Architecture-function analysis of the kinetochore reveals the mechanism of spindle assembly checkpoint signaling

by

Pavithra Aravamudhan

A dissertation submitted in partial fulfillment
of the requirements for the degree of
Doctor of Philosophy
(Biophysics)
in The University of Michigan
2015

Doctoral Committee:

Assistant Professor Ajit P. Joglekar, Chair
Professor Ari Gafni
Professor Duncan G. Steel
Professor Kristen J. Verhey
Associate Professor Yukiko Yamashita

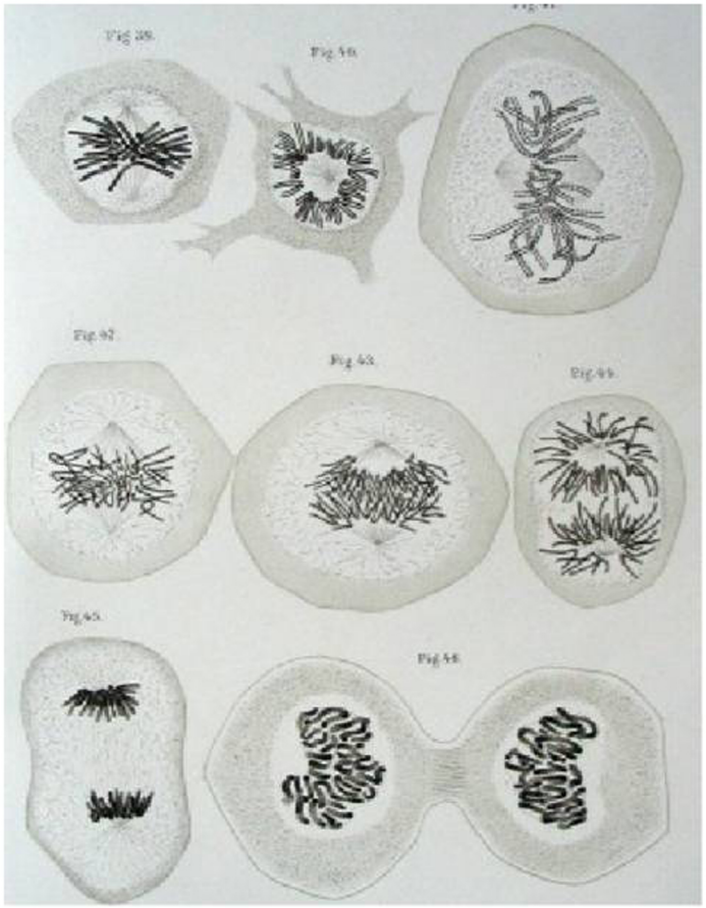

Earliest Drawing of Mitosis
Walther Flemming circa 1882

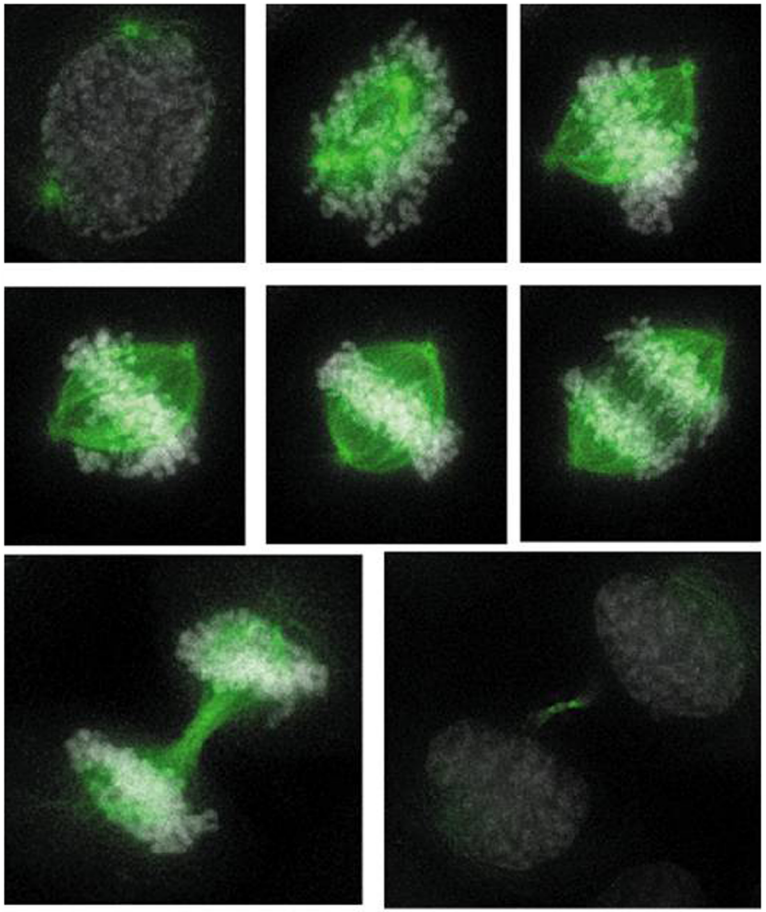

Mitosis : Fluorescence Microscopy
Adapted from Geert Kops

You are the sum total of everything you've ever seen, heard, eaten, smelled, been told, forgot - it's all there. Everything influences each of us, and because of that I try to make sure that my experiences are positive.

- Maya Angelou

ACKNOWLEDGEMENTS

I would like to dedicate this thesis work to every person and experience that has been a part of my life, from floor seating in the class rooms of Innambur, to the contrasting grandeur at the University of Michigan. Here, I would like to specifically acknowledge some people that have been a part of this journey, and I apologize ahead for any oversight.

First of all, I would like to thank Ajit for trusting and taking me in as his first graduate student. It was serendipity that brought me into his lab and I feel privileged to have him as my thesis mentor. He has always inspired me with his unabated enthusiasm, passion for science and intellectual acuity. This thesis would not have shaped up this way but for his keen insights, and all the invaluable brainstorming sessions over the weekends. His office door has always been open for discussions. He has never hesitated to listen to any questions or comments, and has always been receptive to criticism. I especially feel indebted to Ajit for all his patience, insightful advice and interest in the next steps of my career.

I am truly fortunate to have a supportive thesis committee and I thank each of the members for their help. Ari and Duncan always have the best interest of their student in mind, and have gone out of their way to help me. I truly admire them for being not just amazing scientists but also for leading as great human beings. Duncan, in particular, has been my go-to person for everything. He has truly been family to

me; without his advice and support, I probably would not have made it through grad school. Kristen is the one who introduced me to cell biology during my first year and ever since then, she has supported me with her valuable advice and suggestions. Yukiko has always blown my mind with her uniquely insightful comments and questions. She is one person who has spent the most time, other than Ajit and Krish, in reading and providing priceless advice all my manuscripts, proposals and fellowship applications. She is a person who has never said no, whenever I have asked for help. She always finds time amidst her busy schedule (and always responds to emails within a few minutes, even past midnight!). And finally, Mara is someone who has helped me both professionally and otherwise through this time, with absolutely no vested interest. She has been an extremely helpful person. whenever I go to her office with a question, she will either know the answer or walk out with me to find someone who knows the answer.

My lab mates made my time in grad school truly enjoyable, and I deeply thank them for making the lab an intellectually stimulating and a fun place for research. Kaushik recruited me to the lab and has ever since been an amazing friend. He was my partner in crime in fixing messed up experiments during my early days in lab. Babhru is the most patient and helpful person I have ever met. His constant motivational statement has been, "If your experiment works, let's go have a shot of whisky; if it doesnt work, well have an extra shot". Vikash has always been helpful with his frank comments both on science and otherwise. I have also enjoyed Laurens company a lot and she makes the place lively with her attitude whenever she is around. She has also always cheered us up with her out-of-the-world cup cakes on everyone's birthday. I should also thank her for proof reading all my writings multiple times. And finally, Palak, despite being in the lab only for a short time has already become such a great friend. She has been of great support during times of finishing this thesis. Thanks

Palak, for all the moral support, nice conversations over coffee/lunch and more importantly, how can I miss all the nice lunch boxes!

Undergraduate researchers in the lab definitely deserve their own mention. Without Alan and Ted, my thesis work would have taken a few more years to be complete. Thank you for working with me to move the research forward. Al has always been the most caring (kid) in the lab, going out of his way to help people. His sincerity with research helped in moving the first part of my thesis work forward, and also shaped up his own research project in the lab. I also thank Al for taking much of my frustration and being supportive during the time I was writing my first manuscript. Ted and Janice worked with me on the work presented in second half of this thesis. Ted has always amazed me with his intellect and smartness. Janice has inspired me with her sincerity and optimistic attitude. And lastly, Simon, thank you for all the fun times and GOT conversations in the lab.

I would like to thank the University of Michigan, PIBS, and Nils Walter, who played an important role in recruiting me to Michigan, for providing me this invaluable opportunity. I thank all the staff members in Biophysics and Cell & Developmental Biology program for all their help and assistance over the years.

And of course, none of this would have been possible without the most important people in my life, friends and family. I have been fortunate to have friends "the mokkai gumbal", who have been family to me and have made Ann Arbor my home. Janani (my long-term roommate) and Vikram have been the closest to me during this time. Vikram has always made the time to listen to my cribbing from time to time, and has been of great support in making important decisions during tough times. I would also like to thank my oldest friends, Vasanth and Peru, and my Ann Arbor

friends Visa, Sethu and Preethi for cheering me up from time to time, and all the rest of my friends around the world, who have supported me through grad school in one way or the other.

Finally, my family - my parents (Sudha and Aravamudhan) and my sister (Mirunalini) have always put up with my idiosyncrasies, adored me for what I am, supported me through tough times and always motivated me to aim for the best. An engineer by training and an artist at heart, my dad has always indulged with me in fun projects right from my pre-school days. In fact, he is my first scientist role model that I have always looked up to over the years. Importantly, my parents supported me to freely pursue my dreams in a society where women are still expected to confine to rules. They have always dedicated their lives to me, and I would not have been the person I am without them. And the last one, I cannot do justice thanking this person in words; Krishnan, my oldest friend, philosopher and mentor, who eventually became my husband. He introduced me to research as an undergraduate student, helped me get into graduate school, and has always inspired me with his fascination for science. Thank you for being a part of everything in my life and through every day of work that went into this thesis. And most importantly, thank you so much for the help with formatting my thesis! I don't know how I would have made it here without you.

TABLE OF CONTENTS

LIST OF FIGURES

Figure

LIST OF TABLES

Table

ABSTRACT

Architecture-function analysis of kinetochore reveals the mechanism of spindle assembly checkpoint signaling

by

Pavithra Aravamudhan

Chair: Ajit Joglekar

Equal segregation of chromosomes in a dividing cell between its two daughters is necessary for accurate genome inheritance. For successful segregation, chromosomes must attach to and move along microtubule tracks provided by the division machinery. A complex, multi-protein machine called kinetochore establishes this attachment and generates force to move chromosomes. It also signals the absence of attachment by triggering a biochemical cascade called the Spindle Assembly Checkpoint (SAC), which in turn stalls the cell cycle. My thesis work provides mechanistic insights into this attachment-sensitive execution of the SAC by kinetochore. These findings have significant implications on understanding how the checkpoint fails in conditions like cancer and Down's syndrome.

Functionality of kinetochore emerges from its 'architecture', defined by the spatial arrangement of multiple copies of > 60 proteins. I first reconstructed this architecture in the presence of microtubule attachment by combining high resolution imaging with FRET microscopy in budding yeast. This allowed me to then probe this architecture

for changes that directly controlled SAC signaling. Using novel methods, I discovered a specific attachment-sensitive change in kinetochore architecture that regulates SAC signaling. Attachment controls the spatial separation between two conserved kinetochore proteins Ndc80 and Spc105 like a mechanical toggle-switch. This nanoscale separation of ≈ 30 nm in turn controls a key phosphorylation event, to turn the SAC on or off.

I then investigated the biochemical reaction cascade that acts downstream from the triggering phosphorylation event to produce the final SAC signal. To understand the operational characteristics of individual steps in this cascade, I perturbed key parameters that govern these reactions and measured its effects on the steady-state concentration of the reaction intermediates in vivo, using quantitative fluorescence microscopy. This revealed novel mechanisms that tune the maximal signaling capacity of unattached kinetochores in the cell. Two commonly occurring regulatory themes, substrate limitation and modulation of binding affinities through negative cooperativity, tune the maximal SAC signal output. These regulations likely enable sensitive detection of unattached kinetochores, while ensuring rapid reversibility of the SAC cascade.

CHAPTER I

Introduction

1.1 Chromosome segregation during cell division

Life begets life. This ability is bestowed by the ability of life, from single-celled organisms to humans, to replicate its informational content and make a copy of itself through the process of cell division. Historically, the idea that cells form the basic constituents of life dates back to the 17th century when Robert Hooke and Anton von Leuwenhoek discovered cells under their earliest microscopes [*Hooke*, 1665]. This discovery sparked an investigation of the components and processes that constitute these building blocks. While early exciting discoveries in cell biology were made over the next two centuries, it was not until 1855 that the process of cell division was discovered by Virchow. This discovery revolutionized the way of thinking about how life in the form of cells can propagate itself. Especially in the case of single-celled organisms like bacteria, a single division or mitosis results in the creation of an entire organism. In the case of multi-cellular organisms, life again originates through mitotic divisions from a single-celled zygote. These divisions are essential not only for the development of an organism but also to replenish dead and damaged cells. In case of humans, cells in our body undergo more than a quadrillion (10^{15}) divisions in an average lifetime.

Each cell division occurs as a part of a longer cell cycle consisting of multiple phases that involve duplicating the genetic material/DNA and preparing the cells to divide (Fig 1.1 Left). Mitosis forms a small yet, crucial part of this process, where the duplicated DNA packaged in the form of chromosomes gets segregated between the dividing daughter cells. The number of chromosomes to be segregated can range from a single circular chromosome in case of most bacteria to 23 pairs in case of humans to even hundreds in case of some butterflies and plants. Mistakes in this process can have deleterious consequences. Abnormal chromosome content or aneuploidy resulting from missegration is a leading cause of miscarriages and birth defects like Down's syndrome. Even as early as 1902, Theodor Boveri proposed a link between aneuploidy and malignant tumors [*Boveri*, 1929]. Even though his idea was received with skepticism during his life time, accumulating evidence further lends supports to this idea [*Holland and Cleveland*, 2009; *Kops et al.*, 2005]. Aneuploidy is also observed in $> 90\%$ of solid tumors. Accuracy in chromosome segregation, therefore, forms a crucial step in faithful replication of the mother in the daughter cell during division.

1.2 Orchestration of chromosome segregation

Eukaryotic cells are faced with the challenge of repeatedly and reproducibly segregating multiple chromosomes across large spatial dimensions. The cells must have a way to move exactly one copy of each duplicated chromosome into each daughter cell. To accomplish this, cells utilize a specialized structure called spindle apparatus, wherein microtubules (MTs) are organized into a bipolar football shaped structure (Fig 1.1 green tracks). Early in mitosis during prometaphase, the duplicated sister chromatids that are held together make connections with the dynamic ends of MTs. By metaphase all chromosomes in the cell attain biorientation, i.e., sister chromatids make connections with MT tips from opposite poles of the cell. This configuration

allows chromatids to track the depolymerizing MT ends into the opposite cells in anaphase, when the connections holding the sisters together are dissolved. For seamless execution of this entire process, cells must accomplish two things:

1. Employ machinery that can couple chromosome movement with MT dynamics
2. Wait until every chromosome makes bipolar attachments before initiating anaphase

Both these processes are orchestrated by a multi-protein machine called the kinetochore. Kinetochore proteins assemble on specialized sequences on chromosomes called the centromere and mediate connections with the dynamic MT tips on the other end. They also drive chromosome movement during division by tapping energy from MT depolymerization [*McIntosh et al.*, 2010; *Grishchuk et al.*, 2005]. kinetochores also communicate with the cell cycle machinery through Spindle Assembly Checkpoint (SAC) signaling to stall division until attachments are made (Fig 1.1 Schematic in the right). This is crucial because premature division in the absence of kinetochore-MT attachment will result in random segregation of chromosomes between the diving cells. This essential role for kinetochores in SAC signaling was first established by Rieder and colleagues [*Rieder et al.*, 1994]. They showed that if the kinetochore on the last unattached chromosome is ablated with a highly focused laser beam, the cells have no way to detect the misaligned chromosome, and proceed through the division and missegregate the pair.

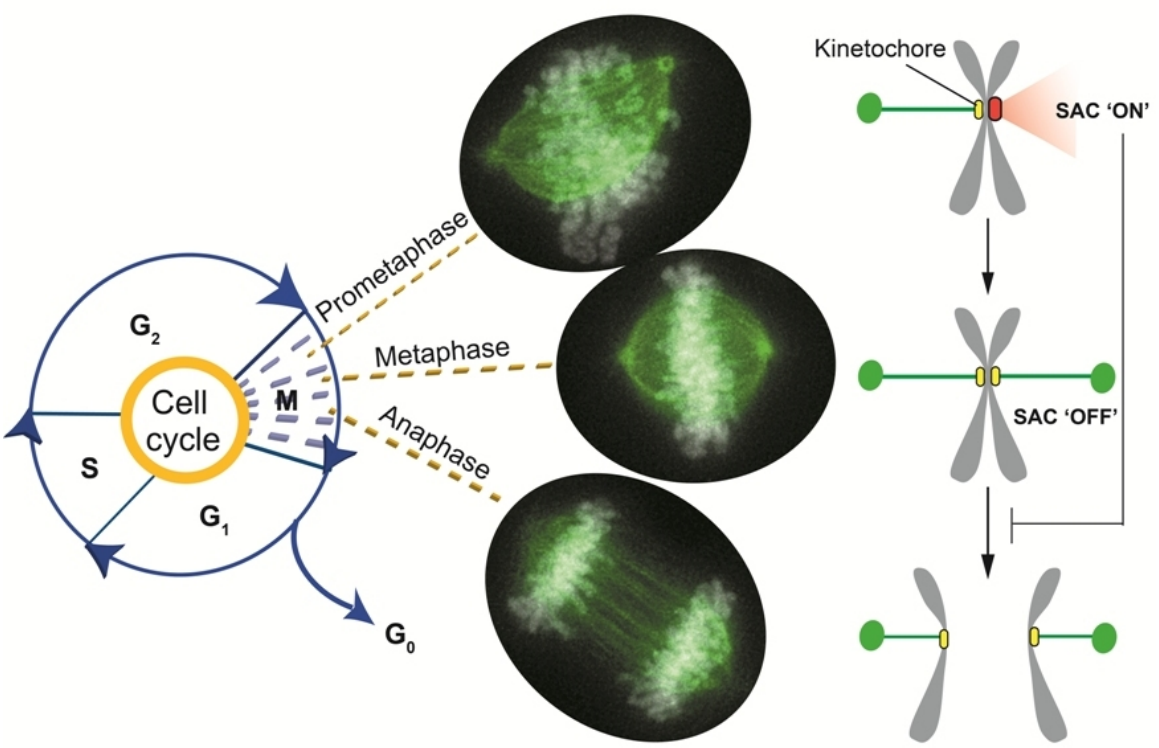

Figure 1.1: **Mitosis and Spindle Assembly Checkpoint** Cartoon in the left depicts different phases of the cell cycle. S represents synthesis phase and M stands for mitosis, which forms a small part of the cell cycle when the duplicated chromosomes are segregated. Representative images of HeLa cells in the middle (adapted from Geert Kops lab) display the spindle morphology in green and the arrangement of chromosomes with in the spindle in grey. Some of the chromosomes are still making attachments in prometaphase. At this point kinetochores assembled on unattached chromosomes activate the spindle assembly checkpoint (SAC) signaling that stalls progression to anaphase. Once all the chromosomes make bipolar attachments and align in metaphase, the SAC gets silenced and this allows progression to anaphase.

In the absence of attachments with MTs, kinetochores activate SAC signaling. They recruit an array of SAC proteins that act together to generate the inhibitory SAC signal that prevents cell cycle progression. Once attachments are established, these proteins dissemble from the kinetochore and the SAC gets inactivated or silenced, and this allows cell cycle progression. Following the discovery of SAC signaling by the kinetochore, tremendous progress has been made over the last three decades in identifying the molecular players that drive the biochemical aspects of SAC signaling (reviewed in [*Musacchio*, 2011; *Murray*, 2011]). Despite this progress, how kinetochore coordinates biochemical events involved in the SAC with its own status of attachment within the spindle has remained a mystery. The complex molecular makeup of the kinetochore forms the bottle neck in understanding this process.

In early electron micrographs of ultra-thin sections of mammalian cells, kinetochore appears as a massive, tri-lamellar structures [*Brinkley and Stubblefield*, 1966; *Rieder*, 1981]. It spreads across $\approx$ 100 nm from the centromeric foundation on chromosomes to spindle MTs. Even the simplest of kinetochores have more than 60 proteins organized into multiple complexes, and each complex is in turn assembled in multiple copies in a hierarchical fashion within the kinetochore (Figure 1.2 and Table 1.1) [*Santaguida and Musacchio*, 2009; *Biggins*, 2013]. Till date, more than a hundred proteins have been identified to function as a part of the kinetochore. The relative arrangement of multiple protein complexes between the centromere and MTs is collectively defined as the 'architecture' of kinetochore. This architecture of the kinetochore determines the emergent function of the kinetochore. This is akin to the example of any machine, a crane in case of the example shown in Fig 1.2 , where the relative arrangement of multiple parts and the flexibilities offered by the linkages define the functionality of this machine.

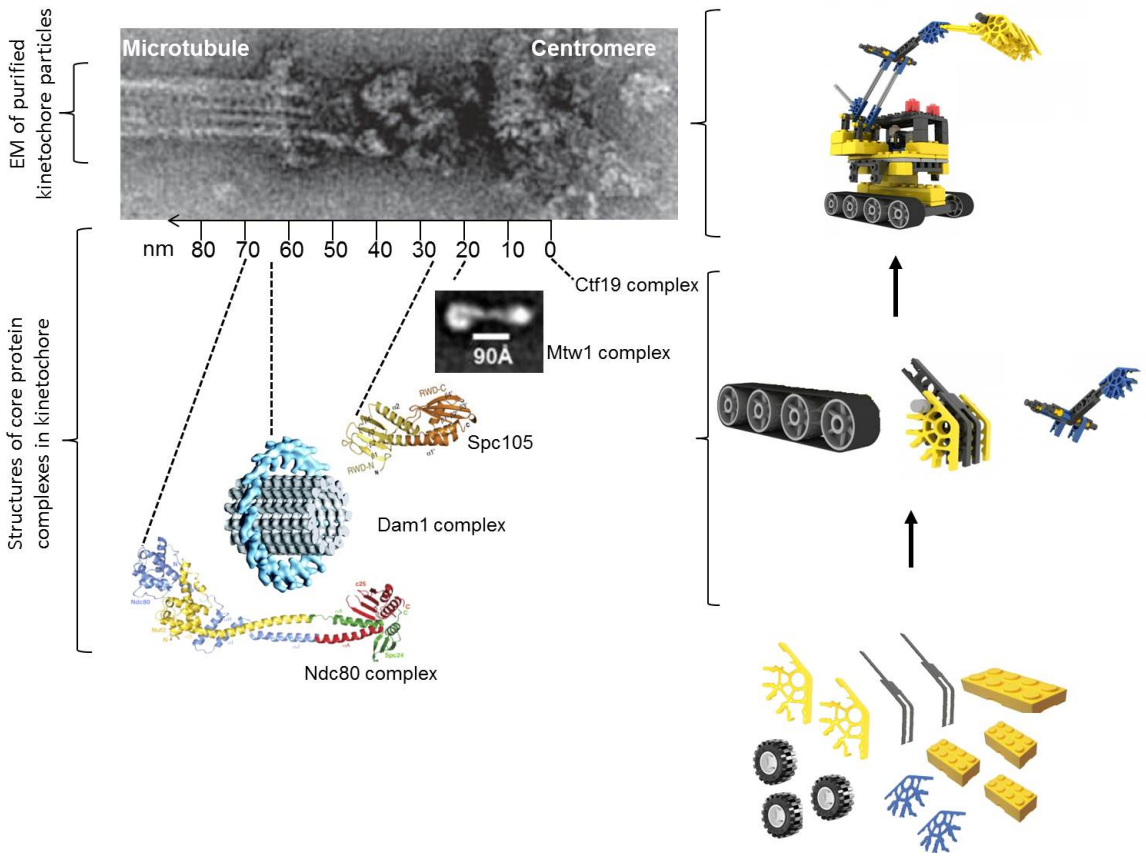

Figure 1.2: **Architecture of the kinetochore** EM structure of purified kinetochore particles is presented at the top left, adapted from ref. [*Gonen et al.*, 2012]. The scale underneath shows the average relative localization of protein complexes within the kinetochore measured in the presence of attachment in budding yeast [*Joglekar et al.*, 2009]. Images at the bottom (adapted from ref. [*Ramey et al.*, 2011; *Hornung et al.*, 2010; *Ciferri et al.*, 2008]) show previously defined structures of core protein complexes. Images on the right present hierarchical assembly of building blocks making up the architecture of a crane. This example is similar to the construction of kinetochore architecture, which is built from the assembly of multiple copies of protein complexes each of which is in turn assembled from multiple proteins (Refer table 1.1)

Importantly knowing the structure of individual parts is not sufficient to decipher how they can act together when present as a part of the entire machine.

Similarly, in case of the molecular machine, kinetochore, multiple protein complexes have been shown to act together in generating force to move chromosomes. Multiple correlations have also been observed with overall changes in kinetochore architecture and the status of SAC signaling in the cell [*McIntosh*, 1991; *Maresca and Salmon*, 2009; *Wan et al.*, 2009]. However, the exact nature of these changes and how they control SAC signaling are not known. A thorough understanding of the attachment-dependent protein architecture of the kinetochore is therefore a fundamental step in defining how it communicates with the SAC machinery.

Downstream from the attachment-dependent initiation of SAC, a biochemical cascade generates the inhibitory signal that stalls cell cycle. The cumulative flux of signal from unattached kinetochores in a cell in turn will determine whether and how long the SAC can stall the cell cycle. On one hand this signal has to be optimal to stall cycle progression even in the presence of a single unattached kinetochore but on the other hand it should also allow quick dissipation once the attachments are made. While the former is essential to avoid errors in chromosome segregation, the latter is important in avoiding unnecessary delays with cell cycle progression. The latter becomes important especially in case of embryogenesis, where delays in coordinated division can have significant implications on development. Therefore, the cells need to optimize the operation of SAC to strike a balance between speed and accuracy in chromosome segregation. Understanding how cells accomplish this requires knowledge of the operation of biochemical steps that generate the SAC signal from the kinetochore. Such an understanding is also crucial to gain insights into how the SAC signaling fails in conditions like cancer.

My thesis work focuses on understanding how the protein architecture of kinetochore allows it to distinguish its status of attachment with the spindle MTs and convey this information to the SAC machinery. It further expands on how cells modulate the SAC signaling cascade, for its optimal operation in ensuring accurate chromosome segregation.

1.3 Building the kinetochore architecture

Cell biology is replete with examples of multiprotein structures, such as ribosomes, nuclear pore proteins [*Schwartz*, 2005], flagella [*Chevance and Hughes*, 2008], endocytic machinery [*Kaksonen et al.*, 2005] etc., where spatial and temporal assembly of multiple proteins gives rise to emergent functions of these complexes. An important aspect in understanding the function of these complexes is not defining the structure and functions of individual parts but rather in defining the composition, molecular linkages, and structure of the resulting macromolecular complex. This is because the functions of individual constituents in a multi-protein system are often contextual - i.e., function of the complex is not simply the sum of parts, but rather emergent in most cases.

Kinetochore, comparable in scale and complexity to these well-studied structures also shares another feature in common: its functions rely on its architecture, as described earlier. The structure and biochemical properties of individual protein complexes that make up the kinetochore have been very well studied. The average localization of individual protein complexes along the kinetochore-MT axis has also been defined using high resolution microscopy [*Joglekar et al.*, 2009]. However, the axial and circumferential distribution of multiple copies of protein complexes that

defines an important aspect of architecture is poorly understood. Defining this architectural aspect *in vivo* is difficult due to the density and dimension of kinetochore falling outside the resolution limits of conventional techniques. From the centromeric foundation to MT attachment, the kinetochore spans $\approx$ 70-100 nm, a distance that is not resolvable using conventional light microscopy. Even further, $>$ 200 core proteins are densely packed with in a cylindrical volume of 10^{-4} μm^3 (Figure 1.2) and thus separations between individual proteins do not fit the resolution of even super-resolution microscopy. Reconstitution *in vitro* for structural studies is also challenging due to the number of proteins involved and the dynamic nature of links that make up the kinetochore. The kinetochore is not a rigid structure but one that actively responds to attachment and MT dynamics [*Akiyoshi et al.*, 2010]. For instance, attachment enforces architecture, and tension directly stabilizes attachment of kinetochore proteins with MTs. These activities can be mimicked, yet difficult to recapitulate *in vitro*. In a remarkable effort, Biggins, Gonen and colleagues isolated kinetochore particles from budding yeast through careful pull down of an inner kinetochore protein [*Gonen et al.*, 2012]. These reconstituted kinetochores could establish MT attachments and track depolymerizing ends *in vitro*. However, the ultra-structure of this reconstituted complex is not at sufficient resolution to establish the identity and geometry of arrangement of individual protein components.

In ***Chapter 2****, along with my colleagues, I utilized a Forster Resonance Energy Transfer or FRET-based microscopy technique developed in the laboratory to define the nanoscale in vivo architecture of the budding yeast kinetochore in the presence of MT attachment.* The protein separations within the kinetochore fall in the ideal range for measurement of proximities using FRET. Using a sensitized emission based FRET technique, we built the axial and circumferential distributions of 4 major protein complexes that make up the core kinetochore machinery, with respect to the MT

axis. This work laid the foundation for understanding how this architecture differs from the one in the absence of attachment, and how these architectural differences regulate SAC signaling.

1.4 Dissecting the mechanism of attachment-dependent operation of the SAC

To execute attachment-dependent signaling, the SAC signal has to be initiated only from unattached kinetochores. The localization of SAC proteins only to unattached kinetochores suggests that the SAC proteins can identify structural or conformation changes that are unique to unattached kinetochores [*Howell et al.*, 2004]. However, the identity of these changes remains unknown and is important in understanding the mechanism of attachment-sensitive SAC signaling. Multiple architectural changes can happen at the kinetochore in the absence of attachment. At the nano-scale, multiple correlations have been reported between changes in the relative organization of kinetochore proteins and the state of SAC signaling [*Maresca and Salmon*, 2009; *Uchida et al.*, 2009; *Wan et al.*, 2009]. However, specific architectural changes that directly trigger SAC signaling are difficult to isolate. The kinetochore proteins can undergo a myriad of changes*in vivo* in the absence of MTs and it is not experimentally feasible to test the influence of specific changes on one or more steps in SAC biochemistry. Therefore, we utilized a unique approach to address this problem based on our known knowledge of the budding yeast kinetochore in the presence of MT attachment.

*In **chapter 3**, we tested how the architecture of attached kinetochore (built in chapter 2) prevented SAC signaling.* We utilized an inducible dimerization system to ectopically localize SAC proteins at defined positions in the kinetochore and assayed their position-dependent ability to signal from attached kinetochores. The results

from this assay revealed regions in the kinetochore that are sensitive to the presence of SAC protein activity. This knowledge allowed us to identify and test specific architectural changes in the kinetochore upon MT attachment that are essential to silence the SAC. This led us to the elegant switch-like mechanism behind attachment-dependent SAC signaling by the kinetochore: MT attachment to the kinetochore controls the physical separation between two kinetochore proteins, Ndc80p and Spc105p, like the two terminals of a toggle-switch. This separation in turn controls a phosphorylation event that is essential for SAC signaling.

1.5 Operational characteristics of kinetochore-based SAC biochemistry

The switch-like execution of SAC by the kinetochore ensures that the SAC responds to the attachment status of the kinetochores. However, the flux of inhibitory signal generated downstream from this mechanism will determine whether this signal can accomplish cell cycle arrest. The aim of SAC signaling is to inhibit the activity of Anaphase Promoting Complex (APC) that mediates metaphase to anaphase transition. Elegant work by the Gerlich and Pines groups showed that each unattached kinetochore generates a finite amount of signal per unit time [*Dick and Gerlich*, 2013a; *Collin et al.*, 2013]. This capacity is determined by the amount of SAC proteins that each kinetochore can accommodate and the efficiency of kinetochore-localized proteins in catalyzing the generation of the SAC signal. Although the signal at the kinetochores may be further amplified by cytosolic reactions, net signal generated and the accompanying cell cycle delay remains proportional to the capacity of each kinetochore, and does not get amplified to a level that can accomplish cell cycle arrest [*Collin et al.*, 2013; *Dick and Gerlich*, 2013a; *Kamenz and Hauf*, 2014; *Ciliberto and Shah*, 2009; *De Antoni et al.*, 2005]. For instance, an unattached kinetochore

Protein complex	Proteins within the complex	#Copies per kinetochore in budding yeast [*Joglekar et al.*, 2006]	Localization in kinetochore	Structure reference
COMA	Ctf19p, Okp1p, Mcm21p, Ame1p	2	Inner kinetochore	[*Schmitzberger and Harrison*, 2012]
Mtw1	Mtw1p, Nsl1p, Dsn1p, Nnf1p	5	Inner kinetochore	[*Hornung et al.*, 2010]
Spc105	Spc105p, Kre28p	5	Inner kinetochore	[*Petrovic et al.*, 2014]
Ndc80	Ndc80p, Nuf2p, Spc24p, Spc25p	8	Outer kinetochore	[*Wang et al.*, 2008]
Dam1	Dam1p, Dad1p, Dad2p, Dad3p, Dad4p, Ask1p, Spc34p, Spc19p, Duo1p, Hsk3p	16	Outer kinetochore	[*Ramey et al.*, 2011]

Table 1.1: **Core protein complexes that make up the kinetochore-MT attachment in budding yeast** The proteins that are present within different kinetochore complexes carry the suffix '*p*' to distinguish them from the entire protein complex with the same name.

generated in the cell in late metaphase cannot stall cell cycle, if it does not have time to generate sufficient signal that can block APC, before committing to anaphase [*Dick and Gerlich*, 2013a]. The flux of this signal is determined by the scaffold that each kinetochore can provide to drive the SAC biochemistry. While this capacity has to be high in the presence of a single unattached kinetochore in the cell, the cumulative signal output from multiple kinetochores need not be proportional. In other terms, although the response of kinetochores to attachment has to be switch-like in triggering the SAC, the downstream signaling pathway has to be modulated for efficient performance (Fig 1.3). Cells can tweak both kinetochore-intrinsic and extrinsic parameters at multiple layers in the biochemical cascade of SAC to achieve efficient signaling [*Zhang et al.*, 2014; *Krenn et al.*, 2014; *Heinrich et al.*, 2013; *Shen*, 2011]. For instance, phosphoregulation can regulate the receptivity of the kinetochore for SAC proteins, while cellular concentrations of SAC proteins and their affinities for binding partners at the kinetochore will further regulate the number of functional SAC complexes that assemble at each kinetochore.

To understand how these processes are regulated*in vivo, in* ***Chapter 4****, we studied how individual steps in SAC biochemistry responded to perturbations in different biochemical parameters that influence SAC signaling.* We measured how these perturbations altered key protein interactions that are essential for SAC signaling. Utilizing quantitative fluorescence microscopy, we quantified the steady-state concentration of SAC reaction intermediates that bound to individual kinetochores in budding yeast. Our data demonstrate that the cellular concentration of a key SAC protein, Bub1 is a critical parameter that determines the maximal signaling capacity in the present of multiple unattached kinetochores, whereas the lower threshold is defined by the affinity of Bub1 for the kinetochore protein Spc105p, which provides the scaffold for SAC protein assembly.

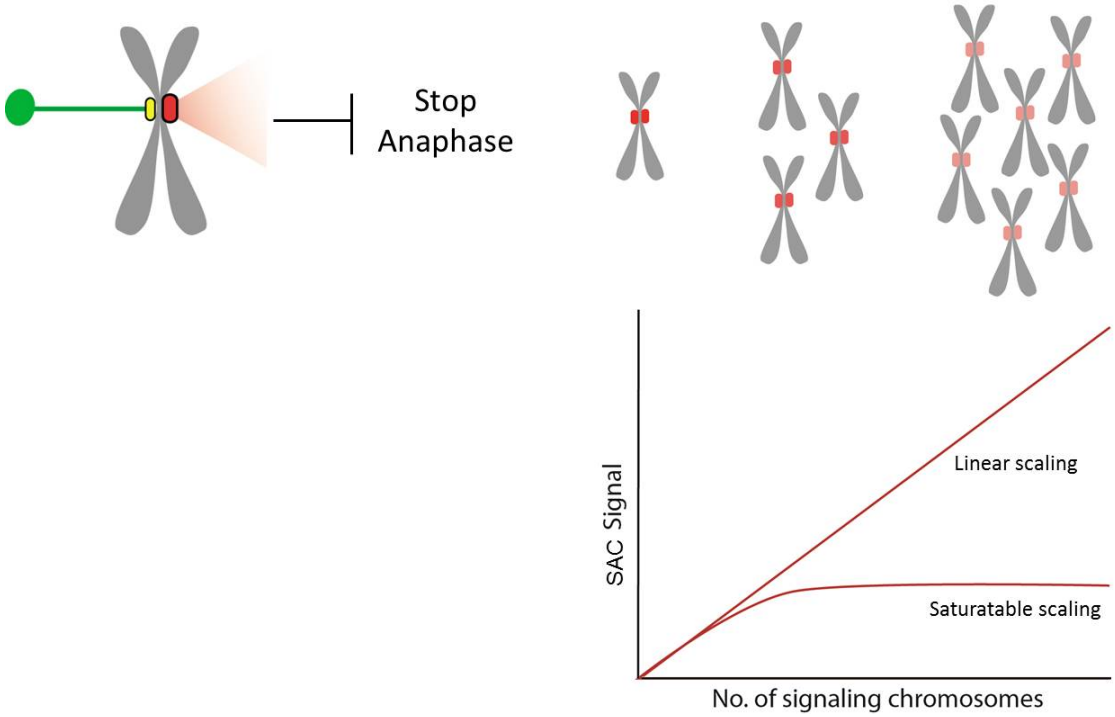

Figure 1.3: **Scaling of the SAC signal** The aim of a single unattached kinetochore is to generate enough SAC signal that can stall the cell cycle. In this case, signaling from multiple unattached kinetochores need not scale proportionally. The cells could potentially tweak biochemical parameters to saturate the net SAC signal at an optimal maximum.

In summary, my thesis work provides mechanistic insights into the initiation and execution of SAC signaling at the kinetochore, which is a fundamental mechanism that ensures fidelity in chromosome segregation. The first part of this work provides the three-dimensional architecture of eukaryotic kinetochore in the presence of MT attachment. This architecture defines the arrangement of core MT-binding components, knowledge of which is essential to understand how kinetochore generates force to move chromosomes. This sets the platform to explore how mutations or post-translational modifications in kinetochore proteins affect the functionality of kinetochore. Knowledge of kinetochore architecture enabled us to dissect the mechanism of attachment-sensitive SAC signaling, which remained a fundamental open question in cell biology for more than 30 years. The mechanism demonstrated here showcases the importance of macromolecular protein architecture of the kinetochore in SAC signaling. The relative placement two protein domains in the context of kinetochore architecture endows their functionality in SAC; the kinetochore encodes the molecular linkages that control the separation between these proteins in an attachment-dependent fashion to control the SAC. This mechanism provides an excellent example of the emergent function of proteins within macromolecular complexes. The described mechanism further allows us to probe how the molecular properties of kinetochore proteins enable optimal function in both force generation and SAC signaling.

The last part of this thesis describes key parameters that control SAC signal generation from unattached kinetochores. We identified novel mechanisms to regulate the biochemistry at multiple steps in the SAC cascade. A quantitative measure of the parameters that cells utilize in each of these steps sets up the stage to investigate how mutations in SAC proteins and perturbations in SAC protein concentrations affect the strength of SAC signal. This can further be used to understand the basis of genetic instability in cancer cells which are often correlated with changes in the

expression of SAC proteins.

CHAPTER II

Reconstruction of the protein architecture of the budding yeast kinetochore-MT attachment using FRET

2.1 Introduction

The relative arrangement of more than a hundred proteins within the kinetochore defines its architecture. This arrangement extends between the centromeric DNA on one end and connects to MTs from the spindle on the other end. Kinetochore architecture determines the mechanism of kinetochore function in generating force to move chromosomes and in executing attachment-dependent SAC signaling. Therefore, understanding the kinetochore architecture becomes a prerequisite in understanding its emergent functions. Here, we reconstruct the architecture of core protein complexes within kinetochore in the presence of MT attachment in budding yeast, using a FRET methodology previously developed in the laboratory.

Based on the morphological features observed from electron micrographs, the proteins that make up the kinetochore can be divided into the inner and outer kinetochore

layers. At the inner kinetochore, the centromere associated proteins lay the foundation to build kinetochores. Multiple protein complexes build on this foundation to establish connections with spindle MTs at the outer kinetochore. Below, I discuss the known molecular and architectural features the kinetochore before diving into our approach to dissect the poorly understood features.

2.1.1 Centromere scaffolds the construction of the kinetochore

The centromeric DNA lays the foundation to build the kinetochore. Walter Flemming (in 1880) identified centromeres as regions on the chromosomes where the sisters constrict and are held together [*Flemming, W. Zellsubstanz*, 1882]. These regions are marked by the non-canonical histone variant, CENP-Ap (Cse4p in budding yeast; 'p' represents individual proteins that may be present as a part of a protein complex) and recruit proteins that direct kinetochore assembly (CENP-Cp) [*Quénet and Dalal*, 2012]. Thus, the centromere provides the scaffold on which the kinetochore proteins assemble, and thereby plays a founding role in defining the kinetochore architecture.

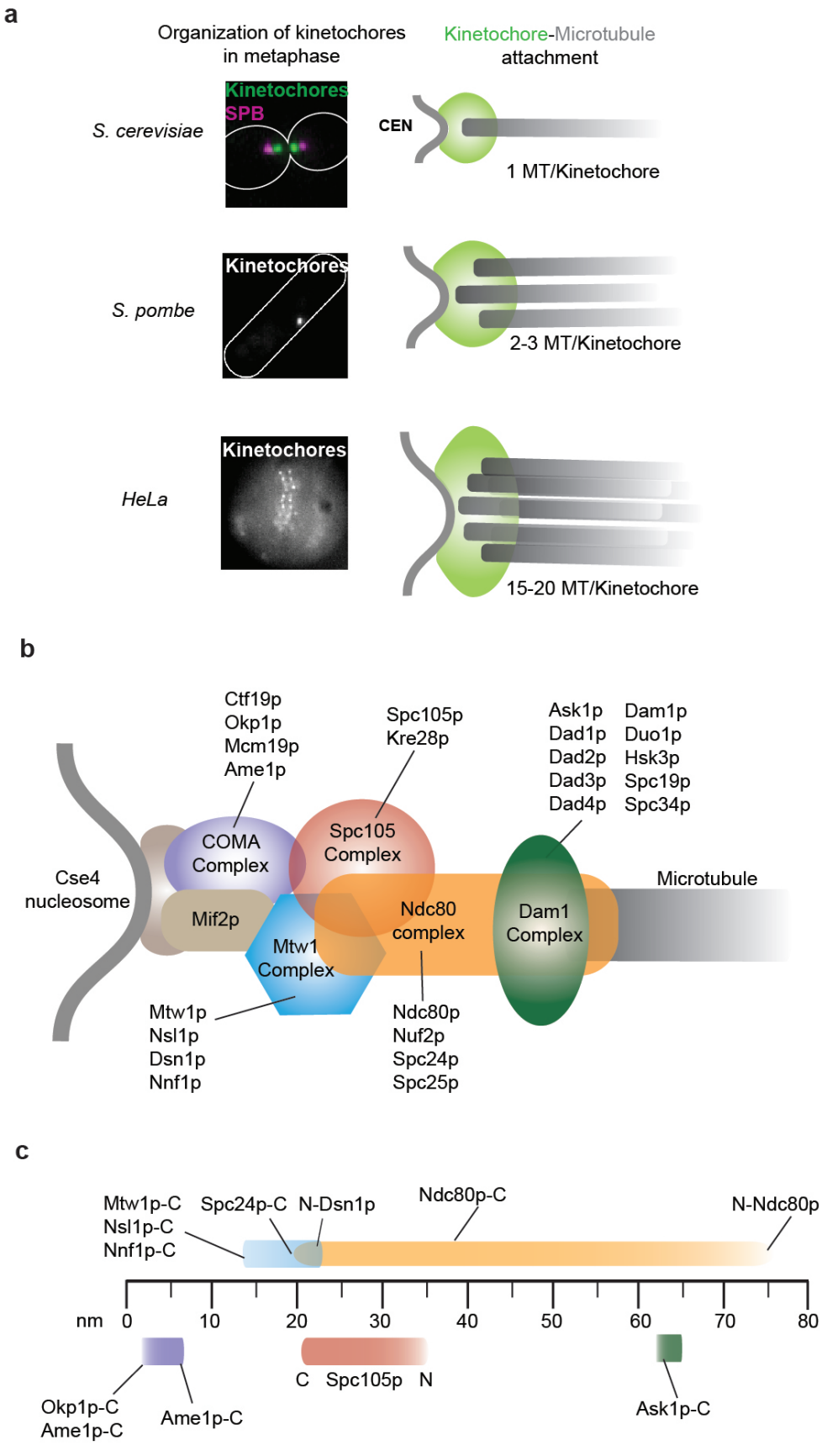
a
Organization of kinetochores in metaphase
Kinetochore-Microtubule attachment
S. cerevisiae
Kinetochores
SPB
CEN
1 MT/Kinetochore
S. pombe
Kinetochores
2-3 MT/Kinetochore
HeLa
Kinetochores
15-20 MT/Kinetochore
b
Ctf19p
Okp1p
Mcm19p
Ame1p
Spc105p
Kre28p
Ask1p Dam1p
Dad1p Duo1p
Dad2p Hsk3p
Dad3p Spc19p
Dad4p Spc34p
COMA Complex
Spc105 Complex
Cse4 nucleosome
Mif2p
Mtw1 Complex
Ndc80 complex
Dam1 Complex
Microtubule
Mtw1p
Nsl1p
Dsn1p
Nnf1p
Ndc80p
Nuf2p
Spc24p
Spc25p
c
Mtw1p-C
Nsl1p-C
Nnf1p-C
Spc24p-C
N-Dsn1p
Ndc80p-C
N-Ndc80p
nm 0 10 20 30 40 50 60 70 80
C Spc105p N
Okp1p-C
Ame1p-C
Ame1p-C
Ask1p-C

Figure 2.1: **Known features of the kinetochore-MT attachment.** (a) Kinetochore-MT attachment in different organisms. Budding yeast has a single MT attachment per kinetochore, whereas this number can be 3 MT attachments in case of fission yeast to 16-20 in case of vertebrates. In vertebrates, part of the kinetochore sites may not be occupied with MTs even in late metaphase when the SAC is satisfied. (b) Composition of kinetochore protein complexes that form the core attachment between the centromere and MTs. (c) Average relative localization of proteins along the kinetochore-MT axis [*Joglekar et al.*, 2009].

The sequence and the length of the centromeric DNA vary widely between organisms. Although there are some specific sequences associated with the centromeres, they are mostly defined epigenetically [*Amor et al.*, 2004]. Length of the centromere varies from short 125 nucleotide sequences in case of budding yeast (defined as point centromere [*McAinsh et al.*, 2003; *Henikoff and Henikoff*, 2012]) to tens of kilobases in case of fission yeast S. *pombe*, to several megabases in case of animals and some plants cells (defined as regional centromeres). These sequences can further occupy a single stretch on the chromosome (monocentric) or extend across the entire length of the chromosome, as found in case of C. *elegans* (holocentric) [*Maddox et al.*, 2004]. The differences in the length and the organization of the centromeric DNA can in turn define the three-dimensional architecture on which the kinetochore is built. The centromere geometry can also determine how the kinetochore proteins are organized into modules that make connections with individual MTs at the other end.

The kinetochore is built inward out from the centromere. The kinetochore proteins are classified as inner or outer kinetochore proteins based on their proximity to the centromere or MTs, respectively. CENP-Cp, associated with the centromere, directs the assembly of the conserved KMN network: Knl1, Mis12 and Ndc80 complexes (Spc105, Mtw1 and Ndc80 complexes, respectively in budding yeast) [*Cheeseman et al.*, 2006; *De Wulf et al.*, 2003; *Biggins*, 2013]. These proteins form the core connection between the inner kinetochore and the spindle MTs.CENP-C directly interacts with a member of the Mtw1 complex, which acts as the hub for outer kinetochore assembly by recruiting the Spc105 and Ndc80 complexes [*Petrovic et al.*, 2010]. The order of assembly and the dynamics of association of these proteins with the centromere differ between organisms. The kinetochore proteins are disassembled at the end of mitosis in humans [*Gascoigne and Cheeseman*, 2013], whereas they remain associated with centromeres in budding yeast, which undergoes closed mitosis [*Marston*,

2014; *Roy et al.*, 2013].The specificity provided by centromere-associated proteins to assemble the kinetochore also becomes important in aiding accurate chromosome segregation. For instance, recruiting CENP-Cp to an ectopic position on chromosomes directs kinetochore assembly that can establish connections with MTs [*Gascoigne and Cheeseman*, 2011]. The presence of multiple such kinetochores on the same chromosome lead to aberrant segregation phenotypes [*Shen*, 2011; *Vig et al.*, 1989].

2.1.2 Organization of the outer kinetochore

At the other end from centromeres, the kinetochore protein linkages build up to establish connections with the tips (plus ends) of spindle MTs at the outer kinetochore. The number of MTs that associate with each kinetochore differs between organisms (Fig 2.1a). The four sub-unit Ndc80 complex primarily mediates these interactions with MTs and thereby connects chromosomes with MTs. Conserved calponin-homology (CH-) domains within the amino-terminus of Ndc80p bind at the interface of the repetitive α/β -tubulin subunits that constitute MTs [*Alushin et al.*, 2010; *Wang et al.*, 2008] (Fig 2.1b and Fig. 2.2a). This interaction is further promoted by an ≈ 113 amino acid long unstructured tail in the N-terminus of Ndc80p [*Alushin et al.*, 2012; *Demirel et al.*, 2012]. Since CH-domains recognize repetitive units on the cylindrical surface of MTs, multiple copies of Ndc80p with in an attachment site can randomly bind anywhere along the length/circumference of the MT, and thus be staggered or aligned relative to each other (Fig 2.2b). However, the connectivity to the inner kinetochore and the foundation provided by the centromere can enforce a favored relative organization/orientation on multiple Ndc80 molecules. Such relative arrangement of multiple copies of molecules forms an important aspect of the kinetochore architecture that would directly influence how it holds on to dynamic MT ends (discussed below). This architecture will also have significant implications on

the SAC signaling.

2.1.3 The kinetochore architecture encodes its functions

A lot of information is available on the structure and biochemical activity of individual protein components that make up the core of the kinetochore. The Ndc80, Mis12/Mtw1 complexes and the kinetochore binding domain of Knl1p (Spc105 homolog) have all been reconstituted *in vitro* and their individual structures, interaction with other components of the kinetochore and biochemical activities have all been well-studied [*Hornung et al.*, 2010; *Wei et al.*, 2005; *Wang et al.*, 2007] (Fig 2.1b and Fig 1.2). However, a cohesive picture of the architecture of the kinetochore and the emergent functions of individual protein components imposed by this architecture is lacking.

Knowledge of the kinetochore architecture is crucial to understand how kinetochore proteins act together to hold on to dynamic MT ends and couple chromosomes movement with MT dynamics. Mechanisms underlying the generation of force to drive chromosome movement depend on both, the MT-binding properties of kinetochore proteins and their nanoscale organization. For example, the Ndc80 complex has been shown to bind and track along with MT ends *in vitro*. However, given the poor affinity of CH-domains, whether individual domains can processively track MT depolymerization to drive chromosome movement becomes questionable [*Ciferri et al.*, 2005; *Wei et al.*, 2005; *Cheeseman et al.*, 2006]. The persistence of this motility will depend on the copy number of Ndc80 molecules in each kinetochore and their distribution relative to the MT tip [*Powers et al.*, 2009; *Joglekar et al.*, 2010]. In addition, the 10-subunit Dam1 complex that forms a ring around MTs *in vitro*, can aid MT tip-tracking by Ndc80, in budding and fission yeasts [*Tien et al.*, 2010; *Lam-*

pert et al., 2010]. The presence of Dam1 complex in reconstituted systems improves processivity *in vitro* [*Tien et al.*, 2010; *Grishchuk et al.*, 2008]. Even though this complex is not conserved, an equivalently positioned Ska complex in metazoa (present in plants, vertebrates, nematodes and humans) might form the functional homolog supporting a similar role [*Schmidt et al.*, 2012; *Welburn et al.*, 2009]. However, force coupling properties of the MT-binding Dam1 complex and, the biophysical mechanism of Dam1-coupled motility depend on its oligomerization state *in vivo*, which has not been proven, and also on its positioning relative to the Ndc80 complex [*Grishchuk et al.*, 2008; *Efremov et al.*, 2007]. Thus, the nanoscale organization of MT-binding proteins within the kinetochore becomes critical in understanding how they act together to track the dynamic MT ends. The copy numbers of core proteins incorporated by each kinetochore, the arrangement of these proteins at the kinetochore-MT interface, and how these molecules are in turn linked to the centromeric foundation, all form important aspects of the architecture.

Architecture of the kinetochore that promotes effective force generation is also intrinsically tied to the organization that satisfies SAC signaling. Logically, geometries of attachment that promote faithful segregation must also satisfy the SAC and promote cell cycle progression. In the absence of MT attachment, multiple kinetochore proteins act together to generate the SAC signal. Understanding how these proteins spatially coordinate to generate the inhibitory SAC signal only in the absence of MT attachment, requires knowledge of differences in their organization based on the attachment status.

2.1.4 Budding yeast as the model system to understand kinetochore architecture

We used budding yeast as the model organism to understand how the organization of MT-binding proteins shapes the mechanisms of kinetochore movement and SAC signaling. The copy number of MT-binding proteins and kinetochore proteins that function in SAC, as well as their average relative organization along kinetochore-MT axis are both known in budding yeast (Fig. 2.1c). Furthermore, the kinetochore assembled on each point centromere interacts with exactly one MT in budding yeast, whereas in case of vertebrates, the number of connections can vary from 15-20 at each kinetochore [*McEwen et al.*, 2001] (Fig. 2.1a). The former therefore offers a unique advantage in studying individual attachment sites that are in either 'attached' or 'unattached' states, rather than the partially attached/occupied states observed in case of vertebrates even in late metaphase. Importantly, despite these differences, the core protein complexes that constitute kinetochore-MT attachment, and the protein composition of each attachment site are conserved between organisms. This implies that the architecture and the enforced functionality of kinetochore are also likely conserved [*Joglekar et al.*, 2009, 2008, 2006; *Johnston et al.*, 2010; *Wan et al.*, 2009]. The core kinetochore-MT attachment machinery in budding yeast consists of four components: Ndc80 complex, Dam1 complex, Spc105p and Mtw1 complex. The yeast kinetochore incorporates an invariant copy number of each protein (complex): at least 16-20 copies of Dam1, and 5-8 copies of Spc105p, Ndc80 and Mtw1 complexes, positioned at well-defined average locations along the kinetochore-MT attachment (Fig. 2.1b and Fig. 2.1c) [*Joglekar et al.*, 2006; *Aravamudhan et al.*, 2013; *Joglekar et al.*, 2009; *Lawrimore et al.*, 2011; *Coffman et al.*, 2011]). Despite this thorough knowledge, two critical facets of kinetochore organization remain unknown (Fig. 2.2a): (1) the distribution of multiple copies of each protein/complex about its average position, and (2) their distribution around the MT circumference. These data are necessary

to define the nanoscale organization of the yeast kinetochore, and to understand how this organization influences force generation and SAC signaling.

2.1.5 Approach to construct the kinetochore architecture using FRET

A FRET-based technique was previously developed in our laboratory to reconstruct nanoscale distributions of kinetochore proteins [*Joglekar et al.*, 2013; *Muller et al.*, 2005]. Here, we extend this to build the protein architecture of budding yeast kinetochore in the presence of MT attachment in metaphase. We made two kinds of FRET measurements between kinetochore proteins tagged with GFP(S65T) or mCherry. To elucidate axial protein distribution (i.e. along the length of the kinetochore-MT attachment), we measured FRET between the labeled protein and suitable reference points in the kinetochore. To obtain circumferential protein distribution, we measured FRET between neighboring copies of the same protein in heterozygous diploid strains.

We built the kinetochore architecture outward-in starting at the MT-binding interface of the Ndc80 complex. Fixing the axial and circumferential distributions of Ndc80 subunits allowed me to use this protein complex as a reference to measure the relative proximity of inner kinetochore proteins such as Spc105p and the Mtw1 complex proteins (Fig. 2.1b and Fig. 2.2a). Combining the FRET measurements with known kinetochore protein structures, copy numbers, and localizations, we reconstructed the *in vivo* architecture of the metaphase kinetochore-MT attachment.

2.2 Methods

2.2.1 Strains and Media

Budding yeast strains were grown in Yeast Peptone Dextrose (YPD) medium. For imaging, mid-log phase cells were rinsed and concentrated in synthetic media supplemented with essential amino acids and the appropriate carbon source. Cells were immobilized on ConA coated coverslips and sealed with VALAP to prevent evaporation. Imaging lasted for < 30 minutes.

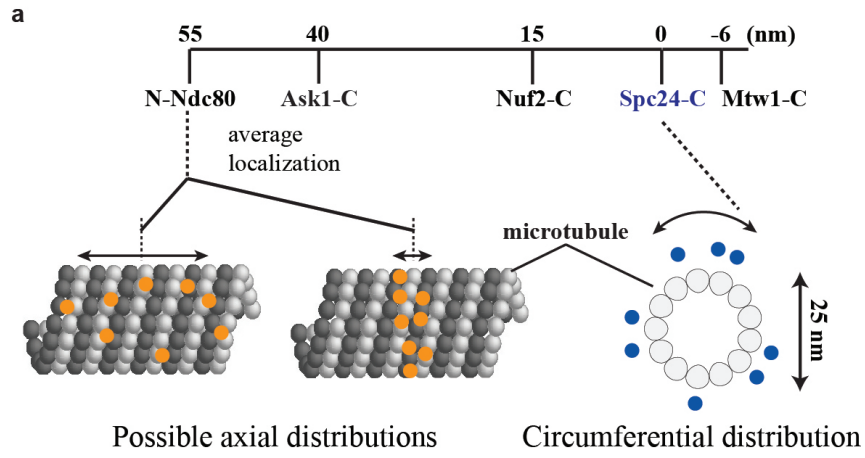
a
55
40
15
0
-6 (nm)
N-Ndc80
Ask1-C
Nuf2-C
Spc24-C
Mtw1-C
average localization
microtubule
25 nm
Possible axial distributions
Circumferential distribution

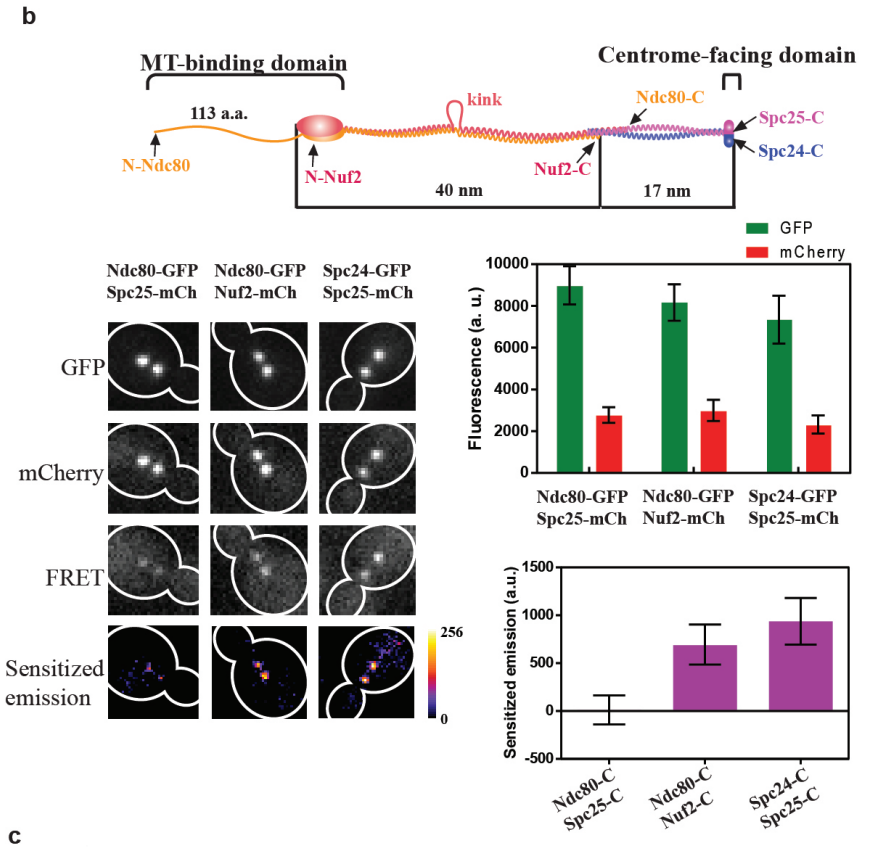
b
MT-binding domain
Centrome-facing domain
113 a.a.
kink
Ndc80-C
Spc25-C
Spc24-C
N-Ndc80
N-Nuf2
Nuf2-C
40 nm
17 nm
Ndc80-GFP Spc25-mCh
Ndc80-GFP Nuf2-mCh
Spc24-GFP Spc25-mCh
GFP
mCherry
FRET
Sensitized emission
256
0
GFP
mCherry
Fluorescence (a. u.)
10000
8000
6000
4000
2000
0
Ndc80-GFP Spc25-mCh
Ndc80-GFP Nuf2-mCh
Spc24-GFP Spc25-mCh
Sensitized emission (a.u.)
1500
1000
500
0
-500
Ndc80-C Spc25-C
Ndc80-C Nuf2-C
Spc24-C Spc25-C

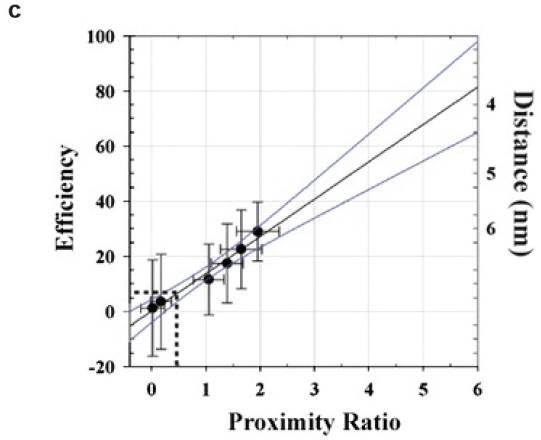
c
Efficiency
100
80
60
40
20
0
-20
0
1
2
3
4
5
6
Proximity Ratio
Distance (nm)
4
5
6

Figure 2.2: **Employing FRET to measure proximity between kinetochore proteins.** (a) Top: The known average positions of kinetochore proteins along the kinetochore-MT attachment [*Joglekar et al.*, 2009]. Nanoscale protein distributions along the MT axis (possibilities indicated in the cartoon) or around the circumference of the MT are unknown. (b) Top. Physical dimensions and subunit organization of the Ndc80 complex. Bottom: Metaphase cells expressing two labeled Ndc80 subunits (indicated the top) as observed in the GFP, mCherry, and FRET channel. Heat maps of sensitized emission intensity were calculated by subtracting contributions of GFP bleed-through and mCherry cross-excitation (estimated using the GFP and mCherry signals measured in the respective images), and cellular auto-fluorescence from the FRET image. Quantification of the GFP, mCherry and sensitized emission intensity per kinetochore cluster (mean±s. d.) shown on the right. Reduction in the GFP signal is due to FRET [*Joglekar et al.*, 2013]. (c) Proximity ratio computed from the measured sensitized emission correlates linearly with FRET efficiency (data reproduced from [*Joglekar et al.*, 2013]).

2.2.2 Microscopy

Imaging was conducted on a Nikon Ti-E inverted microscope with a 1.4 NA, 100x, oil immersion objective. The Lumencor LED light engine (472/20 nm for GFP and 543/20 nm or 575/20 nm for mCherry) was used for fluorophore excitation. Dual-band excitation filter ET/GFP-mCherry (59002x), excitation dichroic (89019bs) and emission-side dichroic (T560lpxr), emission filters: ET525/50m and ET595/50m from Chroma were used for FRET imaging. Kinetochore clusters that were separated by $\approx$ 0.8 to 1 μm were designated as metaphase kinetochore clusters, while those separated by more than 2 μm were designated as late anaphase/telophase kinetochore clusters [*Joglekar et al.*, 2006].

Quantification of FRET was conducted using a semi-automated graphical user interface in Matlab [*Joglekar et al.*, 2013]. Briefly, the total fluorescence from kinetochore clusters was measured in the in-focus plane (containing the brightest pixel within the kinetochore cluster image) in all three channels independently. The GFP fluorescence in strains expressing GFP fusions of subunits of Ndc80 and Mtw1 complexes was statistically indistinguishable, as expected [*Joglekar et al.*, 2006]. mCherry fluorescence showed significant variation from strain to strain even for the same kinetochore protein. Since the GFP fluorescence does not change in this manner, we concluded that the variation in mCherry fluorescence is due to changes either in the brightness or maturation efficiency. We limited variation in the mCherry signal to $< 20\%$ about the average by selecting strains exhibiting the highest fluorescence after each yeast transformation. It was previously shown that for a fixed number of GFP molecules, the proximity ratio (a measure of FRET, defined in results) scales linearly with the mCherry number [*Joglekar et al.*, 2013]. However, the observed mCherry variation does not change any of the conclusions based on comparisons of FRET measurements. Therefore, we report the uncorrected proximity ratio values. We used the

Wilcoxon rank-sum test for all pairwise comparisons of proximity ratios.

2.3 Results

2.3.1 Establishing a measure of FRET efficiency

To measure FRET, selected proteins, e.g. subunits of the Ndc80 complex (Fig. 2.2b), were fused to either GFP(S65T) (the donor) or mCherry (the acceptor) and expressed from the endogenous locus. FRET is quantified as the sensitized emission intensity, which is the acceptor fluorescence due to FRET, emanating from the two kinetochore clusters, each containing 16 kinetochores, seen in haploid cells in metaphase (Fig. 2.2b, micrographs). The fluorescence measured in the FRET channel includes two contaminating signals: GFP bleed-through into the FRET channel and mCherry cross-excitation at the GFP excitation wavelengths. For the imaging conditions used, the GFP bleed-through is 5.8 $\pm$ 0.01 % of the signal measured in the GFP channel, while mCherry cross-excitation is 6.1 $\pm$ 0.02 % of the mCherry signal [*Joglekar et al.*, 2013]. We used these factors and the GFP and mCherry fluorescence measured for each cluster to estimate the contaminating fluorescence due to GFP bleed-through and mCherry cross-excitation. These fluorescence values were subtracted from the fluorescence measured in the FRET image to obtain sensitized emission, which is the acceptor fluorescence due to FRET.

Since we hold the fluorophore excitation conditions constant in all experiments, the sensitized emission from the kinetochore cluster is directly related to the number of FRET pairs and to the average FRET efficiency [*Joglekar et al.*, 2013]. Furthermore, we construct strains wherein the labeled kinetochore subunits generate the same number of FRET pairs per kinetochore cluster. In such strains, the measured sensitized emission intensity depends only on the FRET efficiency, and hence the

average donor-acceptor separation. Therefore, comparison of sensitized emission intensities can reveal relative proximities between labeled proteins.

Since FRET quantitation is obtained from fluorescence intensity, it is affected by cell-to-cell variation in GFP and mCherry maturation, and the distance of the kinetochore cluster from the coverslip [*Joglekar et al.*, 2006] [*Joglekar et al.*, 2013]. To minimize the effects of this experimental variation, we normalized the sensitized emission intensity for each cluster by dividing it with the sum of GFP bleed-through fluorescence and mCherry fluorescence due to cross-excitation [*Joglekar et al.*, 2013]. This normalized sensitized emission, termed as Proximity Ratio, is 0 when FRET efficiency is negligible, and directly proportional to non-zero FRET efficiency values [*Joglekar et al.*, 2013].

$$\text{Proximity ratio} = \frac{\text{Sensitized Emission}}{\text{GFP ``bleed-through''} + \text{mCherry ``cross-excitation''}} \tag{2.1}$$

Previous work from the lab also established the relationship between the measured proximity ratio and FRET efficiency through measurements of donor quenching and sensitized emission from FRET pairs designed within the known structure of Ndc80 complex (Fig. 2.2c).

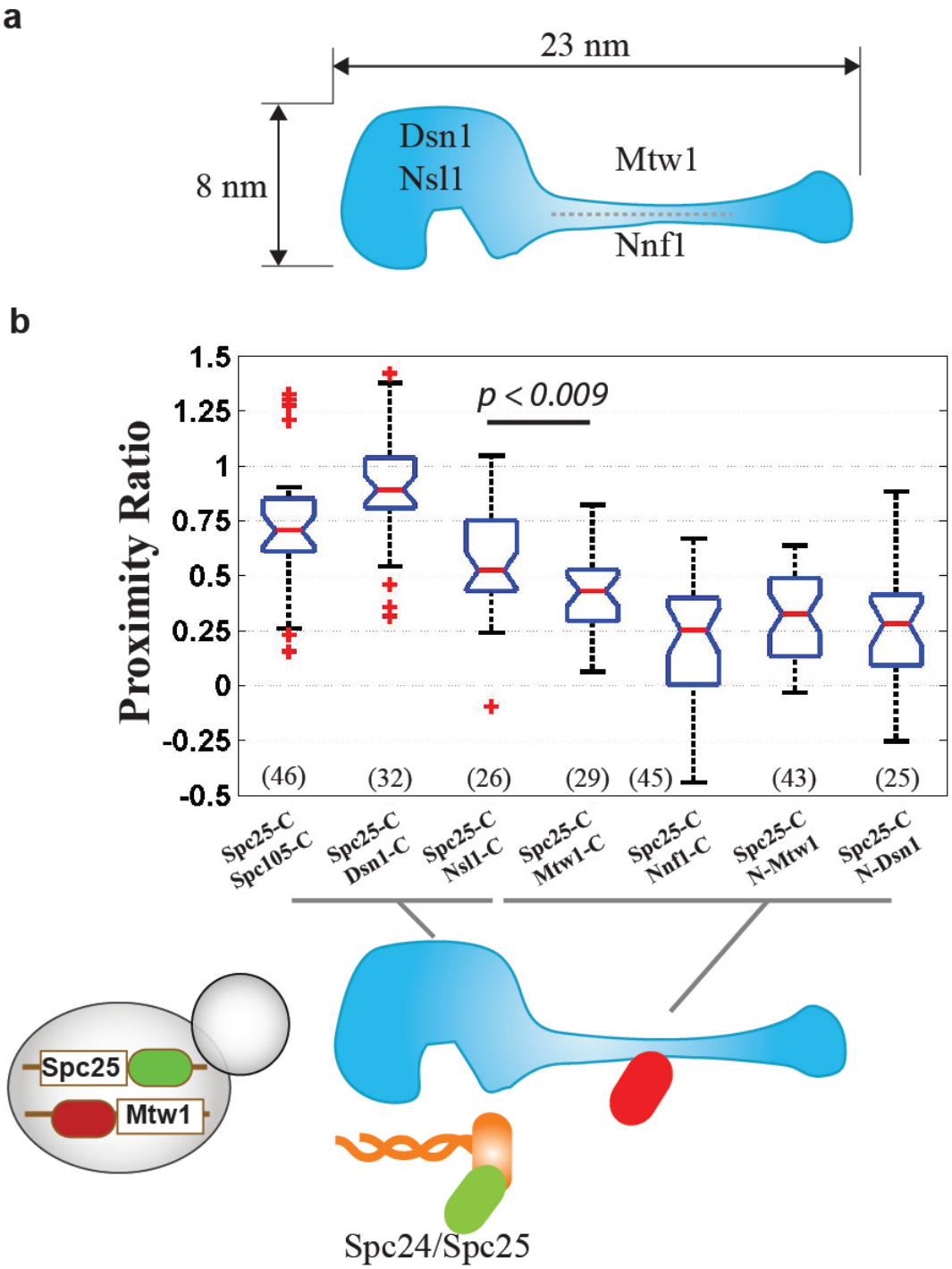

Figure 2.3: **Metaphase architecture of the Mtw1 complex.** (a) Architecture of the Mtw1 complex based on ref. [*Hornung et al.*, 2010; *Maskell et al.*, 2010]. (b) Box and whisker plot for proximity ratios quantifying FRET between Spc105p-C or

Mtw1 subunits, and Spc25p-C. The horizontal blue lines of each box represent the 25th and 75th percentile values, and the whiskers display the extreme values. Red line in each box indicates the median; red crosses display outliers. Non-overlapping notches on the box plots signify statistically significant differences in mean values ($p < 0.05$ using the Wilcoxon rank-sum test). The number of measurements for each dataset is indicated at the bottom.

2.3.2 Organization of the Mtw1 complex and Spc105p relative to the Ndc80 complex

In parallel effort, my colleagues established the organization of Ndc80 and Dam1 complexes at the KT-MT interface. I used this as a reference to build the architecture of Mtw1 complex, which connects up Ndc80 complex to the centromere, and Spc105, which forms an essential part of the kinetochore-based SAC machinery. The four-subunit Mtw1 complex incorporates the proteins Dsn1p, Nsl1p, Mtw1p and Nnf1p in equal stoichiometry (Fig. 2.3a). It connects Ndc80 to the centromere via physical interaction between the Mtw1 subunit and the centromeric protein CENP-C [*Westermann et al.*, 2003; *Petrovic et al.*, 2014; *Screpanti et al.*, 2011]. High resolution colocalization data place the C-termini of Mtw1 complex subunits as well as Spc105p within $\approx$ 10 nm of Spc25p-C, a member of the Ndc80 complex (Fig. 2.1c) [*Joglekar et al.*, 2009]. Therefore, I selected Spc25p-C as the reference point to measure the distribution of Mtw1 subunits. Nsl1p-C and Dsn1p-C as well as Spc105p-C are proximal to Spc25p-C, as evidenced by the high FRET between these termini and Spc25p-C (Fig. 2.3b). FRET between Spc25p-C and Nnf1p-C, Mtw1p-C, N-Dsn1p or N-Mtw1p was lower, indicating a larger separation. These data are largely consistent with the subunit organization of the Mtw1 complex predicted by structural studies [*Hornung et al.*, 2010; *Maskell et al.*, 2010].

Lastly, I attempted to localize the N-terminus of Spc105p within the kinetochore. This region is predicted to be highly unstructured, contains the conserved MELT motifs that serve to recruit the SAC proteins at unattached kinetochores [*London et al.*, 2012; *Petrovic et al.*, 2014]. The N-terminus of Spc105p was previously localized proximal to the Ndc80p-C[*Joglekar et al.*, 2009]. However, I did not detect any FRET between the two.

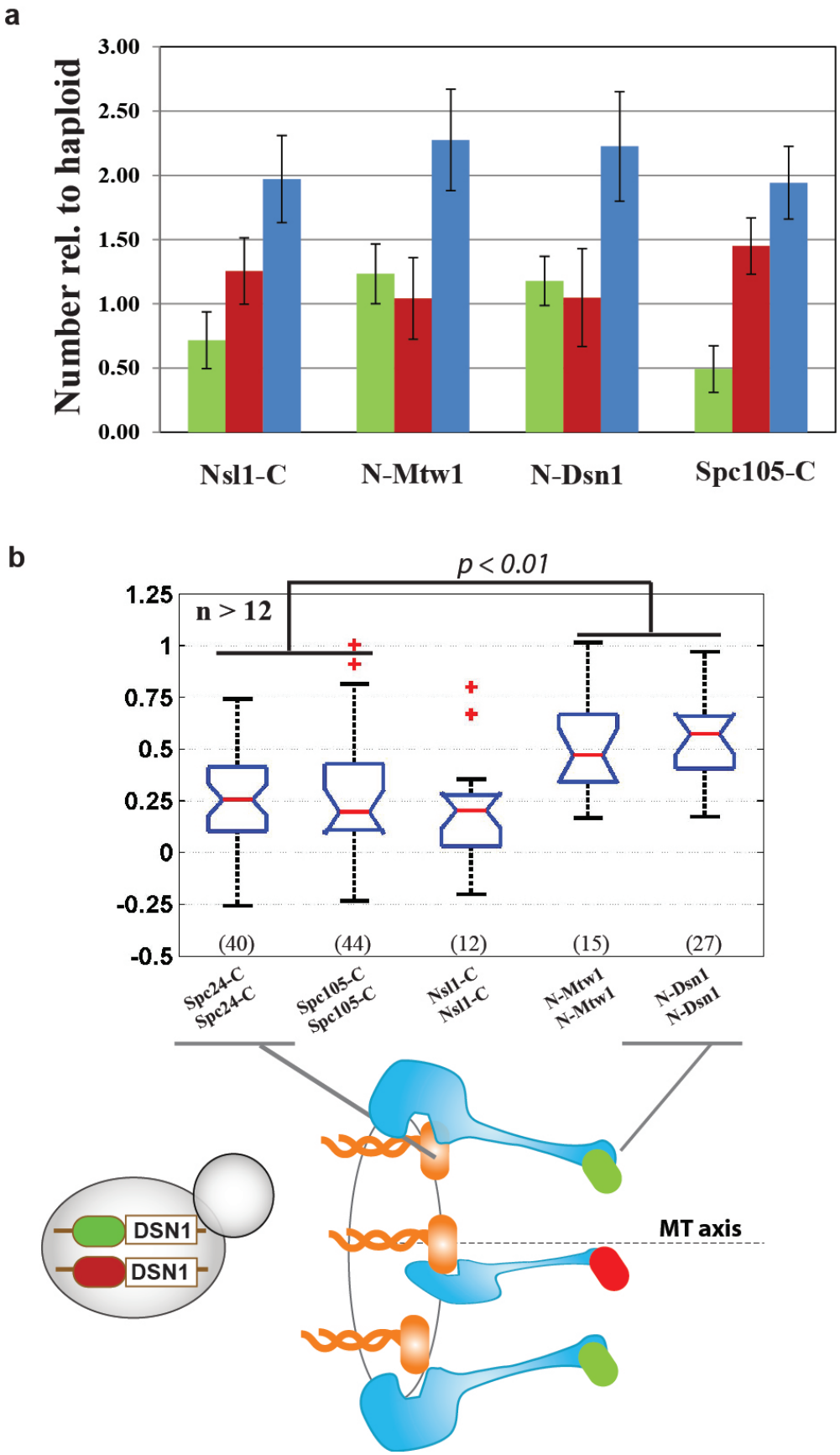
a
Number rel. to haploid
3.00
2.50
2.00
1.50
1.00
0.50
0.00
Nsl1-C
N-Mtw1
N-Dsn1
Spc105-C
b
p < 0.01
n > 12
1.25
1
0.75
0.5
0.25
0
-0.25
-0.5
(40)
(44)
(12)
(15)
(27)
Spc24-C Spc24-C
Spc105-C Spc105-C
Nsl1-C Nsl1-C
N-Mtw1 N-Mtw1
N-Dsn1 N-Dsn1
DSN1
DSN1
MT axis

Figure 2.4: **Distribution of Mtw1 complex around MT lattice.** (a) Relative abundance was calculated as the ratio of average fluorescence from kinetochore clusters in diploid strains expressing GFP- and mCherry-fusions of a protein to the average fluorescence for kinetochore clusters in haploid strains expressing the same subunit fused with either GFP only or mCherry only (mean±s.d. standard deviation calculated using error propagation; [*Bevington and Robinson*, 1969]). The ideal value of this ratio is 1. Since diploid kinetochore clusters carry twice as many molecules as haploid clusters, the addition of the two ratios (Total) should then equal 2. Ideal or close to ideal values for these ratios ensure that the kinetochore clusters contain the maximum possible number of FRET pairs [*Joglekar et al.*, 2013]. (b) FRET between neighboring Spc105 or Mtw1 complex proteins.

2.3.3 Circumferential distribution of Mtw1 subunits around the MT axis

Next, I focused on measuring the circumferential distribution of multiple copies of Mtw1 complex proteins and Spc105p around the MT-axis. For this purpose, I quantified inter-complex FRET in heterozygous diploid strains that express two versions of a selected subunit: one labeled with GFP and the other with mCherry (Fig. 2.4a). The kinetochores in such strains incorporate GFP and mCherry labeled molecules randomly. For accurate comparison of proximity ratios, it is essential that the average number of GFP and mCherry labeled molecules per kinetochore cluster in each strain is equal [*Joglekar et al.*, 2013]. I verified this by comparing the average GFP and mCherry fluorescence per kinetochore cluster in diploid strains with the kinetochore cluster fluorescence in haploid strains that express only GFP or only mCherry labeled subunits (Fig. 2.4a).

In diploid strains, FRET can occur only if adjacent complexes labeled with GFP and mCherry are located within 10 nm. Furthermore, if the neighboring complexes are parallel to and aligned with each other, then FRET will be similar along their entire length of the complex. Modest inter-molecular FRET was detected for Nsl1p-C and Spc105p-C, indicating that at least some of copies of these proteins are located < 10 nm from each other (Fig. 2.4b). The proximity ratios were also indistinguishable from that of Spc24p-C, which is expected from the direct binding between Mtw1 and Ndc80 complex. Surprisingly, inter-complex FRET was significantly higher for both N-Mtw1p and N-Dsn1p indicating a narrower spacing between adjacent copies of these two termini (schematic, Fig. 2.4b).

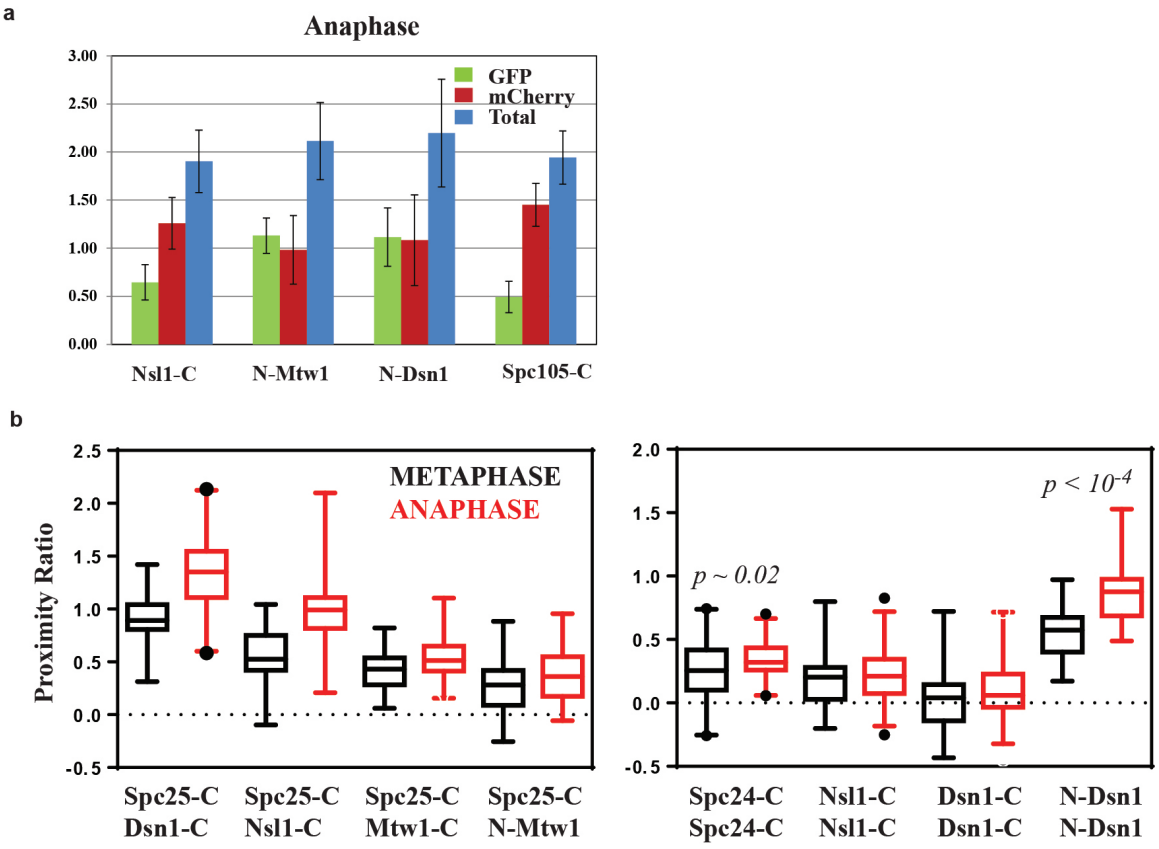

Figure 2.5: **Comparison of FRET measurements between metaphase and anaphase.** (a) Relative abundance measurements as in fig. 2.4a from late anaphase kinetochore clusters. (b) A small, consistent increase in FRET is observed in anaphase for most FRET pairs tested, when compared to metaphase.

2.3.4 Kinetochore subunit organization is maintained in late anaphase/telophase

As the cell cycle transitions from metaphase to late anaphase, Dam1 complex and the centromere-bound CBF3 complex partially dissociate from the kinetochore [*Joglekar et al.*, 2006; *Bouck and Bloom*, 2005]. In this scenario the tension between sister kinetochores is also absent, and these changes can effect substantial changes in kinetochore. Such changes in kinetochore architecture between metaphase and anaphase have also been previously reported [*Joglekar et al.*, 2009]. Comparison of FRET measurements between metaphase and anaphase did not reveal any significant changes in the organization of the tested kinetochore proteins relative to one another. However, the kinetochore was more compact as evidenced by a systematic increase in FRET (Fig. 2.5b).

2.4 Discussion

Combining the FRET and high-resolution colocalization data for Mtw1 complex and Spc105p with that established for Ndc80 and Dam1 complexes provide novel insights into the physiological organization of the kinetochore-MT attachment. We combined these insights with structural data and previously reported protein counts to reconstruct a 3-D visualization of the metaphase kinetochore-MT attachment (Fig. 2.6).

2.4.1 Impact of fluorophore size on FRET measurements

The large size of GFP and mCherry (3 nm diameter x 4 nm height, with fluorophore located at the center) generally discourages the use of these proteins as a FRET pair, where the donor-acceptor separation is the parameter of interest [*Piston*

and Kremers, 2007]. Although this large size can be problematic when using FRET for deducing protein architecture, our experimental design ensures that it has minimal effect on the main conclusions. We used FRET only to compare: (a) proximity between different subunits of the same heteromeric complex and one reference point, or (b) proximity between adjacent copies of subunits of the same heteromeric complex. This design ensures that each experiment involves similar numbers of FRET pairs and differences in proximity ratios result from differences in FRET efficiencies. We also confirmed each key conclusion with multiple measurements using similarly situated kinetochore subunits (by virtue of their known average position or because they belong to the same complex).

We also previously determined that the maturation efficiency of mCherry is only 30-50% relative to GFP [*Joglekar et al.*, 2013; *Padilla-Parra et al.*, 2009]. However, inefficient mCherry maturation is systematic to all the reported measurements, and it only lowers the sensitized emission intensity in all the measurements [*Joglekar et al.*, 2013]. It does not affect the comparison of proximity ratios used here. Therefore, the organization of MT-binding proteins revealed by the FRET data can be used to elucidate protein functions.

2.4.2 Metaphase kinetochore architecture and relevance to SAC signaling

In another part of this work (ref. [*Aravamudhan et al.*, 2014; *Joglekar et al.*, 2013]) not reported here, my colleagues established the architecture of Ndc80 and Dam1 complexes relative to each other and relative to the MT tip. These measurements revealed that adjacent copies of Ndc80 complex are aligned along the length, forming a narrow foot print along MT axis (Fig. 2.6). Multiple copies of Dam1 complex form a ring that is located in the close vicinity of the MT-binding domain of Ndc80

complex.

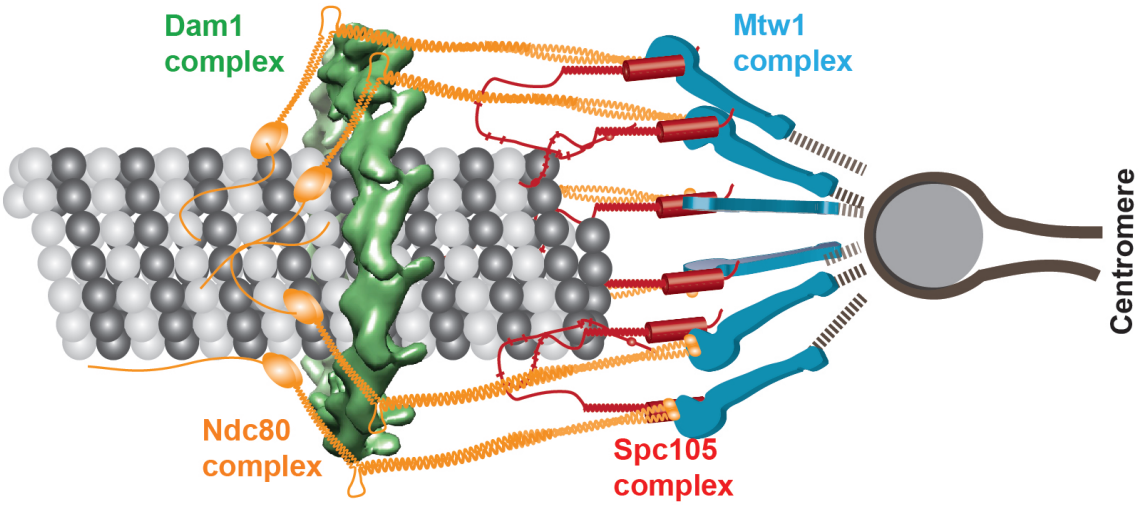

Figure 2.6: **Visualization of the budding yeast kinetochore-MT attachment in metaphase.** Multiple copies of Ndc80 complex are aligned along the MT axis and are not staggered relative to each other. The Dam1 subunits are concentrated close to the MT binding domain of Ndc80p, potentially forming a ring around the MT. The Mtw1 complex forms the connecting link between the MT and converges towards the centromere forming a narrow footprint. Spc105p-C localizes at the junction of Mtw1 and Ndc80 complexes. The exact localization and conformation of the unstructured N-terminus os Spc105p is not known.

Since the Mtw1 complex is physically connected with the Ndc80 complex, the above results suggest that multiple copies of Mtw1 complex and Spc105p are also aligned relative to each other, with Nsl1p-C, Dsn1p-C and Spc105p-C localizing proximal to the Ndc80 complex, and Nnf1p-C, Mtw1p-C, N-Dsn1p and N-Mtw1p localizing away from the Ndc80 complex, pointing towards the centromere. We were not able to localize the N-terminus of Spc105p using FRET. This can be due to two reasons: (1) The N-terminal region of Spc105p is predicted to be unstructured and can possibly assume various positions within the kinetochore, thereby reducing the overall FRET efficiency or (2) Spc105p N-terminus has been shown to bind MTs in other organisms [*Espeut et al.*, 2012]. Such MT-binding may also organize the N-terminus away from Ndc80p-C as the latter is displaced by $\approx$ 10 nm from the MT lattice [*Aravamudhan et al.*, 2014].

The circumferential distribution of Ndc80 and Mtw1 complexes cannot be determined directly. However, detectable inter-complex FRET in both cases suggests that it cannot be symmetric, because symmetric placement of 8 Ndc80 complexes over the MT lattice $>$ 25 nm in diameter translates into an inter-complex spacing $>$ 10 nm. As the simplest case, we depict Ndc80 and the connected Mtw1 complexes as randomly distributed around the MT circumference (Fig. 2.6).

The architecture of the metaphase kinetochore presented here satisfies the SAC. In other words, this architecture precludes the SAC biochemistry that can happen at unattached kinetochores. Understanding how attachment accomplishes this will provide insights into the mechanism of SAC silencing at attached kinetochores and forms the focus of the next chapter. Two aspects of this architecture are highly relevant to SAC functionality: (1) the MT-binding domain of Ndc80p will be the best sensor for MT-attachment as it directly binds MTs. Accordingly, it also plays an essential, yet

unknown, role in SAC signaling. A change in position, conformation or biochemical activity of this domain upon MT binding can serve in precluding or silencing SAC signaling; (2) N-terminus of Spc105p provides the platform at the kinetochore for SAC signaling. Again, the presence of MT can change the position, conformation or access of this domain for SAC protein binding, in order to silence the SAC.

Knowing the exact architecture of the metaphase kinetochore allows us to test the influence of this architecture on the activity of SAC proteins. The architecture presented here also reveals that equivalent positions in multiple copies of the different kinetochore proteins are aligned along MT axis and therefore SAC proteins binding to equivalent points should also be aligned relative to each other. The architecture presented here, therefore, serves as a frame work to test the position-dependent functionality of SAC proteins within the kinetochore.

CHAPTER III

The kinetochore encodes a mechanical switch to disrupt spindle assembly checkpoint signaling

3.1 Introduction

3.1.1 What is sensed by the SAC machinery? Tension vs. attachment

The aim of the SAC is to stall cell cycle progression in the absence of 'correct' connections between chromosomes and spindle MTs that will allow accurate chromosome segregation. This requires amphitelic attachments, where the sister chromatids need to connect to MTs from opposite poles of the spindle. Such amphitelic attachments biorient the kinetochores and also generate tension across the sister chromatids as a consequence of MT dynamics, like in a tug-of-war situation. However, if both sisters make attachments to the same pole (syntelic), cells must have a way to detect these tensionless attachments and resolve them before the cell cycle proceeds. Whether the SAC exclusively identifies unattached kinetochores or it also recognizes the lack of tension in the presence of improper attachments has been a source of debate in the field [*Nezi and Musacchio*, 2009; *Khodjakov and Pines*, 2010].

To examine whether the SAC senses both tension and attachment, it becomes imperative to isolate or generate either condition independently. But generating such a system is complicated by the fact that tension and attachment are inherently coupled. The absence of tension destabilizes kinetochore-MT attachments, while tension selectively stabilizes attachments [*King and Nicklas*, 2000; *Akiyoshi et al.*, 2010]. Furthermore, in order to correct syntelic attachments, the incorrect attachments should be selectively relieved, in order to provide the kinetochores with a chance to make the right attachments. Therefore, unattached kinetochores become necessary intermediates in establishing amphitelic attachments. This brings back the question of whether these unattached intermediates act as unique beacons for the SAC or whether the lack of tension can also directly activate the SAC.

Classic experiments by Nicklas and Koch demonstrated that the absence of tension across sister kinetochores in monotelic attachments can cause cell cycle delay. By artificially applying tension across the sisters through micromanipulation, they were able to show that tension across the sisters is required for cell cycle progression in meiotic insect cells [*Li and Nicklas*, 1995; *Nicklas and Koch*, 1969]. On the other hand, the major evidence for the SAC exclusively sensing attachment and not tension came from experiments in budding yeast. Biggins and colleagues showed that the absence of tension created unattached kinetochores through the action of Aurora B/Ipl1 [*Biggins and Murray*, 2001]. This kinase has a well-established role in error correction and acts on multiple kinetochore substrates, Ndc80 and Dam1 complexes to regulate attachments. The unattached kinetochores thus generated in the absence of tension were shown to activate the SAC. Conversely, inhibition of Aurora B led to missegregation in the absence of tension; the SAC could not detect tension defects and stall the cell cycle. However, creating unattached kinetochores using the MT destabilizing drug nocodazole was sufficient to activate the SAC, even in the absence

of Aurora B activity. These results provided strong support to the model that the SAC senses only attachments, and the lack of tension feeds into this pathway by creating unattached kinetochores. However, proving this idea in higher eukaryotes gets complicated due to the requirement for Aurora B in SAC signaling, even in the absence of attachments [*Santaguida et al.*, 2011; *Kuijt et al.*, 2014; *Ballister et al.*, 2014]. Therefore the question still remains in these systems. However, for the purpose of this thesis, where budding yeast is employed as the model system, I will focus on the mechanisms that act downstream from the error correction pathway, in sensing unattached kinetochores to generate the SAC signal.

3.1.2 Generating the SAC signal

To achieve cell cycle arrest, the SAC communicates with the cell cycle machinery through two primary targets - Cyclin B and Securin. Cyclin B is the mitotic Cdk1 activator and its degradation promotes mitotic exit [*Coudreuse and Nurse*, 2010]. Securin sequesters separase, an enzyme that cleaves cohesin, which holds the sister chromatids together after duplication [*Nasmyth and Haering*, 2009]. Both cyclinB and securin are targeted for destruction by the ubiquitin ligase activity of the Anaphase Promoting Complex (APC). In the presence of unattached kinetochores, active SAC signaling serves to sequester Cdc20, the activating subunit of APC in the form of Mitotic Checkpoint Complex (MCC), and this prevents anaphase onset. When all the kinetochores in the cell form attachments, the SAC gets satisfied and the MCC is dissembled to release Cdc20, which activates APC and targets Cyclin B and Securin for degradation. This allows mitotic exit and sister chromatid separation into the dividing daughters.

The SAC effector, MCC is generated through a biochemical cascade that is pro-

moted only at unattached kinetochores. This kinetochore-based biochemical cascade that generates the SAC signal is well-understood (Fig. 3.2a). Members of the SAC cascade were first identified through genetic screens in budding yeast [*Li and Murray*, 1991; *Hoyt et al.*, 1991]. The kinase activity of Mps1 and Ipl1 (Aurora B) form essential components that trigger and regulate the SAC signaling, and the PP1 phosphatase counteracts the kinase activity and aids in silencing the SAC once MT attachments form [*Funabiki and Wynne*, 2013]. This phosphoregulation controls the assembly of SAC proteins: Bub1, Bub3, Mad1, Mad2 and Mad3 (BubR1) at the kinetochore. A lot of these conserved proteins are known to localize to kinetochores only in the absence of MT attachment and are removed soon after attachments form [*Howell et al.*, 2004]. Once assembled at the unattached kinetochore, the SAC proteins act together to generate the inhibitory signal.

The interaction partners of SAC proteins at the kinetochore have been established over the last 5 years through biochemical and structural efforts from multiple groups. The kinetochore proteins, Ndc80 and Spc105 have emerged as the key regulators of SAC signaling at the kinetochore [*Bollen*, 2014; *Martin-Lluesma et al.*, 2002]. Two independent studies identified conserved motifs in the N-terminus of Spc105 with the amino acid sequence 'MELT' to recruit the Bub3-Bub1 complex, only when phosphorylated by Mps1 [*London et al.*, 2012; *Shepperd et al.*, 2012; *Kiyomitsu et al.*, 2007]. Further structural data revealed that the conserved MELT motifs in Spc105 upon phosphorylation by Mps1 directly interact with Bub3-Bub1 complex [*Primorac et al.*, 2013]. Further phosphorylation of Bub1 at multiple sites by Mps1 allows subsequent recruitment of Mad1-Mad2 heterodimeric complex through interaction with the RLK motif in Mad1, at least in budding yeast [*London and Biggins*, 2014]. In vertebrates, the interaction of Mad1 with the kinetochore requires further elements and the regulation of these interactions remain unknown [*Burke and Stukenberg*, 2008;

Moyle et al., 2014].

Mad1 and Mad2 form a tight hetero-tetramer in the cell and are normally associated with the nuclear envelope. A pool of Mad1-Mad2 complex translocates to unattached kinetochores [*Howell et al.*, 2004]. It is known that Mad1 gets heavily phosphorylated by Mps1 during the SAC and this phosphorylation may serve in releasing the nuclear pore associated Mad1 and/or aid its binding to the kinetochore. Mad1-Mad2 complex, once assembled at the kinetochore, catalyzes the generation of a conformational isomer of Mad2 called closed-Mad2 from the diffusible cellular pool of an open conformer of Mad2 [*Vink et al.*, 2006; *De Antoni et al.*, 2005; *Sironi et al.*, 2002]. The closed-Mad2 forms the primary inhibitory signal generated at the kinetochore, which along with Bub3 and Mad3 sequesters Cdc20 in MCC. It is not clear what confers the catalytic activity to Mad1-Mad2 complex only at the kinetochore during mitosis. In fact, the Mad1-Mad2 complex drives MCC generation even from attached kinetochores when artificially localized [*Ballister et al.*, 2014; *Kuijt et al.*, 2014]. However, this also requires the activity of Mps1 and Ipl1, and other SAC proteins Bub1 and Bub3. This provides a clue that the concentration of all the above components only at unattached kinetochores is essential in catalyzing the formation of closed Mad2. This concentration of SAC proteins only at unattached kinetochores also couples the SAC signal generation with the attachment status of the kinetochore. This specificity becomes important because aberrant generation of MCC can compromise the viability of cells. However, what couples the attachment status of the kinetochore with the assembly and function of SAC proteins has remained an open question.

Early cell biological observations that MT attachment generates tension across sister chromatids led to the hypothesis that a mechanical change within the kineto-

chore induced by the tension-generating, end-on MT attachment controls the SAC signaling [*McIntosh*, 1991]. Concurrent changes in the state of SAC signaling and the nanoscale separations between multiple kinetochore proteins support this hypothesis [*Maresca and Salmon*, 2009; *Wan et al.*, 2009; *Uchida et al.*, 2009]. However, the causative link between specific changes in kinetochore architecture induced by MT attachment and the disruption of specific steps in SAC signaling is missing. This is mainly because the kinetochore is a highly complex machine that contains multiple copies of more than 60 different proteins [*Santaguida and Musacchio*, 2009]. A change in the structure, conformation, and/or architecture of any of these proteins induced by MT attachment can affect SAC signaling. Consequently, the molecular basis for the mechanosensitivity of SAC signaling is unknown.

Here we investigate how the architecture of the kinetochore-MT attachment in the budding yeast Saccharomyces cerevisiae disrupts SAC signaling. We find that the phosphorylation of of the kinetochore protein Spc105 by Mps1 kinase is both necessary and sufficient to initiate the SAC cascade. End-on kinetochore-MT attachment restricts Mps1 kinase activity to the outer kinetochore and maintains the phosphodomain of Spc105 in the inner kinetochore to disrupt this crucial first step in the SAC cascade to silence the SAC.

3.2 Results

3.2.1 Mps1, when artificially localized to the kinetochore, phosphorylates Spc105 and activates the SAC

MT attachment to the kinetochore may silence the SAC by promoting the dissociation of SAC proteins from the kinetochore (Figure 3.2a). If this is true, then persistent localization of key SAC proteins at the kinetochore should constitutively

activate the SAC. To test this hypothesis, we used rapamycin-induced dimerization of 2xFkbp12 and Frb to artificially localize or anchor key phosphoregulators and SAC proteins [*Haruki et al.*, 2008]: Mps1, Ipl1 (Aurora B), Glc7 (PP1), or Mad1 within the kinetochore (Figure 3.2b). In the absence of rapamycin, each Frb-tagged protein retained its normal cellular distribution.

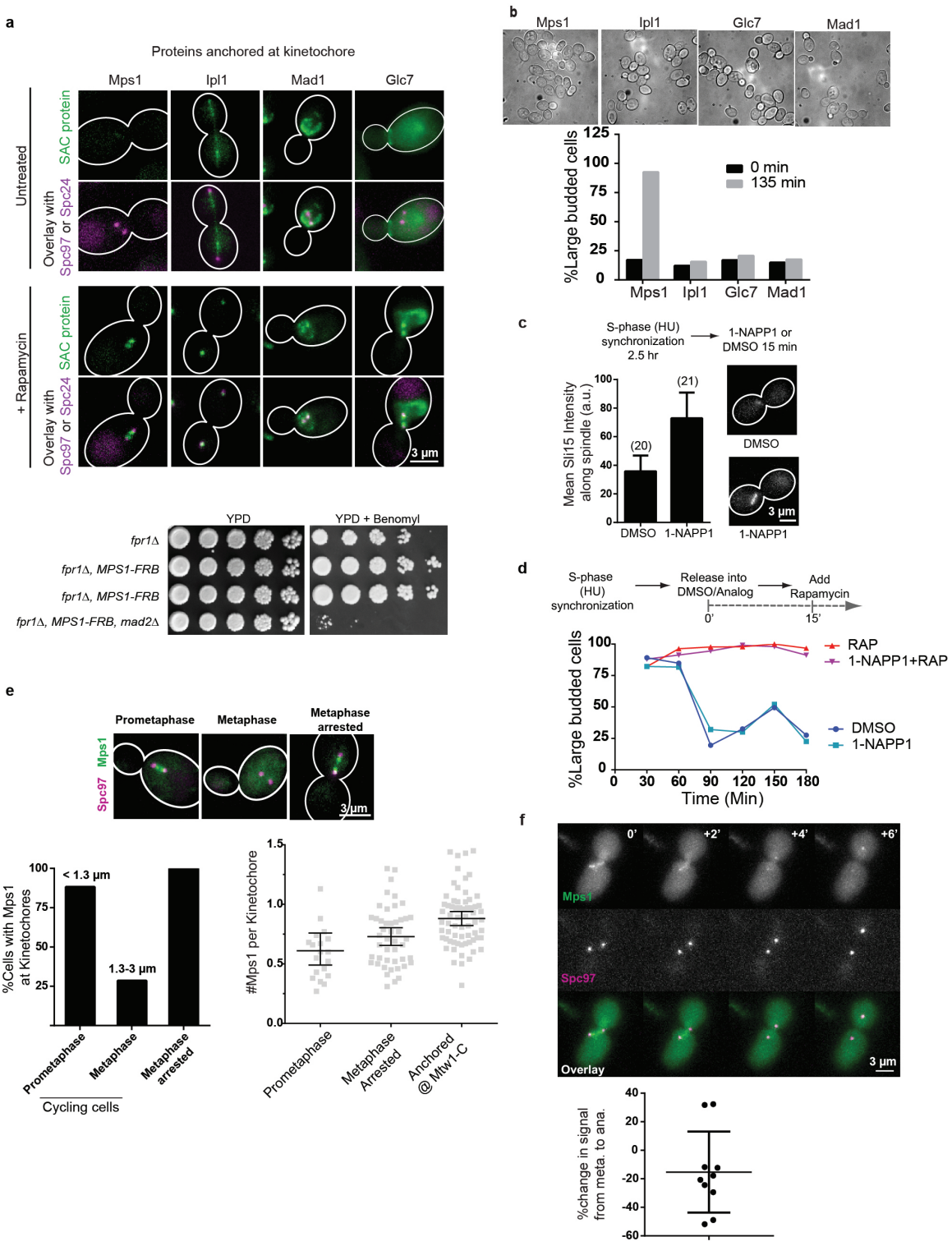

Figure 3.1: **Effects of anchoring key SAC regulators to Mtw1-C on the cell cycle** (a) Top: Representative images display the expected localization of SAC

proteins tagged with Frb-GFP in untreated cells and one hour after the addition of rapamycin. Bottom: Benomyl sensitivity of indicated strains.

(b) Representative transmitted light micrographs of four strains treated with rapamycin for 135 minutes to anchor Mps1, Ipl1, Mad1, or Glc7, at Mtw1-C. The bar graph displays the percentage of large-budded in each case averaged from two independent experiments (more than 50 cells were scored in each trial.

(c) Effect of the ATP analog 1-NAPP1 on the localization of the Ip1l substrate Sli15-GFP in cells expressing ipl1-as6, an analog-sensitive allele of the Ipl1 kinase67. Representative pre-anaphase cells expressing Sli15-GFP are shown on the right. Quantification of Sli15-GFP fluorescence on the spindle (mean ± s.d. from a single experiment; number of cells scored are displayed at the top) shown on the left. Consistent with published results67, spindle localization of Sli15-GFP significantly increased following 1-NAPP1 treatment indicating that the analog inhibits ipl1-as6. (d) Cell cycle kinetics following the release of S-phase synchronized cells into media containing 1-NAPP1 and rapamycin. Blocking ipl1-as6 activity did not have any effect on SAC activation induced by Mps1 anchored at Mtw1-C. The experiment was performed once and more than 70 cells were scored for each time point. (e) Bar graph: Frequency of prometaphase and metaphase cells with kinetochore-localized Mps1 (representative micrographs displayed at the top; 18, 12 and 45 cells were analyzed, from left to right). Spindle length was used to classify cells as prometaphase or metaphase cells. Scatter plot (mean ± 95% confidence interval; n = 21, 46 and 66 kinetochore clusters from left to right) displays the abundance of kinetochore-localized Mps1-Frb-GFP in prometaphase, metaphase-arrested cells (by repressing CDC20), and when it is anchored to Mtw1-C in heterozygous diploid strains. Each experiment was performed once. (f) Quantification of Mps1 localization to kinetochores soon after release from metaphase compared to that in anaphase (n = 10 from one experiment). Micrographs on the right show localization of Mps1 relative to spindle pole bodies over a period

of 6 minutes during the metaphase to anaphase transition.

Addition of rapamycin to the culture media rapidly anchored it to the kinetochore subunit tagged with 2xFkbp12 (Figure 3.2c, right and Figure 3.1a).

Mps1 anchored at Mtw1-C in this manner led to the accumulation of large-budded cells that were arrested in metaphase (Figure 3.2d-e). The kinetochores in these cells recruited both Bub1 and Mad1, indicating that the arrest was mediated by the SAC (Figure 3.2d). These observations are consistent with previous reports that Mps1 fused to kinetochore proteins activates the SAC [*Jelluma et al.*, 2010; *Ito et al.*, 2012]. Other SAC proteins tested: Ipl1, Mad1, and Glc7, did not delay the cell cycle when anchored to Mtw1-C (Figure 3.1b). The phosphorylation of the kinetochore protein Spc105 at one or more of its conserved 'MELT motifs was necessary for the anchored Mps1 to activate the SAC [*London et al.*, 2012] (Figure 3.2e). Importantly, these effects did not require the kinase activity of Ipl1, suggesting that the anchored Mps1 did not activate the SAC indirectly by disrupting either MT attachment or force generation [*Pinsky et al.*, 2006] (Figure 3.1c-d). This observation is consistent with data from other organisms and with the dispensability of Ipl1 for SAC signaling in budding yeast [*Biggins et al.*, 1999; *Heinrich et al.*, 2012]. Thus, anchoring Mps1 to the kinetochore is sufficient for constitutive SAC signaling.

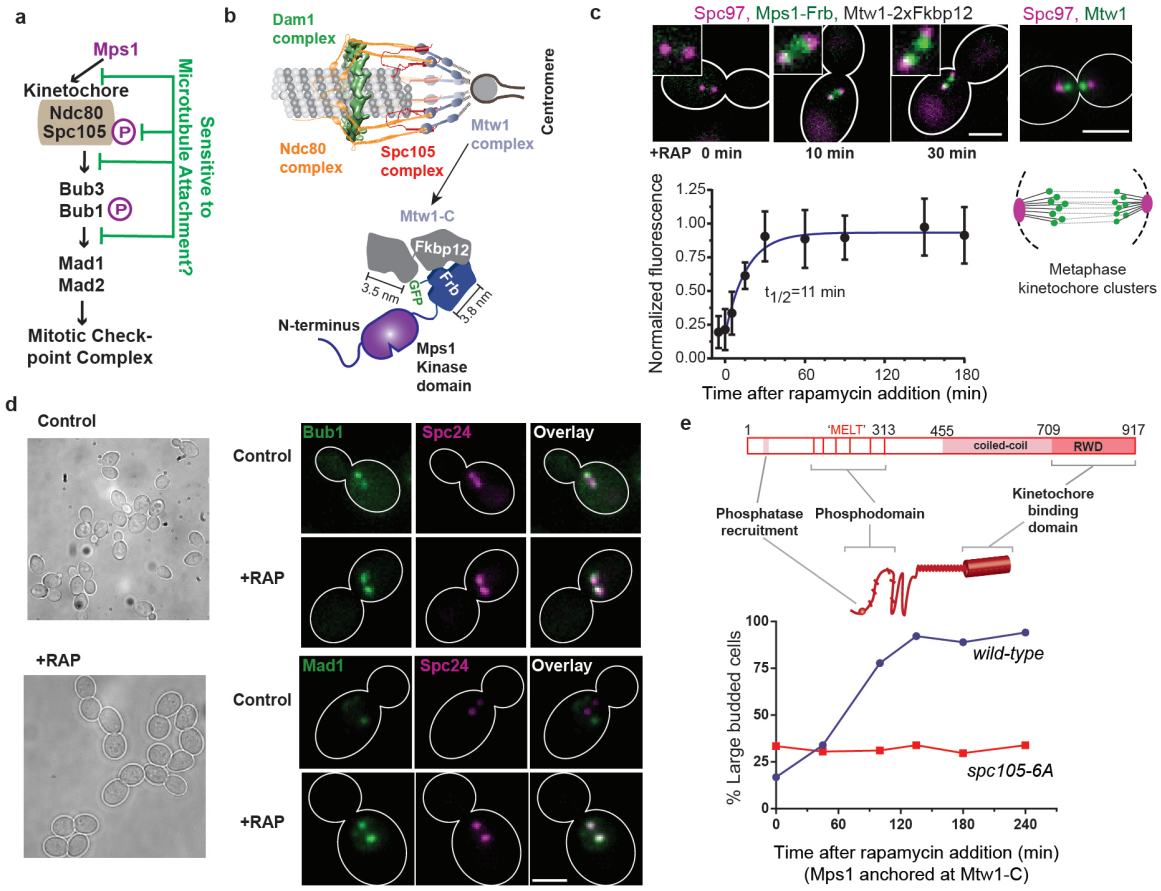

Figure 3.2: **Cell cycle effects of anchoring Mps1 to the kinetochore using rapamycin-induced dimerization :** (a) The steps in the kinetochore-based signaling cascade of the SAC (magenta Ps indicate Mps1-mediated phosphorylation) that may be disrupted by MT attachment. (b) Top: Protein architecture of the metaphase kinetochore-MT attachment [*Aravamudhan et al.*, 2014]. Bottom: Schematic of the rapamycin-induced dimerization technique used to anchor Mps1 to the carboxyl terminus of Mtw1 (Mtw1-C). (c) Top: Micrographs show the anchoring of Mps1-Frb-GFP at Mtw1-C (time after rapamycin addition indicated; scale bar ≈ 3 μm). The stereotypical distribution of kinetochores in metaphase visualized with Mtw1-GFP, spindle poles visualized using Spc97-mCherry is shown in the right. Cartoon underneath depicts the metaphase spindle morphology. Bottom: kinetics of rapamycin induced anchoring of Mps1-Frb-GFP to Mtw1-C. Error bars represent mean $\pm$ s.d.

of n = 10, 11, 8, 13, 14, 18, 24, 16 and 11 kinetochore clusters analyzed from -5 to 108 min. (d) Left: Representative transmitted-light images before and 1 hour after the addition of rapamycin to anchor Mps1 at Mtw1-C. Right: Localization of Bub1-GFP and Mad1-GFP, and kinetochores (visualized by Spc24-mCherry) in untreated cells (control) and in cells that have Mps1 anchored at Mtw1-C (+RAP). Scale bar $\approx$ 3 μm. (e) Top: Domain organization of Spc105. The end-to-end length of the unstructured domain of Spc105 (amino acids 1-455) is predicted to be 11.7 $\pm$ 5 nm (mean $\pm$ s.d. using the worm-like chain model [*Zhou*, 2004]). The maximum length of it -helical region (a.a. 455-709) is 38 nm (3.6 amino acids per turn/ 0.54 nm pitch). The predicted kinetochore-binding domain (RWD*) is $\approx$ 6 nm long [*Petrovic et al.*, 2014]. Other than these estimated dimensions, the structure and organization of Spc105 is unknown. Therefore, the depiction is not drawn to scale. The six Mps1 phosphorylation sites (consensus sequence MELT) are depicted as bars. Bottom: Cell cycle progression of asynchronous cells with the indicated genotypes observed upon anchoring Mps1 at Mtw1-C. Accumulation of large budded cells indicates mitotic arrest. Plotted points represent the average values calculated from 2 independent experiments. More than 50 cells were scored for each time point.

3.2.2 SAC proteins that act downstream from Mps1 can function within attached kinetochores

The above experiments were performed in asynchronous yeast cultures. Consequently, we could not ascertain whether the anchored Mps1 activated the SAC mostly in prometaphase, before all kinetochores attach to MTs, or if Mps1 can re-activate the SAC when anchored within stably attached kinetochores. To test this, we repressed CDC20, the gene that encodes the activating subunit of the Anaphase Promoting Complex (APC), to prevent yeast cells from entering anaphase even after all the kinetochores were attached and the SAC was satisfied [*Yeong et al.*, 2000]. We anchored Mps1 at Mtw1-C in such cells, released them from the arrest by inducing CDC20 expression, and then monitored cell cycle progression (Figure 3.3a). We found that cells that had Mps1 anchored at Mtw1-C underwent a persistent cell-cycle arrest, whereas control cells completed anaphase within 20 minutes (Figure 3.3a). Thus, Mps1 can re-activate the SAC, when it is anchored to kinetochores with stable MT attachments.

These results also show that SAC proteins downstream from Mps1 can bind to and function from attached kinetochores. It is possible that the anchored Mps1 facilitates SAC protein binding by changing the overall organization of the kinetochore. However, we did not detect significant changes when we compared the nanoscale separation between key kinetochore domains in metaphase and rapamycin-treated cells using high-resolution colocalization (Figure 3.3b). Even if architectural changes that facilitate SAC protein binding do occur, they can do so when the kinetochore is attached. Based on these data, we concluded that MT attachment to the kinetochore must hamper either Mps1 localization to the kinetochore or its kinase activity in order to silence the SAC.

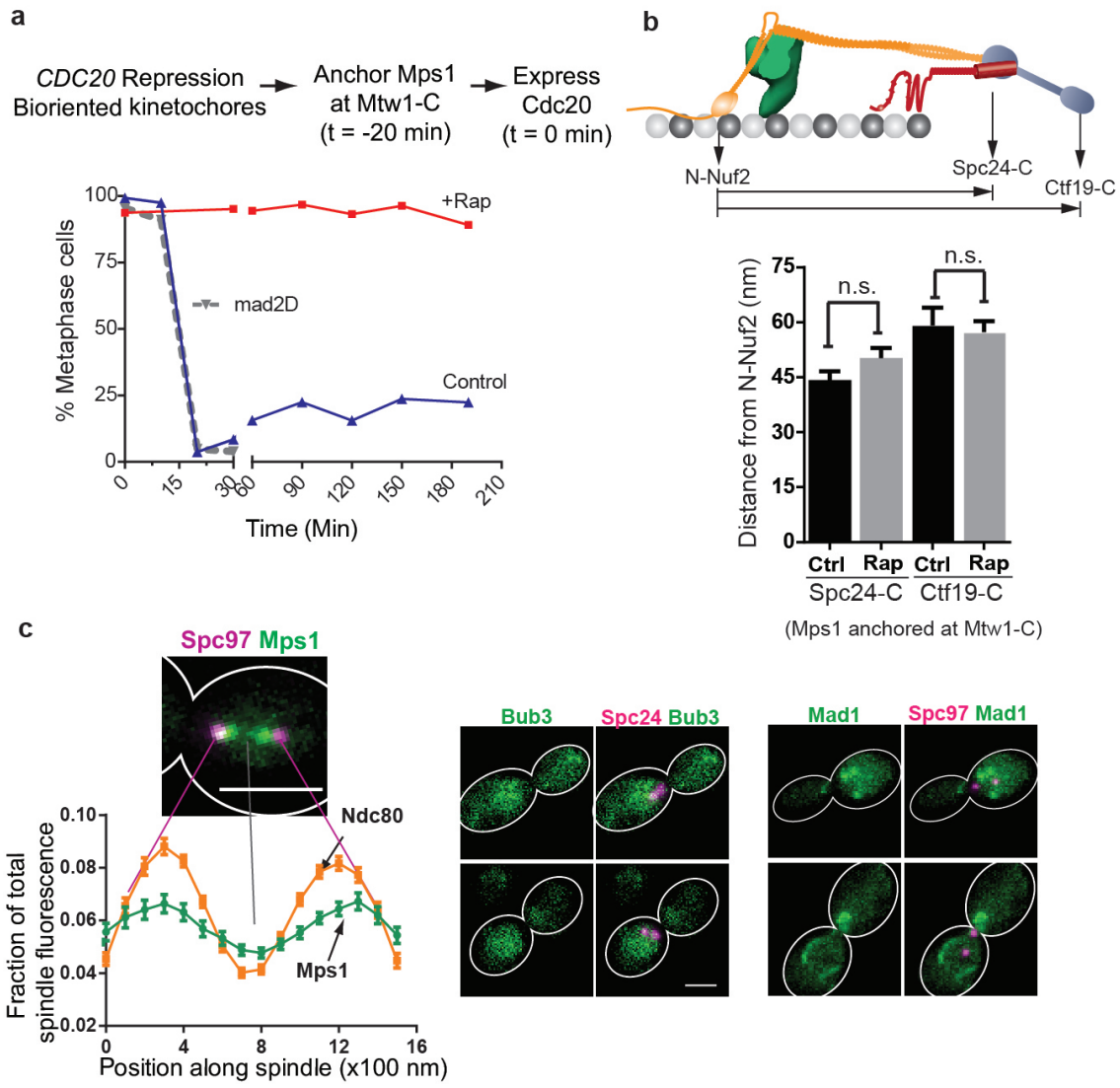

Figure 3.3: **Testing the sensitivity of SAC signaling steps to the attachment status of the kinetochore.** (a) Cell cycle progression of three different strains following release from metaphase arrest (methodology indicated at the top, see Methods for details). Solid lines indicate cell cycle progress of a strain expressing Mtw1-2xFkbp12 and Mps1-Frb released into media with (red) or without (blue) rapamycin. The dotted gray line indicates cell cycle progression of a mad2 strain similarly released from metaphase arrest. Plotted points represent the average values calculated

from 2 independent experiments. (b) Separation between the centroids of fluorescently labeled kinetochore proteins along the spindle axis obtained by high-resolution colocalization in unperturbed metaphase cells (ctrl.) and rapamycin treated cells (rap. rapamycin added to anchor Mps1 at Mtw1-C; mean ± s.e.m.; n = 61, 49, 19, 42 cells were analyzed (from left to right). Data were pooled from 2 independent experiments. n. s. not significant, p-value > 0.05 using Mann-Whitney test). (c) Left: Fractional intensity distributions of Mps1-Frb-GFP (that autonomously localizes along the spindle in the absence of rapamycin) and Ndc80-GFP along the spindle in cells arrested in metaphase using CDC20 repression (spindle pole bodies visualized using Spc97-mCherry). Error bars represent s.e.m. from n = 38 and 57 cells for Mps1 and Ndc80, respectively. The experiment was repeated twice and graph presents mean data pooled from 2 independent experiments. Right: Bub3 and Mad1 do not localize to kinetochores under the same conditions. Mad1 puncta correspond to its known localization to the nuclear envelope [*Scott et al.*, 2005]. Scale bar ≈ 3 μm.

3.2.3 Endogenous Mps1 binds to attached kinetochores

MT attachment may inhibit Mps1 function by simply promoting its dissociation from the kinetochore [*Jelluma et al.*, 2010]. Indeed, Mps1 gradually disappears from the kinetochore clusters as yeast cells progress from prometaphase to metaphase (Figure 3.1e). However, Mps1 is targeted for degradation by the APC [*Palframan et al.*, 2006]. This process may contribute to the disappearance of Mps1 either directly or indirectly. Consistent with this hypothesis, when we inactivated the APC using CDC20 repression, Mps1-Frb-GFP autonomously localized to attached kinetochores (Figure 3.3c, left). Importantly, this autonomously-localized Mps1 did not activate the SAC, because both Bub3 and Mad1 were absent from the kinetochores (Figure 3.3c, right). Furthermore, these cells entered anaphase without any detectable delay upon release from the metaphase block (Figure 3.3a, dotted gray line). Finally, Mps1 was present at the kinetochore even as these cells entered anaphase (Figure 3.1f). Thus, the removal of Mps1 from the kinetochore is not necessary for either SAC silencing or anaphase onset.

It is notable that the Mps1 molecules that autonomously localize to attached kinetochores do not activate the SAC, but a similar number of Mps1 molecules anchored at Mtw1-C activate it constitutively (Figure 3.1e). The inability of the autonomously localized Mps1 to activate the SAC could be due to: (a) its inability to reach and phosphorylate Spc105 from its endogenous binding position in the kinetochore, (b) the inhibition of the kinetochore-bound Mps1 kinase, or (c) the up-regulation of Glc7 phosphatase activity in attached kinetochores [*Rosenberg et al.*, 2011; *Pinsky et al.*, 2009]. Up-regulation of Glc7 activity for SAC silencing is unlikely to be the main mechanism, because Glc7 is not necessary for anaphase onset [*Pinsky et al.*, 2009]. Therefore, we investigated how MT attachment affects Mps1 kinase activity within the kinetochore.

3.2.4 The ability of Mps1 to activate the SAC depends on its position within the kinetochore

We first tested whether the binding position of Mps1 within the kinetochore can affect its ability to phosphorylate Spc105 and initiate SAC signaling. In metaphase, the budding yeast kinetochore spans ≈ 80 nm, from the N-terminus of Ndc80 to the centromeric nucleosome [*Joglekar et al.*, 2009]. It contains ≈ 8 copies of Ndc80 complex and Spc105 molecules distributed with an average inter-molecular spacing of ≈ 8 nm around the MT circumference [*Aravamudhan et al.*, 2013; *Joglekar et al.*, 2006], and with little intermolecular staggering along the length of the MT [*Aravamudhan et al.*, 2014] (Figure 3.2b). This architecture suggests that the proximity of Mps1 to Spc105 along the length of the kinetochore can affect its ability to phosphorylate Spc105.

Rapamycin induced dimerization must stably anchor and confine Mps1 at specific kinetochore positions in order to reveal its position-specific activity. We determined this to be the case using three measurements (Figure 3.4a-c). First, we found that the anchoring was stable, as indicated by negligible turn-over of Mps1-Frb-GFP anchored at Ndc80-C (Figure 3.4a). Although this high stability is ideal for studying position-specific activity, it is likely to be non-physiological [*Howell et al.*, 2004]. Second, Frster Resonance Energy Transfer (FRET) measurements suggested that the anchored protein is likely confined within a 10 nm region around the anchoring point (Figure 3.4b). Finally, the total number of molecules anchored within the kinetochore was determined by the abundance of the anchored protein [*Ghaemmaghami et al.*, 2003] and also its kinetochore anchor [*Aravamudhan et al.*, 2013] (Figure 3.4c). For low abundance proteins such as Mps1 and Ipl1, the entire nuclear pool was anchored at the selected kinetochore position.

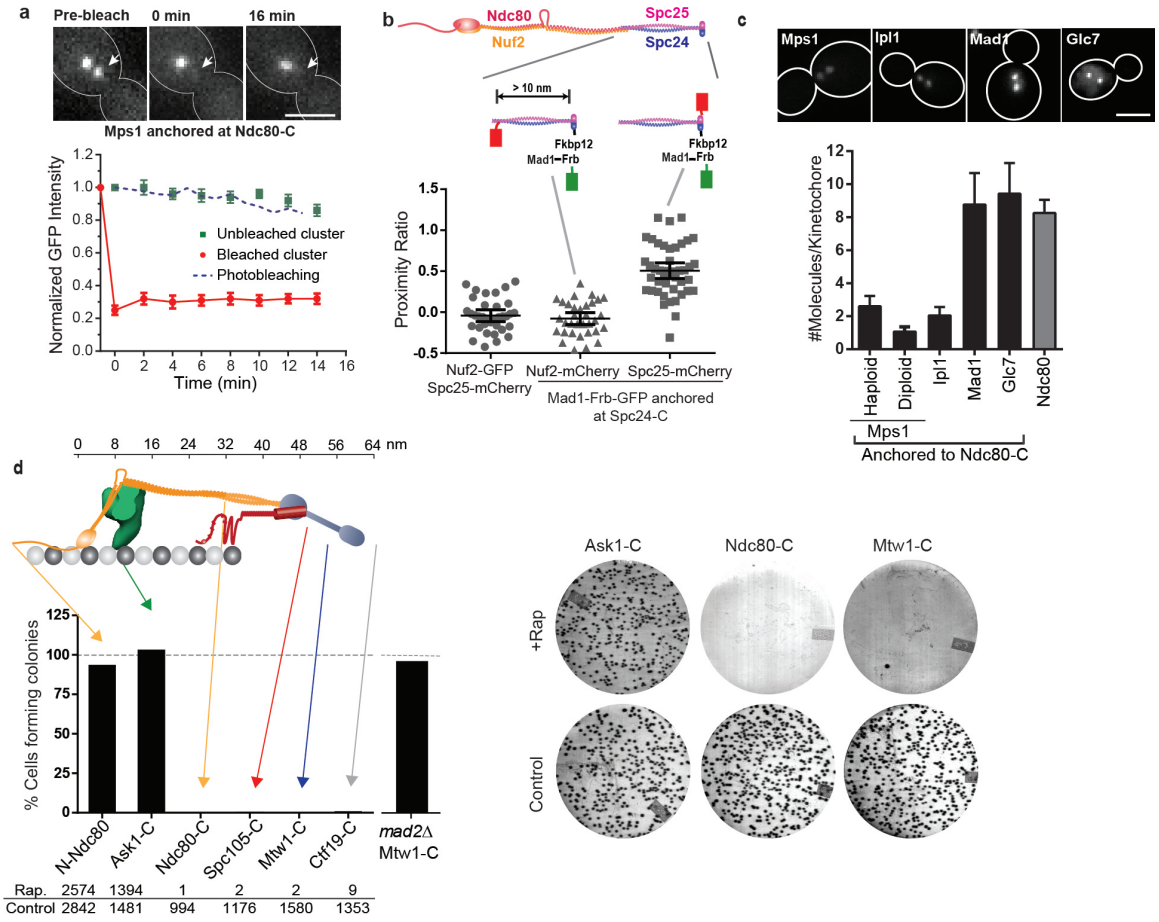

Figure 3.4: **The ability of Mps1 to activate the SAC depends on its position in the kinetochore.** (a) Fluorescence recovery after photobleaching of Mps1-frb-GFP anchored at Ndc80-C (red circles), and loss of anchored protein from the unbleached cluster (green squares). Blue dashed line displays the expected rate of photobleaching as a result of imaging determined in cells expressing Ndc80-GFP (mean ± s.e.m. from n = 8 and 11 clusters for bleached and unbleached clusters, respectively; data pooled from 2 independent experiments). Scale bar ≈ 3 μm. (b) Top: Structure of Ndc80 complex and the positions of fluorescent tags used for FRET. Scatter plot: Proximity ratio, which is directly proportional to the FRET efficiency [*Joglekar et al.*, 2013], for FRET between Spc25-mCherry or Nuf2-mCherry and Mad1-Frb-GFP anchored to Spc24-C (mean ± 95% confidence interval from n = 35, 33 and 44

kinetochore clusters analyzed, from left to right. The experiment was repeated twice and graph presents mean data pooled from 2 independent experiments). Proximity ratio is defined as the acceptor fluorescence resulting from FRET normalized by the sum of direct excitation of mCherry on exciting GFP and GFP emission bleed-through into the mCherry imaging channel [*Joglekar et al.*, 2013]. FRET between the anchored donor, Mad1-Frb-GFP, and the acceptor, Spc25-mCherry, was readily detected, but it was absent when the mCherry was fused to Nuf2-C. Spc25-C is $<$ 3 nm away [*Wei et al.*, 2006] from Spc24-C, where the donor is anchored, whereas Nuf2-C is $>$ 10 nm away [*Wei et al.*, 2005]. We used Mad1, rather than Mps1, in this experiment to ensure that the number of donors is equal to the number of acceptor molecules (either Spc25-mCherry or Nuf2-mCherry, see (c) below) for accurate FRET quantification [*Joglekar et al.*, 2013]. (c) Number of protein molecules anchored at Ndc80-C, measured 30 min after rapamycin addition (mean $\pm$ s.d. from n = 25, 33, 29, 20, 41, and 30 kinetochore clusters from left to right. The experiment was performed once). Scale bar $\approx$ 3 μm. (d) Top: The organization of yeast kinetochore proteins along the MT axis [*Joglekar et al.*, 2009; *Aravamudhan et al.*, 2014]. The N-terminal half of Spc105 is not drawn to scale. Bottom: Bar graph shows the number of colonies formed on rapamycin-containing plates relative to control plates. The experiment was repeated at least twice and the cumulative number of colonies scored is displayed below the graph. Right: Representative photographs of plates for three strains.

We constitutively anchored Mps1 at six distinct positions selected to sample the 80 nm length of the kinetochore-MT attachment (Figure 3.4d, top). To assess the effects of anchoring Mps1 on the cell cycle, we plated an equal number of cells on control plates and on plates containing rapamycin, and compared the number of colonies formed in each case (Figure 3.4d, right). We performed these experiments in heterozygous diploids with a wild type copy of Mps1, because Mps1 activity is also essential for other cellular functions [*Liu and Winey*, 2012]. Even though the wild-type, diffusible Mps1 provides these essential functions, it is not required for SAC activation (Figure 3.5a-b). Furthermore, haploids expressing only Mps1-Frb displayed identical SAC activation phenotypes (see below and Figure 3.5c).

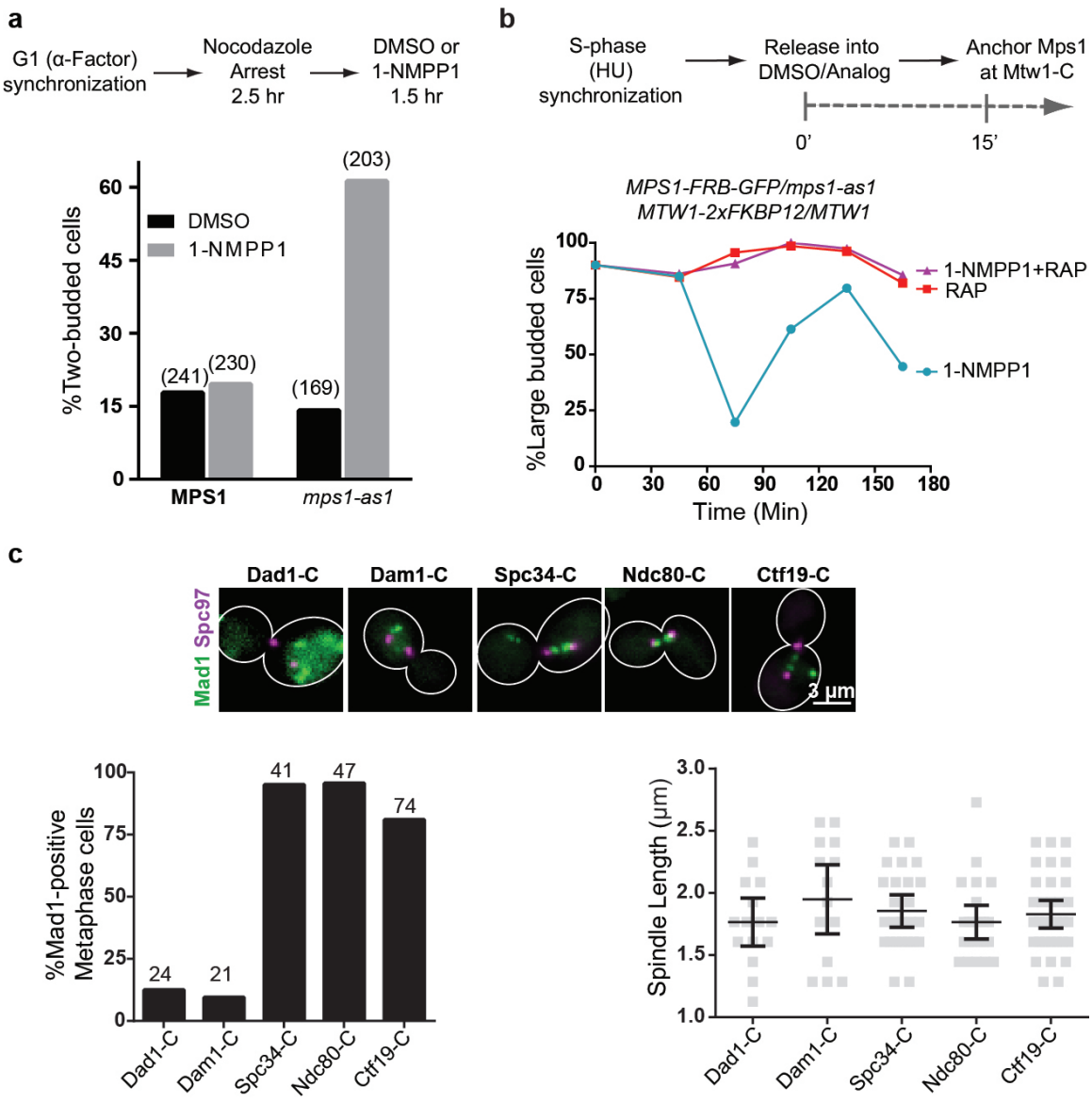

Figure 3.5: **Kinase activity of the kinetochore-anchored Mps1 is sufficient for SAC activation.** (a) Cells expressing the analog-sensitive Mps1 allele, mps1-as1 or wild type Mps1 were treated as indicated at the top. Bar graph displays the percentage of two-budded cells (which form when a mitotic cell fails to sustain the SAC in the presence of a damaged spindle and produce a new bud by re-entering the cell cycle). Bars indicate the average value based on data from two independent experiments. The total number of cells scored is indicated at the top. (b) Inhibition

of the diffusible mps1-as1 does not affect SAC activation by Mps1-Frb anchored at the kinetochore. Heterozygous diploid strains expressing mps1-as1 and Mps1-Frb were synchronized in S-phase and released into 1-NMPP1 for 15 minutes. Rapamycin was then added to anchor Mps1-Frb at Mtw1-C. The anchored Mps1 arrested the cell cycle robustly, and the cells retained the large-budded morphology for a prolonged period of time. The experiment was performed once, and more than 50 cells scored for each time point. (c) Micrographs: Mad1 localization relative to the spindle pole body in haploid cells that have Mps1 anchored to the indicated subunit. Bar graph displays the percentage of cells with visible Mad1 localization in between the spindle poles in each case (number of cells scored in one experiment indicated on top). The corresponding metaphase spindle length in each case is presented in the scatter plot (range: 1.8-1.9 $\pm$ 0.3 μm; mean $\pm$ 95% confidence interval from n = 15, 14, 25, 23 and 33 cells from left to right).

When Mps1 was constitutively anchored at four different locations within the inner kinetochore, ranging from Ndc80-C to Ctf19-C, it completely inhibited colony growth (Figure 3.4d). MAD2 deletion restored colony growth, indicating that the lack of growth was due to constitutive SAC activation (Figure 3.6a and Figure 3.4d). Interestingly, Mps1 anchored at two positions located in the outer kinetochore, N-Ndc80 and Ask1-C (a Dam1 complex subunit), had no effect on colony growth (Figure 3.4d). Although the number of Mps1 molecules anchored in the inner kinetochore positions was 30-50% higher than the number of Mps1 molecules anchored in the outer kinetochore, these differences did not strictly correlate with SAC activation phenotypes (Figure 3.6b). Reducing the length of the linker between Mps1 and Frb-GFP did not affect the observed phenotypes (Figure 3.6c). Finally, the observed effects were specific to Mps1: constitutive anchoring of Ipl1 or Mad1 at the same positions did not result in the same phenotypes (Figure 3.6d-g). These data show that the position of Mps1 within the kinetochore can affect its ability activate the SAC. Since Mps1 must phosphorylate Spc105 to activate the SAC, the observed phenotypes likely reflect whether or not the anchored Mps1 can access the phosphodomain of Spc105. It is notable that Mps1 activates the SAC from different locations over a 30 nm span [*Joglekar et al.*, 2009] (the metaphase separation between Ndc80-C and Ctf19-C), even though its kinase activity is spatially confined to individual locations. To encounter the confined kinase activity over this wide span, the long and unstructured phosphodomain of Spc105 likely assumes variable conformations.

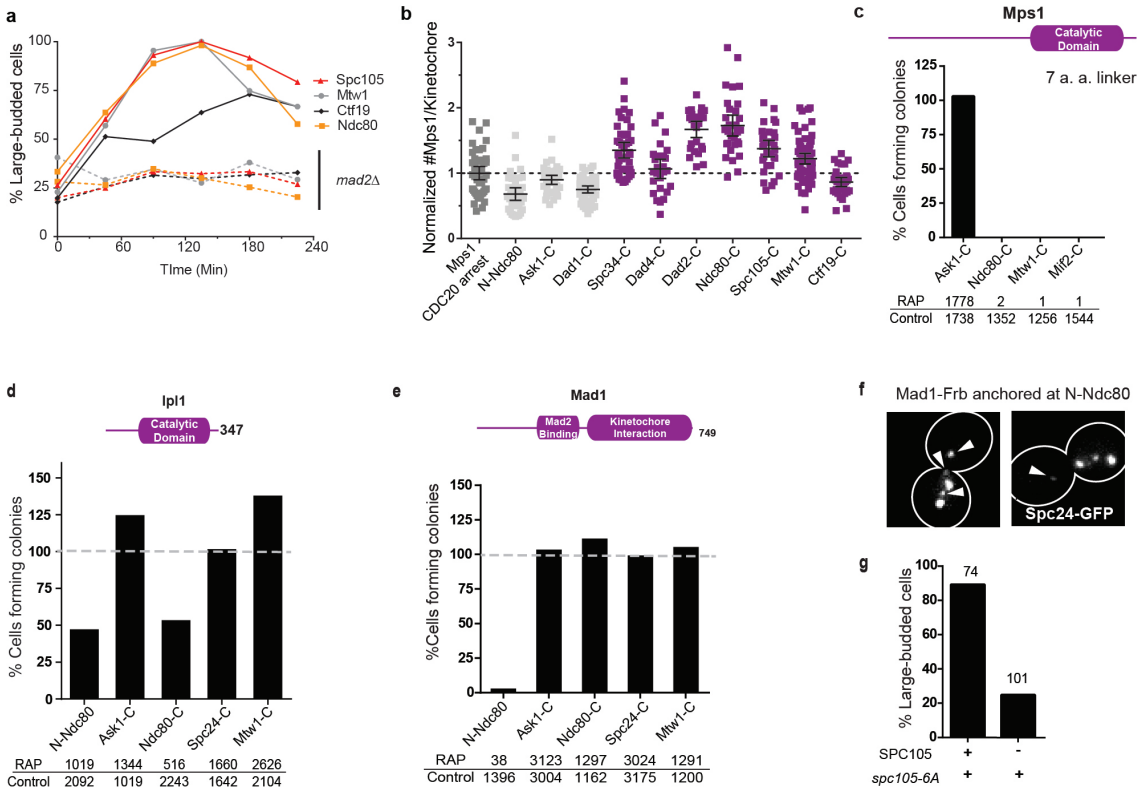

Figure 3.6: **Cell cycle effects of anchoring Mps1, Ipl1 or Mad1 constitutively within the kinetochore** (a) Cell cycle kinetics of asynchronous cultures where Mps1 is anchored at the C-termini of indicated kinetochore subunits in wild-type or SAC null strains (mad2). The experiment was performed once. More than 50 cells were scored for each time point. (b) Quantification of Mps1-Frb-GFP (mean ± 95% confidence interval; n = 35, 36, 47, 43, 27, 26, 33, 31, 66, 35 and 46 kinetochore clusters from left to right) anchored at indicated kinetochore subunits measured 45 minutes after rapamycin treatment and normalized relative to endogenous Mps1 in metaphase-arrested cells. Note that the recruitment of Mps1 at Dad4-C and Ctf19-C that activates the SAC is comparable to that at Ask1-C which does not activate the SAC. (c) Reducing the length of the flexible linker connecting Mps1 and Frb (from 24 to 7 amino acids) did not change the effect of anchoring Mps1 on colony growth. Bars represent the average values calculated from two independent experiments. Cu-

mulative number of colonies counted is displayed at the bottom. (d-e) The number of colonies formed on rapamycin-containing plates relative to control plates, when Ipl1 (in d) or Mad1 (in e) is constitutively anchored at the indicated positions. Bars represent the average values calculated from 3 or 4 independent experiments. The number of colonies on rapamycin-containing plates exceeding that on the control is likely due to pipetting errors. Reduced number of colonies upon anchoring Ipl1-Frb-GFP at Ndc80-C and N-Ndc80 may be due to attachment defects caused by Ipl1-mediated phosphorylation of kinetochore proteins13. The loss of colony formation upon Mad1 anchoring at N-Ndc80 is also likely due to attachment defects (see f-g). (f) Mad1 anchored at N-Ndc80 generates unattached kinetochores (arrowheads) in a large fraction of cells (60 out of 108 cells had visible defects in kinetochore cluster morphology). (g) Graph presents the fraction of cells expressing Spc105-6A or Spc105 that arrested with large-buds when Mad1 was anchored at N-Ndc80 (rapamycin treatment for 4 hours). The experiment was performed once. The number of cells scored is indicated on top of bars.

3.2.5 Mps1 anchored in the outer kinetochore does not activate the SAC

To confirm that the inability of Mps1 to activate the SAC from the outer kinetochore is only because it cannot phosphorylate Spc105, we characterized the effects of anchoring Mps1 to the C-termini of seven other subunits of the heterodecameric Dam1 complex [*Ramey et al.*, 2011] (Figure 3.7a). Similar to Ask1, Mps1 anchored to three other Dam1 subunits did not affect the colony growth (Figure 3.7b and Figure 3.8a). Surprisingly, Mps1 anchored to four other subunits delayed colony formation, but did not appear to affect the number of colonies formed (Figure 3.7b, Figure 3.8a). Slow colony growth was likely due to a transient SAC-mediated delay in the cell cycle (Figure 3.7c, also Figure 3.5c). As before, reduced length of the flexible linker fusing the Mps1 kinase domain to Frb did not affect the observed cell cycle delay (Figure 3.8b).

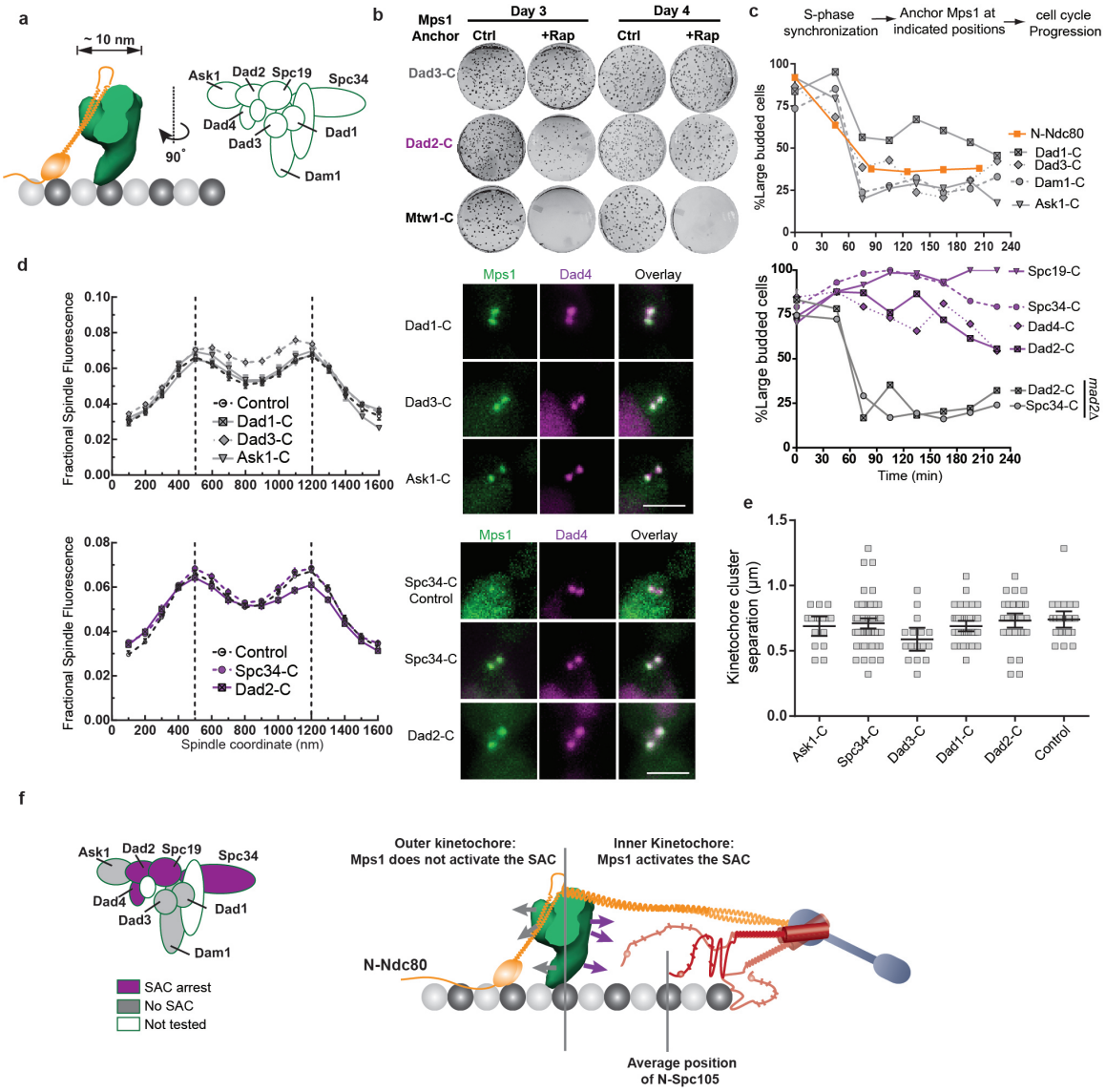

Figure 3.7: **The Dam1 complex defines a boundary for SAC signaling by anchored Mps1.** (a) Cartoon: Position of the Dam1 complex relative to Ndc80 complex [*Aravamudhan et al.*, 2014] and subunit organization within the Dam1 complex [*Ramey et al.*, 2011]. EMD1372 was used to infer the dimensions of the Dam1 complex. (b) Colony growth (also see Figure 3.8a) on control (ctrl.) and rapamycin (+Rap) plates. The number of days after plating is indicated at the top; the anchoring subunit is indicated on the left. (c) Cell cycle progression when Mps1 is anchored to a

Dam1 subunit (indicated on the left) in cells released from an experimentally imposed S-phase arrest. This strategy was used to ensure that the kinetochores formed end-on attachments and loaded Dam1 complex before Mps1 was anchored [*Li et al.*, 2002]. Plotted points represent the average values calculated from 2 independent experiments. (d) Normalized distribution of Dad4-mcherry on the spindle when Mps1 was anchored to the indicated positions for 1 hour (mean ± s.e.m. n = 43, 34, 28, 36, 73 and 38 cells for Dad1, Dad3, Ask1, Ctrl, Spc34 and Dad2, respectively). Control data is from untreated metaphase cells. Micrographs on the right display the localization of Dad4-mCherry relative to that of Mps1-frb-gfp anchored to the indicated subunits (scale bar ≈ 3 μm). (e) The separation between kinetochore clusters in the cells in (d), measured as the separation between maximum intensity pixels in the two Dad4-mCherry puncta in each cell; mean ± 95% confidence interval, n = 43, 16, 16, 25, 72 and 38 cells for Dad1, Dad3, Ask1, Ctrl, Spc34 and Dad2, respectively. Although there is a small decrease in spindle length when Mps1 is anchored at Dad3-C, cell cycle progression is unaffected as seen in (c). (f) Left: Classification of Dam1 complex subunits inferred from the Mps1 anchoring experiments. Right: Activity map of the anchored Mps1 along the length of the kinetochore-MT attachment. Arrows from the Dam1 complex depict the proposed orientation of the C-termini of subunits used as anchors. Possible variations in the conformation of the unstructured phosphodomain of Spc105 are also depicted.

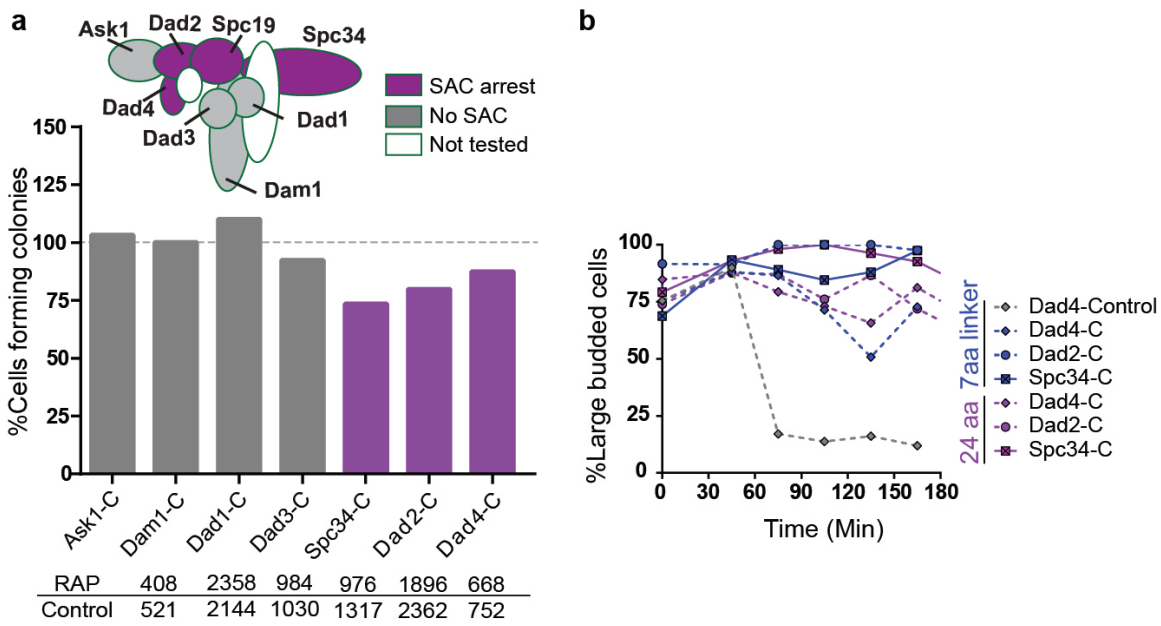

Figure 3.8: **Anchoring Mps1 to Dam1 subunits leads to different phenotypes** (a) Subunit organization of the Dam1 complex is color-coded according to the scheme displayed on the right. The untested subunits are Duo1 and Hsk4. Bar graph displays the number of colonies formed on rapamycin relative to the control plates. Bars represent averages from two independent experiments. The total numbers of colonies scored are displayed at the bottom. (b) Cell cycle kinetics of rapamycin treated (to anchor Mps1 at indicated subunits) or untreated (control) cells. The experiment was performed once and more than 60 cells were scored for each time point. Since Mps1 anchored at Dad2-C, Dad4-C or Spc34-C transiently activated the SAC, we tested if shortening the linker connecting Mps1 and Frb (from 24 to 7 amino acids) eliminates this transient SAC activation by restricting access to N-Spc105. However, anchored Mps1 activated the SAC in spite of the shorter linker.

We also tested whether the anchored Mps1 in these experiments perturbed Dam1 complex localization and function, because Dam1 subunits are known Mps1 substrates [*Ramey et al.*, 2011; *Shimogawa et al.*, 2006]. We quantified the distribution of Dad4 over the mitotic spindle after anchoring Mps1 to other Dam1 subunits (Figure 3.7d). Dad4-mCherry colocalized with the anchored Mps1-Frb-GFP in every case, and its distribution was indistinguishable from Dad4 distribution in untreated cells. Thus, the association of the Dam1 complex with the kinetochore remained unaffected. The separation between kinetochore clusters in rapamycin-treated cells was also indistinguishable from the corresponding length in untreated cells (Figure 3.7e). This indicates that force generation at the kinetochore, a process in which the Dam1 complex is the dominant contributor, was not affected [*Cheeseman et al.*, 2001]. Thus, the anchored Mps1 does not perturb Dam1 complex function, and the observed phenotypes reflect whether or not the anchored Mps1 can phosphorylate Spc105. The strikingly different phenotypes induced by Mps1 anchored to Dam1 subunits are surprising. This is because dimensions of the Dam1 complex [*Ramey et al.*, 2011] and its narrow distribution along the length of the kinetochore-MT attachment [*Aravamudhan et al.*, 2014] suggest that all of the anchoring points are confined within a ≈10 nm wide zone. Although the structure of the Dam1 complex is unknown, it is conceivable that the C-termini of Dam1 subunits face towards or away from the centromere (Figure 3.7f, arrows). This orientation may in turn constrain the orientation of the anchored Mps1, and determine whether or not it can phosphorylate Spc105 to activate the SAC.

3.2.6 The phosphorylation of Spc105 by Mps1 is sufficient to initiate SAC signaling

Our data show that the physical proximity between the Mps1 kinase and the phosphodomain of Spc105 can control the state of the SAC. Therefore, we tested whether

a forced interaction between the two outside the kinetochore is sufficient to activate the SAC. We engineered a minimal, anchorable phosphodomain comprising residues 120-329 of Spc105 (referred to as $Spc105^{120:329}$, Figure 3.9a). It contains all 6 MELT motifs, but no known kinetochore-binding activity. When we anchored $Spc105^{120:329}$ to Mps1-Fkbp12 in asynchronously dividing cells, the cells arrested in metaphase (Figure 3.9b). $Spc105^{120:329}$ also localized to kinetochore clusters under these conditions and recruited Mad1 (Figure 3.9c, Figure 3.10a). The kinetochore-localization of Mad1 and $Spc105^{120:329}$, when the latter anchored to Mps1, is likely mediated by Mps1 binding to the kinetochores. MAD2 deletion abolished the cell cycle arrest indicating that the arrest resulted from SAC activation (Figure 3.9b, dashed line). When $Spc105^{120:329}$:6A, the non-phosphorylatable version of $Spc105^{120:329}$, was anchored to Mps1, it did not activate the SAC (Figure 3.9b-c). Thus, the phosphorylation of MELT motifs in $Spc105^{120:329}$ by Mps1 is necessary for the observed cell cycle arrest.

To test whether kinetochores contributed to the SAC signaling in the above experiment, we used cells carrying ndc10-1, a temperature sensitive allele of gene encoding the centromeric protein Ndc10 (ref. [*Goh and Kilmartin*, 1993]). At the restrictive temperature, these cells cannot assemble functional kinetochores, and are thus unable to activate the SAC. However, when $Spc105^{120:329}$ was anchored to Mps1 at the restrictive temperature, ndc10-1 cells experienced a cell cycle delay similar to the delay seen in NDC10 cells under the same conditions (Figure 3.10b). Thus, the SAC signaling induced by the forced interaction between $Spc105^{120:329}$ and Mps1 does not require functional kinetochores [*Fraschini et al.*, 2001]. Together with our earlier results, these data demonstrate that the interaction between Mps1 and the phosphodomain of Spc105 is both necessary and sufficient to activate the SAC. The kinetochore may primarily serve as the scaffold that makes this interaction sensitive to MT attachment.

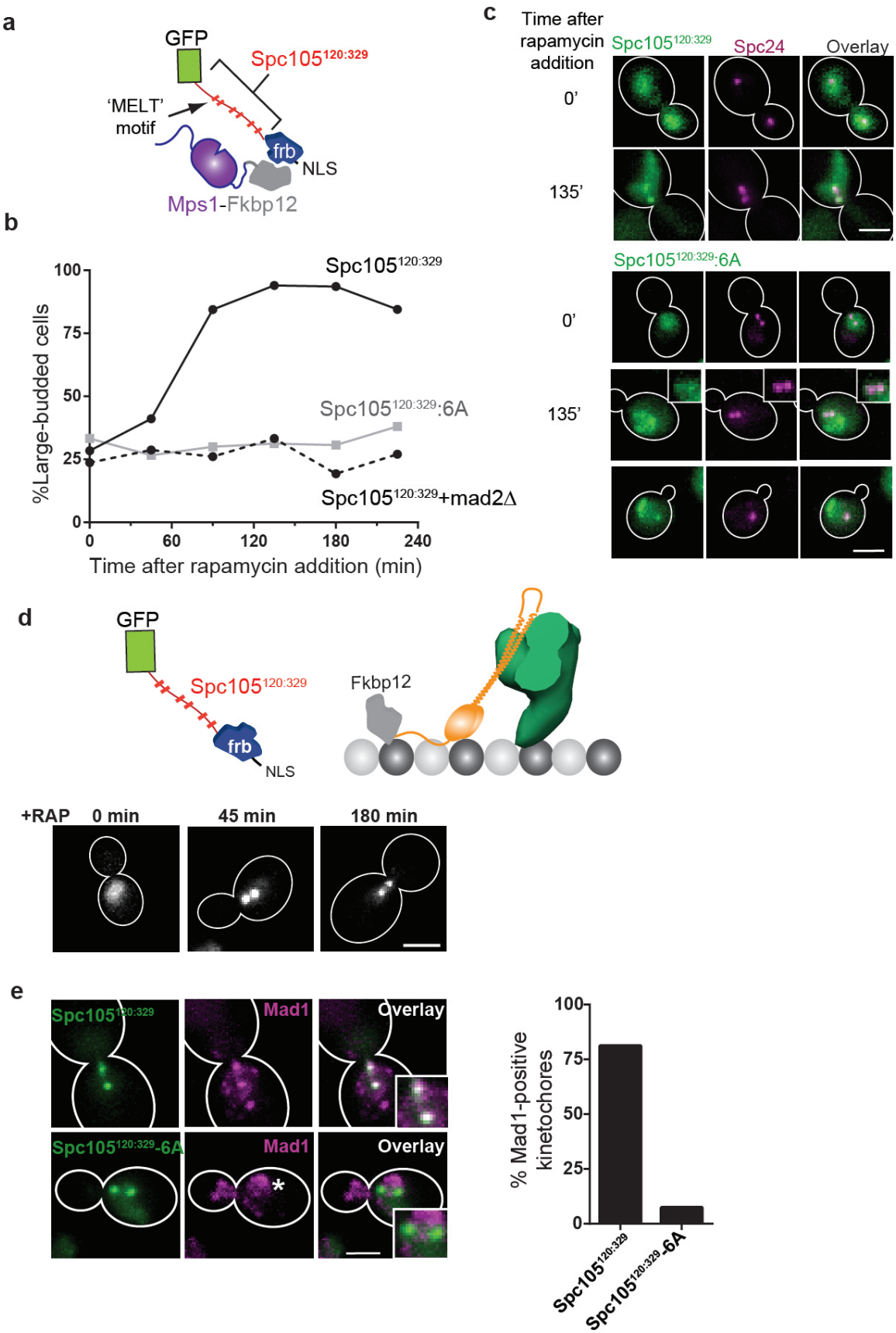
a
GFP
Spc105120:329
'MELT' motif
frb
NLS
Mps1-Fkbp12
b
Spc105120:329
Spc105120:329:6A
Spc105120:329+mad2Δ
%Large-budded cells
Time after rapamycin addition (min)
c
Time after rapamycin addition
Spc105120:329
Spc24
Overlay
0'
135'
Spc105120:329:6A
d
GFP
Spc105120:329
frb
NLS
Fkbp12
+RAP
0 min
45 min
180 min
e
Spc105120:329
Mad1
Overlay
Spc105120:329-6A
% Mad1-positive kinetochores
Spc105120:329
Spc105120:329-6A

Figure 3.9: **The phosphorylation of the Spc105 phosphodomain by Mps1 is sufficient to activate the SAC.**(a) Schematic of $Spc105^{120:329}$: the minimal Spc105 phosphodomain. NLS = Nuclear Localization Signal used to send $Spc105^{120:329}$ to the nucleus. (b) Cell cycle kinetics following rapamycin addition to anchor the phosphorylatable (solid black line) or non-phosphorylatable $Spc105^{120:329}$ (solid gray line) to Mps1-C. Dashed black line shows the cell cycle progression of the mad2 strain after anchoring $Spc105^{120:329}$ to Mps1. Plotted points represent the average values calculated from 2 independent experiments. More than 50 cells scored for each time point in each trial. (c) Localization of $Spc105^{120:329}$ or $Spc105^{120:329}$:6A when anchored to Mps1. Scale bar ≈ 3 μm. (d) Strategy to anchor $Spc105^{120:329}$ at N-Ndc80, and the localization of $Spc105^{120:329}$ at indicated times after rapamycin addition. Scale bar ≈ 3 μm. (e) Recruitment of Mad1 to the kinetochore clusters when $Spc105^{120:329}$ (top) or $Spc105^{120:329}$:6A (bottom) is anchored at N-Ndc80. Bars represent mean data pooled from 2 independent experiments. At least 45 cells were analyzed for each sample in each trial. Asterisk known Mad1 localization at the nuclear envelope. Scale bar ≈ 3 μm.

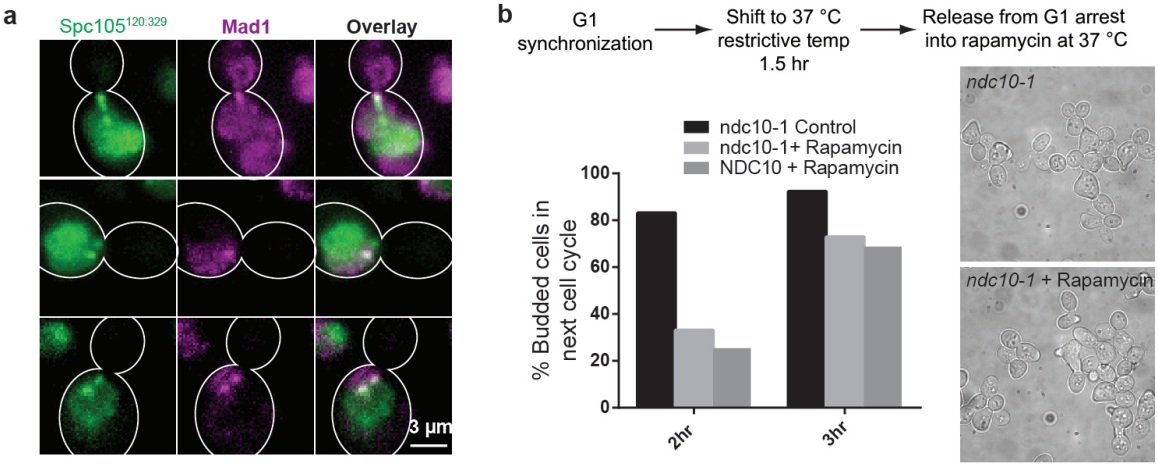

Figure 3.10: **SAC signaling induced by rapamycin-induced dimerization of Spc105$^{120:329}$ and Mps1 does not require functional kinetochores.** (a) Representative images show Spc105$^{120:329}$ anchored to Mps1 (rapamycin treatment for 45 minutes) localizing to the kinetochores. Mad1 also co-localizes with these kinetochore clusters. (b) Cells carrying the temperature-sensitive ndc10-1 allele and expressing Spc105$^{120:329}$ and Mps1-Fkbp12 were treated as indicated at the top. When released at the restrictive temperature from G1 arrest, these cells go through the cell cycle without assembling functional kinetochores and fail in cytokinesis, and give rise to cells with two buds (black bars; also see transmitted light micrograph top-right). However, when the same experiment was conducted in rapamycin containing media, the emergence of two budded cells was delayed by an hour (light gray bars). We attribute this delay to SAC activation, which is also observed when Spc105$^{120:329}$ is anchored to Mps1 in NDC10 cells at 37 C (dark gray bars). Bars represent averages from 2 independent experiments.

3.2.7 Spc105$^{120:329}$ activates the SAC when anchored in the outer kinetochore, but not the inner kinetochore

Our data reveal a potential organization of Mps1 and Spc105 relative to one another that can make their interaction sensitive to the attachment state of the kinetochore. When Mps1 is anchored in the inner kinetochore, proximal to the phosphodomain of Spc105, it activates the SAC constitutively even from attached kinetochores. In contrast, if it is anchored in the outer kinetochore, distal from the phosphodomain of Spc105, it activates the SAC conditionally, only from unattached kinetochores (Figure 3.11). Therefore, to implement attachment-sensitive SAC signaling, endogenous Mps1 should bind to a site within the outer kinetochore. Consistent with this expectation, Mps1 physically interacts with the CH-domain of Ndc80, which is located in the outer kinetochore [*Kemmler et al.*, 2009; *Nijenhuis et al.*, 2013].

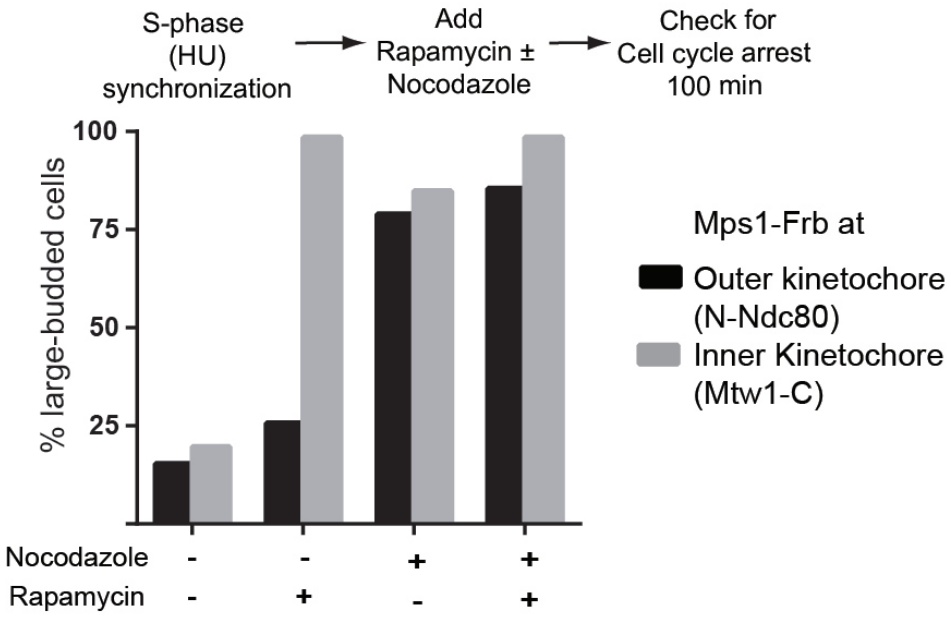

Figure 3.11: **SAC signaling induced by Mps1 anchored at N-Ndc80 depends on the attachment-state of the kinetochore.** S-phase synchronized cells were treated as indicated in the schematic at the top and the percentage of large-budded cells formed after 100 minutes was measured as an indicator of cell cycle arrest Mps1 anchored at Mtw1-C constitutively activated the SAC in the presence of attachments and in nocodazole. However, Mps1 anchored at N-Ndc80 allowed normal cell cycle progression and caused cell cycle arrest only in the presence of unattached kinetochores in nocodazole. Bars represent the average from 2 independent experiments. More than 50 cells were scored for each condition in each experiment.

To test whether endogenous Mps1 binds within the outer kinetochore, we anchored Spc105$^{120:329}$ at N-Ndc80, proximal to the CH-domain (Figure 3.9d, top). In metaphase cells, the anchored Spc105$^{120:329}$ displayed the stereotypical, metaphase kinetochore distribution: two distinct puncta separated by < 1 μm. It also recruited Mad1, and the cells remained arrested for a prolonged period (Figure 3.9d-e). The cell cycle arrest was absent when Spc105$^{120:329}$:6A was anchored to N-Ndc80, revealing that the phosphorylation of the MELT motifs in Spc105$^{120:329}$ by kinetochore-localized Mps1 is required for SAC activation. These results demonstrate that catalytically active Mps1 binds to the outer kinetochore even after stable MT attachments form. We next probed the entire kinetochore for additional Mps1 binding sites (Figure 3.13a). When we anchored Spc105$^{120:329}$ to Dam1 subunits expected to face towards the outer kinetochore (Ask1-C, Dam1-C, or Dad1-C, see Figure 3.7f), the kinetochores recruited Mad1, and the cells arrested in mitosis (Figure 3.13b top and Figure 3.13c). Strikingly, Spc105$^{120:329}$ was anchored to positions in the inner kinetochore, including the Dam1 subunit termini predicted to face towards the centromere (Dad4-C, Spc34-C, and Spc19-C), it had no effect on the cell cycle (Figure 3.13b bottom and Figure 3.13c). As expected, Spc105$^{120:329}$:6A did not affect the cell cycle when anchored at any of the positions (dashed lines in Figure 3.13b). These results demonstrate that catalytically active Mps1 is absent from the inner kinetochore. The N-terminus of Spc105 localizes to the inner kinetochore and contains a Glc7 binding motif [*Rosenberg et al.*, 2011], which is not present in Spc105$^{120:329}$. Therefore, the lack of Glc7 activity in the outer kinetochore, rather than localized Mps1 activity, could also produce the observed SAC activation phenotypes. To test if this is the case, we constructed a phosphodomain that contains the Glc7 binding motif (Spc105$^{2:329}$, Figure 3.13d). Spc105$^{2:329}$ anchored at N-Ndc80 or at Ndc80-C produced the same phenotypes as Spc105$^{120:329}$ (Figure 3.13d, top). We quantified Bub3-mCherry at the kinetochore, which specifically binds phosphorylated MELT motifs [*Primorac et al.*, 2013], after

anchoring either Spc105$^{2:329}$ or Spc105$^{2:329}$ to Ask1-C (Figure 3.13d). Spc105$^{2:329}$ recruited significantly less Bub3 confirming that it recruits Glc7 activity (Figure 3.13d, bottom). These data build an activity map for Spc105$^{120:329}$ and demonstrate that catalytically active Mps1 kinase binds exclusively in the outer kinetochore even after the kinetochore establishes stable MT attachment. Strikingly, this map is the mirror image of the activity map for the anchored Mps1 kinase, with the Dam1 complex demarcating the boundary in both (Figure 3.7f and Figure 3.13e). These data strongly suggest that the Dam1 complex may contribute to SAC silencing by acting as a physical barrier that separates the phosphodomain of Spc105 from Mps1.

3.2.8 Separation between CH-domains of Ndc80 and N-Spc105 changes with the attachment state of the kinetochore

Our data suggest that MT attachment to kinetochore physically separates the CH-domains of Ndc80 and the phosphodomain of Spc105 to silence the SAC. By corollary, unattached kinetochores must bring them in close proximity to activate the SAC. To test if the separation between these two domains and the attachment state of the kinetochore are correlated, we measured FRET between N-Spc105 and either N-Nuf2 or N-Ndc80, which are proximal to the CH-domains (Figure 3.14a, Figure 3.12). In both cases, FRET was undetectable in metaphase as predicted by the $>$ 30 nm separation between N-Spc105 and the two protein termini [*Joglekar et al.*, 2009]. In contrast, moderate FRET was detected in unattached kinetochores created by treating the cells with nocodazole indicating that mCherry and GFP fused to the respective N-termini were, on average, $\approx$ 8 nm apart [*Joglekar et al.*, 2013].

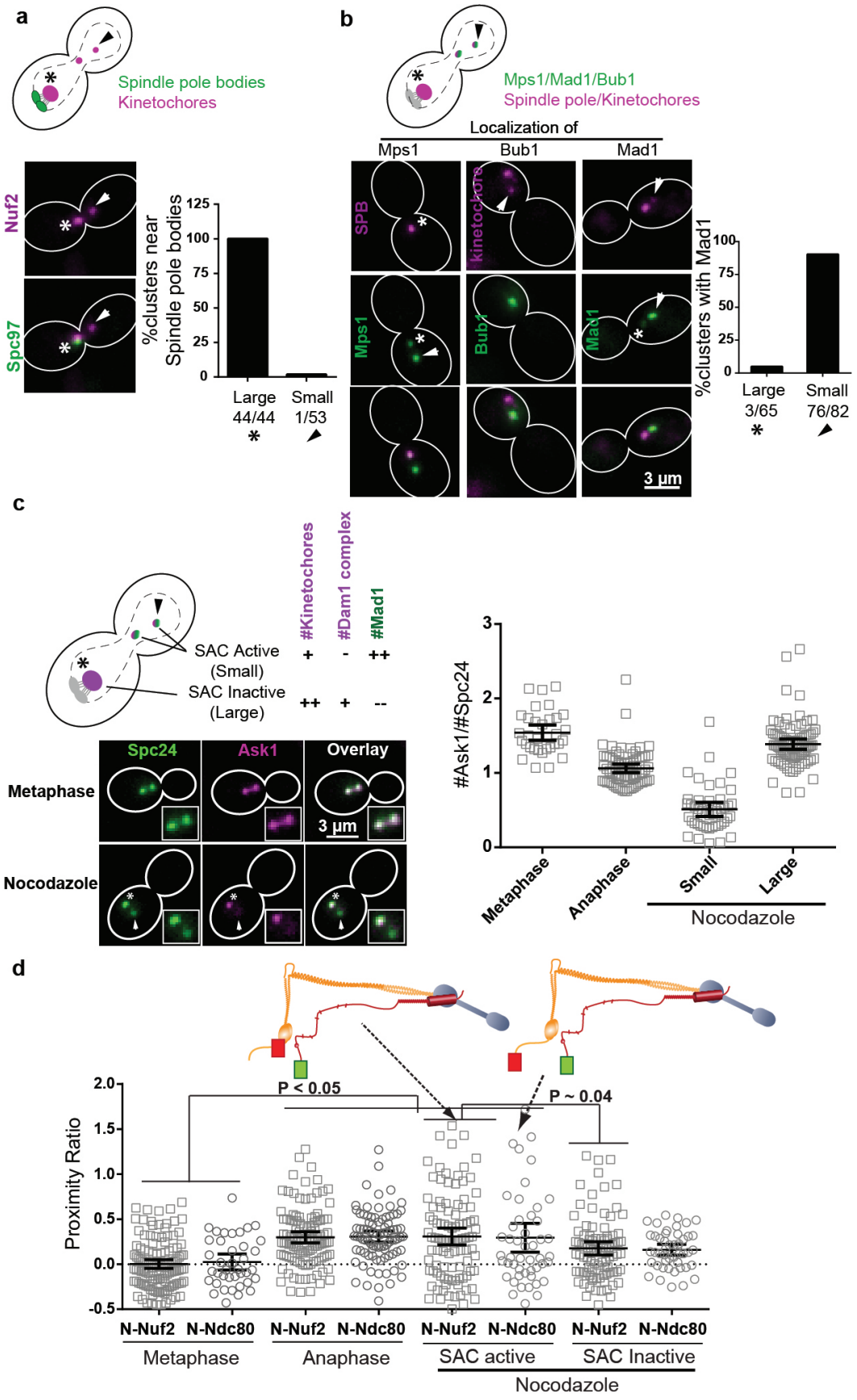
a
Spindle pole bodies
Kinetochores
Nuf2
Spc97
%clusters near Spindle pole bodies
125
100
75
50
25
0
Large
44/44
Small
1/53
b
Mps1/Mad1/Bub1
Spindle pole/Kinetochores
Localization of
Mps1
Bub1
Mad1
SPB
Kinetochores
Mps1
Bub1
Mad1
3 µm
%clusters with Mad1
100
75
50
25
0
Large
3/65
Small
76/82
c
#Kinetochores
#Dam1 complex
#Mad1
SAC Active (Small)
+
-
++
SAC Inactive (Large)
++
+
--
Spc24
Ask1
Overlay
Metaphase
Nocodazole
3 µm
#Ask1/#Spc24
3
2
1
0
Metaphase
Anaphase
Small
Large
Nocodazole
d
P < 0.05
P ~ 0.04
Proximity Ratio
2.0
1.5
1.0
0.5
0.0
-0.5
N-Nuf2
N-Ndc80
N-Nuf2
N-Ndc80
N-Nuf2
N-Ndc80
N-Nuf2
N-Ndc80
Metaphase
Anaphase
SAC active
SAC Inactive
Nocodazole

Figure 3.12: **Effect of spindle disruption on SAC protein recruitment and kinetochore architecture** (a) Spindle disruption with nocodazole generates two or three kinetochore clusters within the nuclei of most budding yeast cells as reported previously. The cluster that contained majority of the kinetochores (large, asterisks) localized proximal to the collapsed spindle pole bodies (visualized by Spc97-GFP). One or two smaller kinetochore clusters (small, arrowheads) were found distal to the spindle pole bodies. Bar graph displays the percentage of large or small clusters that are proximal to the spindle pole body. The cumulative numbers of clusters scored in 2 independent experiments are indicated at the bottom. (b) Consistent with Gillett et al. 2004, the smaller kinetochore clusters (arrowheads) in nocodazole recruit significantly higher levels of Mps1 and Bub1 than the large cluster. Mad1 was undetectable at the large clusters (bars indicate average from 2 independent experiments). 76 out of 82 smaller clusters recruited Mad1, but only 3 out of 65 large clusters had detectable Mad1. Therefore, we classify the smaller clusters as SAC-active and the larger clusters as SAC-inactive. (c) Dam1 complex (visualized with Ask1-mCherry) is retained at the SAC-inactive cluster, whereas it is significantly reduced at the SAC-active clusters in nocodazole. Quantification of Ask1-mCherry fluorescence measured relative to Spc24-mCherry fluorescence is displayed on the right. The experiment was performed once and horizontal bars represent mean ± 95% confidence intervals, n = 33, 72, 45 and 81 kinetochore clusters (left to right). Since MT attachment is necessary for Dam1 recruitment to the kinetochore, this observation suggests that the kinetochores located proximal to the collapsed spindle pole bodies retain MT attachment. (d) Measurement of FRET between GFP-Spc105 and either mCherry-Nuf2 or mCherry-Ndc80 in SAC-active and SAC- inactive kinetochore clusters. The horizontal bars represent mean ± 95% confidence interval; data pooled from more than two independent experiments. P-values were computed using non-parametric Mann-Whitney test; n = 121, 39, 110, 87, 101, 49, 90 and 47 kinetochore clusters from left to

right). FRET between mCherry-Nuf2 (or mCherry-Ndc80) and GFP-Spc105 in the SAC-inactive kinetochore cluster is higher than metaphase FRET value, and significantly lower than the FRET observed in the SAC-active cluster ($\approx 50\%$, p-value ≈ 0.04). Note that the significantly higher FRET in anaphase compared to metaphase clusters is consistent with the previously reported reduction in the length of Ndc80 complex in anaphase.

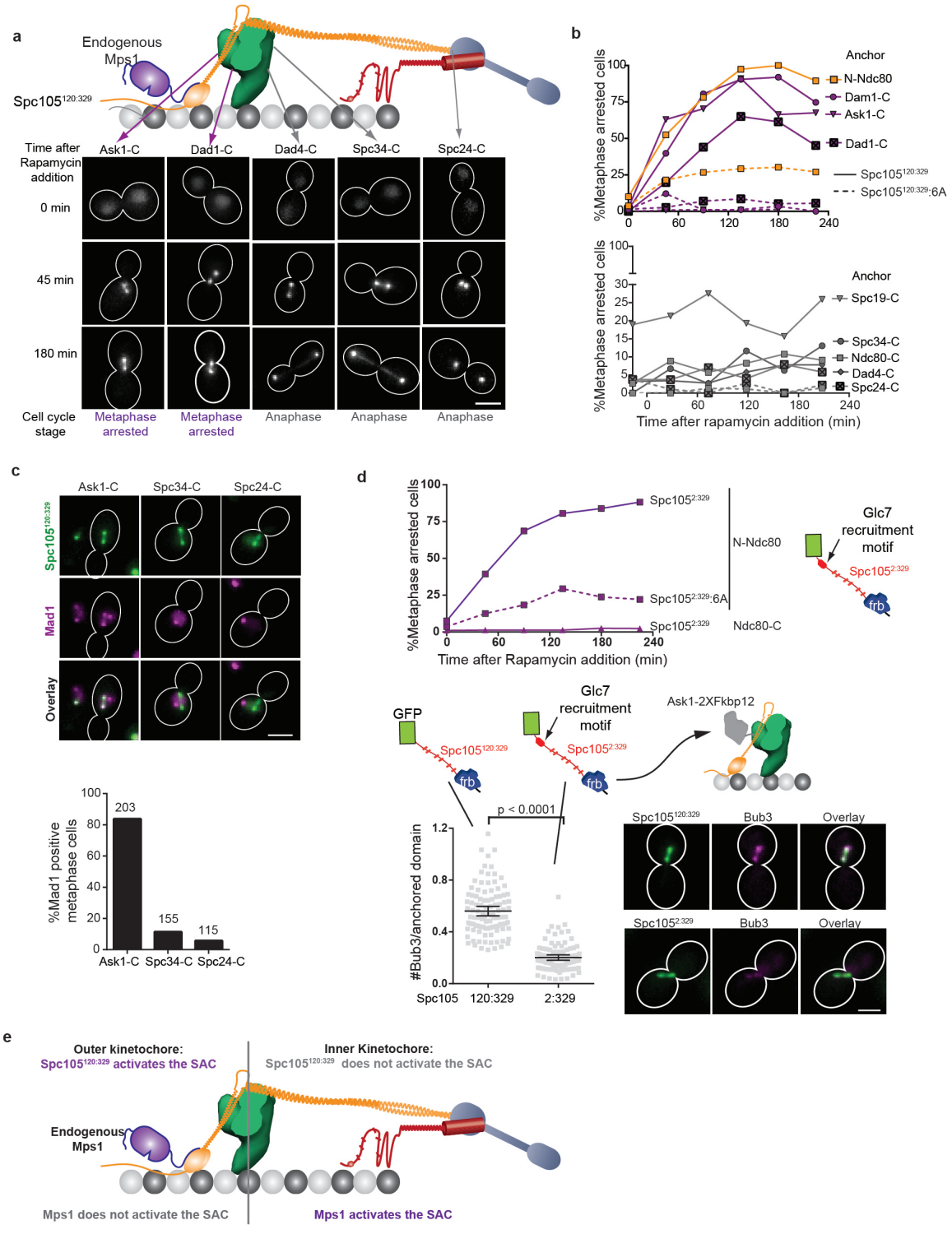

Figure 3.13: **Spc105$^{120:329}$ activates the SAC only when it is anchored in the outer kinetochore.**(a) Representative micrographs of asynchronously dividing cells

showing the localization of $Spc105^{120:329}$ and cell-cycle progression as a function of the anchoring position (indicated at the top; scale bar ≈ 3 μm). Large-budded cells with < 2 μm separation between kinetochore clusters were characterized as metaphase-arrested cells. (b) Accumulation of metaphase-arrested cells after rapamycin addition, when either $Spc105^{120:329}$ (solid lines) or its non-phosphorylatable version, $Spc105^{120:329}$:6A (dashed lines) was anchored at the indicated positions. The experiment was performed once, and more than 70 cells were scored for each time point . (c) Mad1-mCherry localization after anchoring $Spc105^{120:329}$ at indicated positions for 1 hour (scale bar ≈ 3 μm). The bar graph shows the fraction of metaphase cells that recruit Mad1 to the kinetochores in each case. Bars present average values from 2 independent experiments. Total number of cells analyzed in each case is indicated on top of the bars. (d) Top: Cell cycle progression as in Figure 3.13a when a modified version of Spc105 phosphodomain that includes the Glc7 recruitment motif ($Spc105^{2:329}$, solid lines) or its non-phosphorylatable version ($Spc105^{2:329}$:6A, dashed line) was anchored at the indicated kinetochore positions. The experiment was performed once. More than 50 cells were scored for each time point. Bottom: Micrographs (scale bar ≈ 3 μm) and quantification of kinetochore-localized Bub3-mCherry 45 minutes after either $Spc105^{120:329}$ or $Spc105^{2:329}$ was anchored at Ask1-C in cells arrested in metaphase using CDC20 repression (mean $\pm$ 95% confidence interval from n = 102 and 100 kinetochore clusters analyzed for $Spc105^{120:329}$ and $Spc105^{2:329}$ anchoring, respectively). p-values computed using Mann-Whitney test. (e) Map of the SAC activity of the anchored $Spc105^{120:329}$.

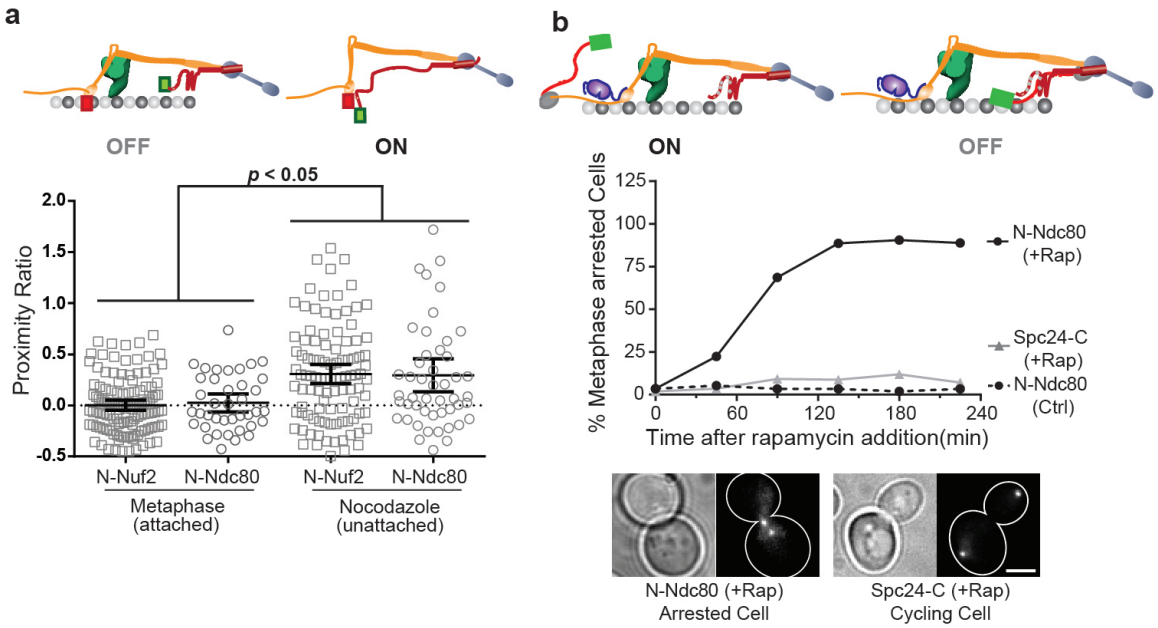

Figure 3.14: **The proximity between the CH-domains of Ndc80 and the phosphodomain of Spc105 within the kinetochore controls SAC signalling** (a) Scatter plot: Proximity ratio measurements for FRET between mCherry-Nuf2 or mCherry-Ndc80 and GFP-Spc105 in attached (metaphase) and unattached (nocodazole-treated) kinetochores. It should be noted N-Ndc80 is connected to the CH-domain via a 113 amino acid long unstructured tail. Data pooled from 3 independent experiments, horizontal bars represent mean ± 95% confidence interval computed from n = 121, 37, 101 and 49 clusters (left to right). p-values were computed using Mann-Whitney test. (b) Cell cycle kinetics after anchoring $Spc105^{120:329}$ at indicated positions in strains expressing spc105-6A. Plotted points represent average values calculated from 2 independent trials. More than 70 cells scored in each trial. Scale bar ≈ 3 μm.

3.2.9 Proximity between the CH-domains and Spc105$^{120:329}$ controls SAC signaling in attached kinetochores independently of the endogenous Spc105

Finally, we tested whether Spc105$^{120:329}$ can restore the SAC in attached and unattached kinetochores in a position-dependent manner in spc105-6A strains that are SAC-deficient. The kinetochore only provides the architectural scaffold in this experiment. Consistent with the previous results, Spc105$^{120:329}$ arrested the cell cycle when anchored proximal to the CH-domains (at N-Ndc80), but not when anchored distal to the CH-domains (at Spc24-C, Figure 3.14b). Even within unattached kinetochores, Spc105$^{120:329}$ restored the SAC when it was anchored at N-Ndc80, as expected (Figure 3.15). However, Spc105$^{120:329}$ anchored at Spc24-C also activated the SAC suggesting that Mps1 can access Spc105$^{120:329}$, even though its anchoring position is expected to be distal to the CH-domains. The inherent flexibility of Ndc80 and Spc105 and the presence of multiple molecules of these proteins in the kinetochore are likely responsible for this unexpected phenotype.

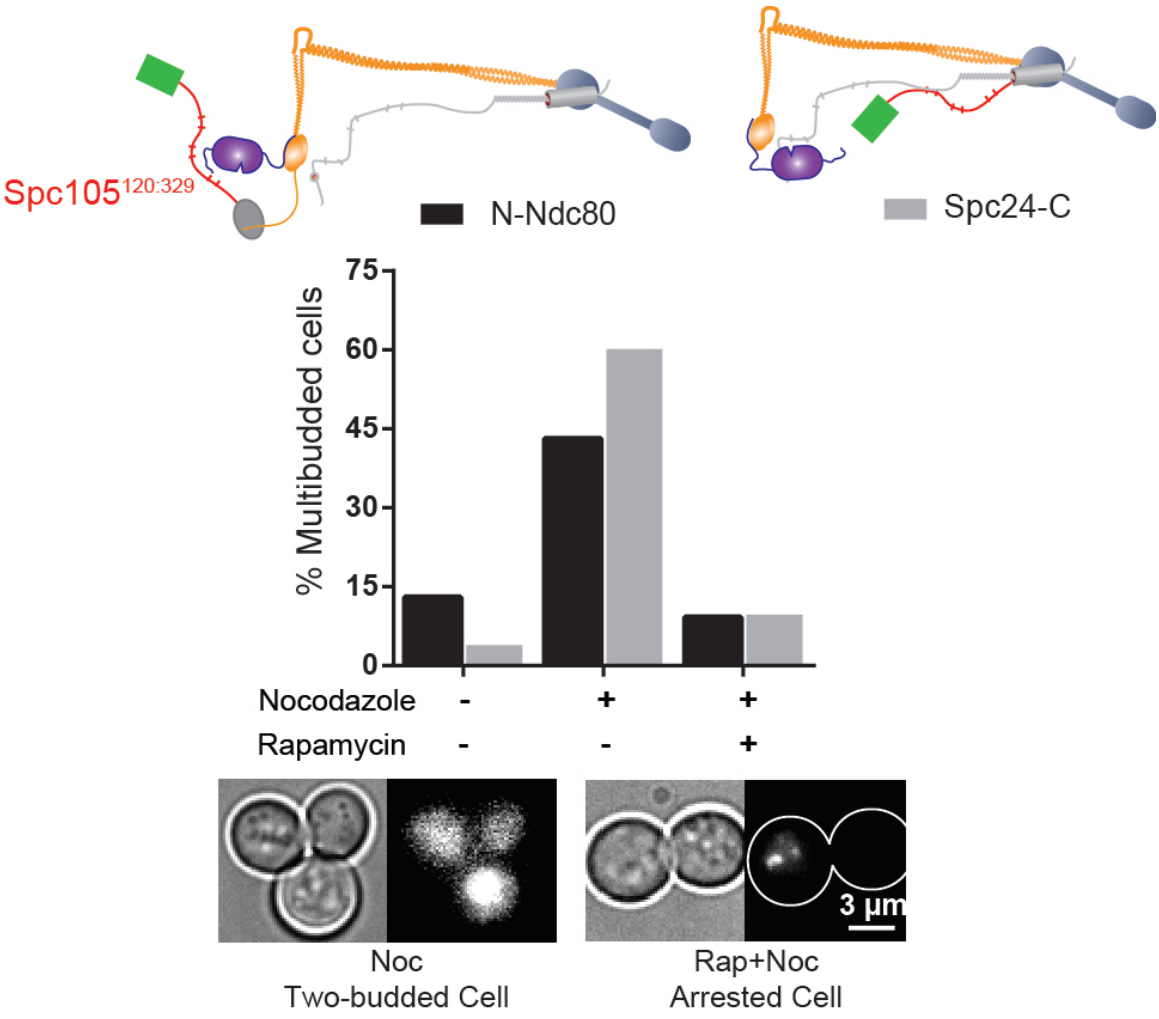

Figure 3.15: **Spc105$^{120:329}$ restores the SAC when it is anchored to unattached kinetochores in SAC-null strains** Top: Experimental scheme. Bar graph: Fraction of nocodazole-treated cells with two buds in the presence and absence of rapamycin in cells expressing spc105-6A (see micrographs on the left). Note the diffuse nuclear localization of Spc105$^{120:329}$ in the absence of rapamycin. When Spc105$^{120:329}$ was anchored either at N-Ndc80 or at Spc24-C, it restored the SAC. The cells arrested with large buds (transmitted light micrograph on the right). In this condition, Spc105$^{120:329}$ is visible as multiple puncta corresponding to kinetochore clusters that form when budding yeast cells are treated with nocodazole. Data represent mean

from 2 independent trials. More than 100 cells were scored for each treatment.

3.3 Discussion

Our work yields critical insights into how the protein architecture of the budding yeast kinetochore enables attachment-sensitive SAC signaling (Figure 3.16a). We find that catalytically active Mps1 binds to a site located in the outer kinetochore even when the kinetochore is attached. Based on our findings and published data [*Kemmler et al.*, 2009; *Nijenhuis et al.*, 2013; *Guimaraes et al.*, 2008], we propose that this site corresponds to the CH-domain of Ndc80. We also demonstrate that a persistent interaction between Spc105 and Mps1 is both necessary and sufficient to activate the SAC. These findings lead to an elegant model for the attachment-sensitive operation of the SAC (Figure 3.16b-c). In unattached kinetochores, close physical proximity between the CH-domains of Ndc80 and the phosphodomain of Spc105 allows Mps1 to phosphorylate Spc105, and also enables subsequent steps in SAC signaling [*Jelluma et al.*, 2010; *Maldonado and Kapoor*, 2011; *Hewitt et al.*, 2010; *Tipton et al.*, 2013; *Kim et al.*, 2010; *London and Biggins*, 2014]. End-on MT attachment to the kinetochore separates the CH-domains and the phosphodomain of Spc105 likely by pulling the CH-domains outwards and by restraining phosphodomain in the inner kinetochore. Additionally, the Dam1 complex, which is recruited after the formation of end-on attachment [*Li et al.*, 2002], may act as a physical barrier that prevents further interaction between Mps1 and Spc105. A combination of these events leads to SAC silencing.

The control of SAC signaling by the physical separation of two protein domains is conceptually equivalent to the operation of a mechanical switch. As the two terminals of this MT-operated switch, Ndc80 complex and Spc105 must be capable of binding MTs and changing their positions and/or conformations in response to MT-binding. Accordingly, the Ndc80 complex binds to MTs via the CH-domains [*Ciferri et al.*, 2008]. Known flexibilities in its structure should also allow it to change conformation

in response to MT binding [*Joglekar et al.*, 2009; *Aravamudhan et al.*, 2014; *Wang et al.*, 2008; *Tien et al.*, 2014; *Wei et al.*, 2006]. Spc105 also binds MTs, and this may play a role in restraining its otherwise unstructured phosphodomain in the inner kinetochore [*Pagliuca et al.*, 2009; *Espeut et al.*, 2012]. Finally, the low cellular abundance of the Mps1 kinase is crucial for the effective operation of this mechanical switch. If Mps1 is highly abundant, it can phosphorylate Spc105 through diffusive interactions, cause aberrant SAC activation, and thus effectively override the kinetochore-based switch [*Fraschini et al.*, 2001; *Hardwick et al.*, 1996].

While our work defines the off state of the mechanical switch, further work is needed to define its on state. The first key question is whether the CH-domain of Ndc80 is the only Mps1 recruitment site that is necessary for SAC signaling. Our findings and published data strongly argue for this to be the case. We find that the phosphorylation of Spc105 by Mps1 is both necessary and sufficient for SAC signaling. Therefore, the only activity that the Ndc80 complex can contribute to the SAC is the recruitment of Mps1. Accordingly, the Ndc80 complex is necessary for SAC signaling [*Pagliuca et al.*, 2009; *McCleland et al.*, 2003; *DeLuca et al.*, 2003], and the CH-domain binds Mps1 [*Kemmler et al.*, 2009; *Nijenhuis et al.*, 2013]. The second key question is how the architecture of the unattached kinetochore, despite its inherent flexibility, promotes optimal interaction between Mps1 and Spc105. Answers to these questions will further validate and complete the cell biological description of the mechanical switch model for the SAC.

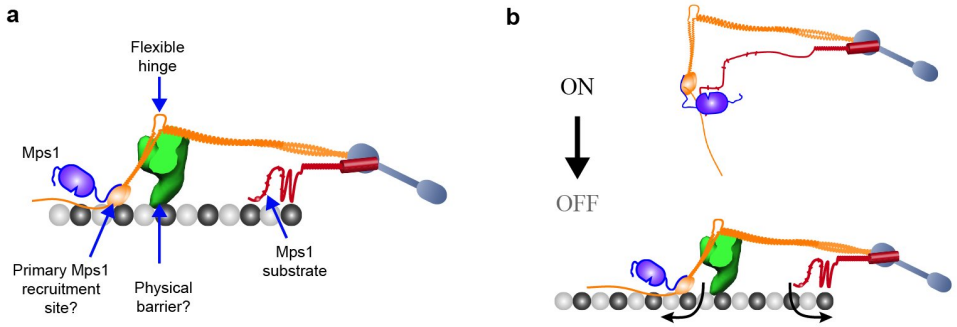

Figure 3.16: **Mechanical switch model for attachment-sensitive SAC signaling.** (a) Key features of the yeast kinetochore-microtubule attachment and their proposed roles in SAC signaling. (b-c) The on and off positions of the mechanical switch.

Whether the mechanical-switch model is applicable to the kinetochore in other eukaryotes is also an important question. Higher eukaryotes employ additional mechanisms that promote SAC silencing [*Nijenhuis et al.*, 2013; *Howell et al.*, 2001]. Moreover, in other organisms, the forced localization of Mps1 in the outer kinetochore or Mad1 in the inner kinetochore activates the SAC [*Ito et al.*, 2012; *Maldonado and Kapoor*, 2011; *Ballister et al.*, 2014; *Kuijt et al.*, 2014]. These differences may be because the budding yeast kinetochore stably binds exactly one MT in metaphase, whereas the kinetochores in most eukaryotes bind dynamically to many MTs. A fraction of these MT-binding sites are unattached even in metaphase [*McEwen et al.*, 1997], creating the possibility of cross-phosphorylation of SAC proteins localized in one attachment site by Mps1 localized within adjacent sites. Despite these differences, key elements of the SAC switch are highly conserved from yeast to humans. Components of the SAC switch: Mps1, the Ndc80 complex, and Spc105, and their nanoscale organization are highly conserved [*Wan et al.*, 2009]. Intriguingly, even though the Dam1 complex is absent in humans, the human kinetochore recruits other MT-binding proteins in the same position as that of the Dam1 complex in the yeast kinetochore [*Zhang et al.*, 2012; *Daum et al.*, 2009; *Varma et al.*, 2012; *Hsu and Toda*, 2011]. This striking conservation of key proteins and their architecture suggests that the kinetochore in other eukaryotes may encode a similar mechanical switch to control the SAC.

CHAPTER IV

Operational characteristics of SAC signaling from unattached kinetochores

4.1 Introduction

Chromosome segregation during cell division requires that the kinetochore, a multi-protein machine built on each chromosome, is stably attached to the tips of spindle MTs. Kinetochores that lack MT attachment recruit an array of proteins and generate a biochemical signal to stall cell cycle progression. Formation of stable MT attachment disrupts the kinetochore-based SAC signal generation, and enables cell cycle progress.

For effective operation, the SAC must meet three requirements: it should be responsive to the attachment state of individual kinetochores; it must be highly sensitive so that even one unattached kinetochore can arrest the cell cycle; and it must be amenable to rapid silencing to avoid unnecessary delays in the progression of the cell cycle [*Nasmyth*, 2005; *Doncic et al.*, 2005; *Sear and Howard*, 2006]. To meet these requirements, the SAC imposes unique and conflicting constraints on the bio-

chemical steps that constitute SAC signaling. The responsiveness of SAC signaling is ensured by its exclusive origin at unattached kinetochores. The kinetochore protein, Spc105/KNL-1 provides the physical platform to recruit SAC proteins. However, highly localized signaling limits the number of SAC proteins that initiate signaling, and therefore the rate of signal generation, to the copy number of Spc105. This number can be very small: a kinetochore in budding yeast contains only 5-8 Spc105 molecules [*Aravamudhan et al.*, 2013; *Joglekar et al.*, 2008, 2009]. Despite this small number, single yeast kinetochores activate the SAC and delay the cell cycle [*Dick and Gerlich*, 2013b; *Collin et al.*, 2013; *Heinrich et al.*, 2013]. Since a single unattached kinetochore can arrest the cell-cycle [*Rieder et al.*, 1994; *Spencer and Hieter*, 1992], it is reasonable to expect that the cumulative signal generated by many unattached kinetochores will not scale proportionally but saturate [*Doncic et al.*, 2005]. Saturation of the cumulative signal will avoid unnecessary cell cycle delays that can lead to apoptosis [*Tanaka et al.*, 2005]. To understand whether and how SAC signaling meets these requirements, it is necessary to define the kinetochore-intrinsic and extrinsic mechanisms that modulate, and potentially optimize, SAC biochemistry.

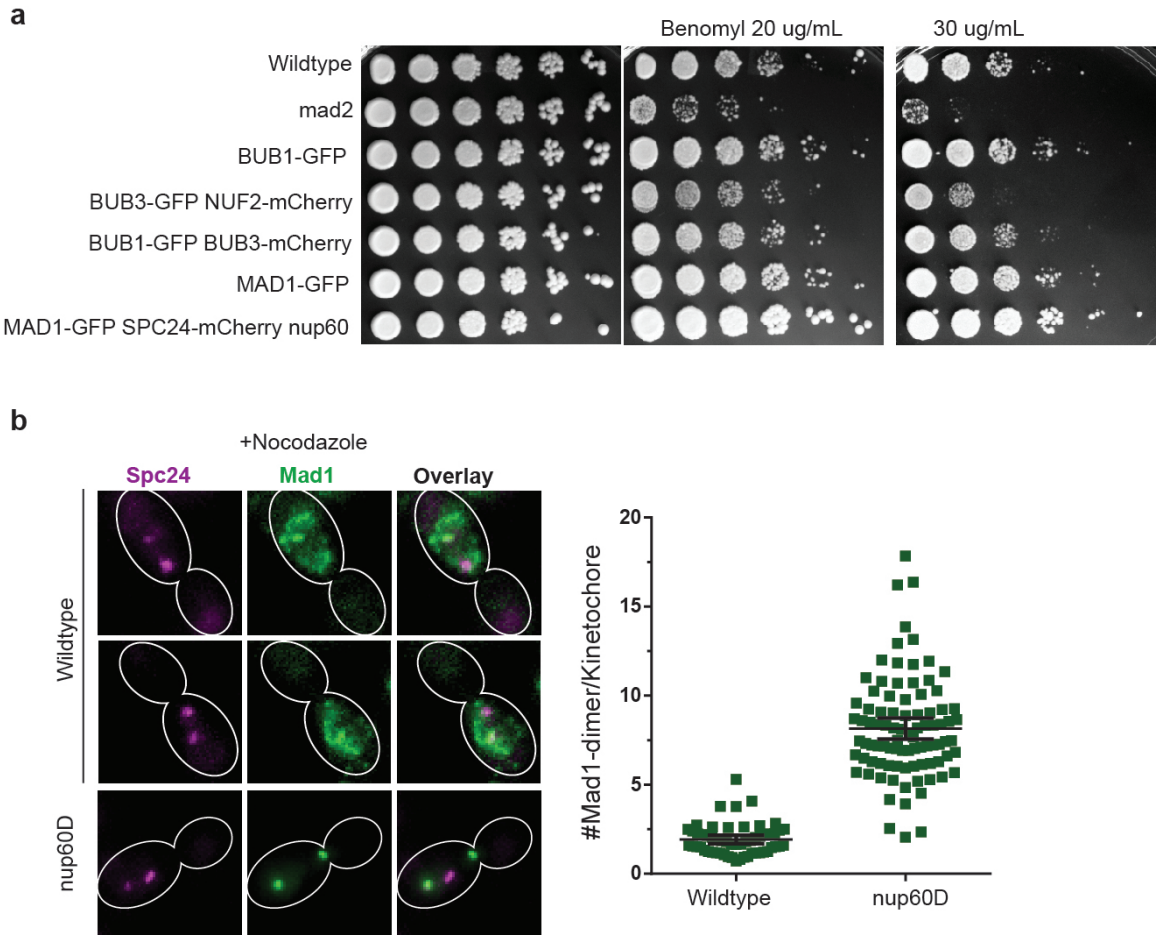

Figure 4.1: **Characterization of experimental strains expressing fluorescent chimeras of SAC proteins** (a) 10-fold serial dilutions of indicated strains frogged on YPD or plates containing 20 or 30 μg/ml of benomyl. Strains expressing Bub1-GFP, Bub3-GFP, and Mad1-GFP are resistant to benomyl. Therefore, the C-terminal fluorescent tags on SAC proteins do not interfere with their SAC functionality. (b) Representative images show the localization of Mad1-GFP following nocodazole treatment in NUP60 or nup60 strains. Quantification for both cases in nocodazole is shown in the right. The SAC-independent localization of Mad1-GFP interferes with accurate measurements of Mad1 localizing to the kinetochores in nocodazole-treated cells. Therefore, we used strains lacking Nup60, a nuclear pore protein responsible for Mad1 localization to the nuclear envelope. This reduced nuclear pore association of Mad1-

GFP. However, it likely increases the effective concentration of Mad1-GFP in the cell and hence the binding at unattached kinetochores. However, as previously reported, the lack of Nup60 does not affect the ability of Mad1 to participate in SAC signaling [*Scott et al.*, 2005] (See (a) above).

4.2 Results

To understand the in vivo operation of the SAC, we quantified the steady-state activity of its kinetochore-based reactions in budding yeast. We conceptualized the highly complex biochemical interactions of the SAC as a cascade of three bi-molecular reactions as a first approximation (Figure 4.2a). In this simple conceptualization, the number of kinetochore-localized SAC proteins directly reveals the respective reaction product. The numbers of kinetochore-localized Bub1 and Mad1 are particularly informative, because they report on the number of Mad1 binding sites and the number of Mad1-Mad2 templates that catalyze the generation of the inhibitory signal [*Dick and Gerlich*, 2013b; *Collin et al.*, 2013; *Heinrich et al.*, 2013; *London et al.*, 2012; *Primorac et al.*, 2013; *London and Biggins*, 2014] (Figure 4.2a). To measure these numbers, we created unattached kinetochores in yeast cells expressing fluorescent protein chimeras from the endogenous promoters. We verified that the chimeras complimented the functions of the respective wild-type proteins (Figure 4.1a). To enable accurate quantitation of kinetochore-localized Mad1, we deleted the NUP60, which encodes the nuclear pore protein that indirectly anchors Mad1 at the nuclear envelope [*Scott et al.*, 2005]. Although this mutation increases the effective concentration of Mad1 in the nucleus, it does not affect SAC signaling negatively (Figure 4.1a-b) [*Scott et al.*, 2005; *Yuen et al.*, 2007]. With this strategy, we can count molecules with single molecule sensitivity [*Aravamudhan et al.*, 2013]. We started our analysis by measuring the number of kinetochore-localized Bub1 and Mad1 molecules in cells containing exactly one pair of unattached sister kinetochores (Figure 4.2b). Molecular details of the biochemical reactions and the known copy number of Spc105 enabled us to calculate the maximum number of binding sites for these proteins (Table 1). With 6 MELT motifs in each Spc105 that binds Bub3-Bub1 upon phosphorylation by Mps1, two unattached kinetochores offer a maximum of 30 binding sites [*London et al.*, 2012; *Primorac et al.*, 2013], and probably the same number of sites for Mad1

dimers that binds Bub1 upon phosphorylation of the latter by Mps1 [*London and Biggins*, 2014]. However we measured only 18.34±6.8 molecules (Figure 4.2b). Thus, on average, only 2 out of the 6 MELT motifs on each Spc105 molecule are occupied by the Bub3-Bub1 complex. Interestingly, the two kinetochores recruited twice as many Mad1 dimers as Bub1 molecules (37.3±8.12 dimers/kinetochore). Since each kinetochore in yeast represents exactly one MT attachment site, these measurements provide the steady-state concentration of the SAC products at the unique resolution of a single-attachment site.

Next, we tested how the cumulative number of SAC proteins recruited by unattached kinetochores scaled as the number of unattached kinetochores increases. We generated two different defined numbers of signaling kinetochores: nocodazole treatment created 10 ± 2 unattached kinetochores, and forcing the localization of Mps1 at the kinetochore by anchoring triggered SAC signaling from all ≈ 32 attached kinetochores (see Methods for details, Figure 4.2c and Figure 4.3a-c). We found an inverse, non-linear correlation between the number of signaling kinetochores and the number of Bub1 and Mad1 molecules recruited by each kinetochore (Figure 4.2d, average number of molecules per kinetochore is shown in Figure 4.3d). In the extreme case, wherein all 32 kinetochores are SAC active, each Spc105 molecule recruited at the most one Bub3-Bub1 complex. This number was independent of the position of anchored Mps1, suggesting that the accessibility of Spc105 by the kinetochore-anchored Mps1 does not affect the SAC signaling induced (Figure 4.3e). Importantly, the number of Mad1-dimers bound to the kinetochore scaled linearly with the number of Bub1 molecules maintaining the 2:1 Mad1:Bub1 stoichiometry in each case, irrespective of the number of signaling kinetochores (Figure 4.2e).

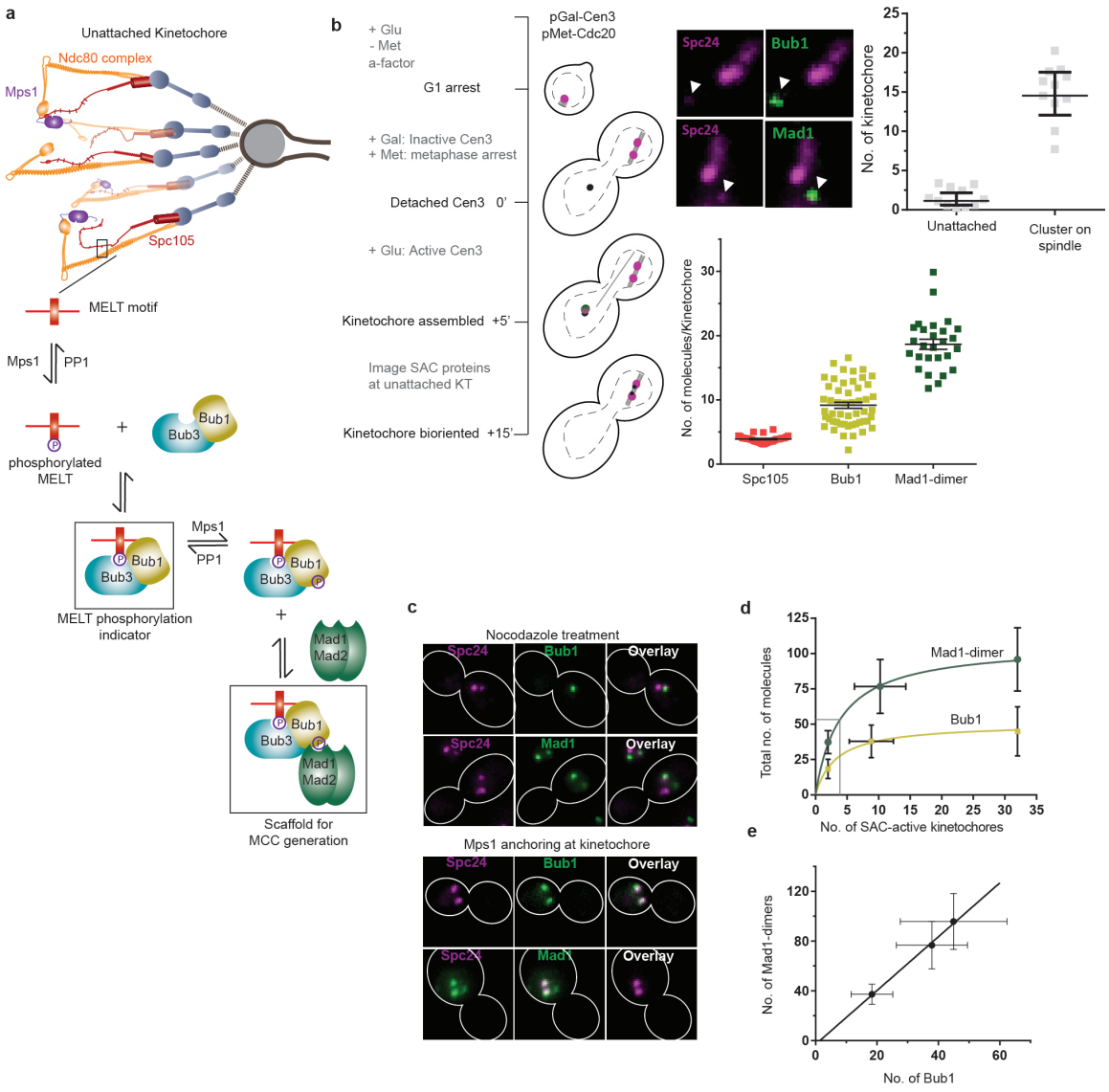

Figure 4.2: **Cumulative signaling capacity of kinetochores saturate with increasing number of unattached kinetochores in the cell** (a) Schematic of biochemical reactions that constitute SAC signaling at the unattached kinetochore. Each step is represented as a bimolecular reaction. Mps1 kinase phosphorylates MELT motifs in Spc105 which promotes binding of Bub3-Bub1 complex [*London et al.*, 2012; *Primorac et al.*, 2013], which in turn recruits Mad1-Mad2 hetero-tetrameric complex upon phosphorylation of Bub1 by Mps1 [*London and Biggins*, 2014]. Mad1-Mad2

bound to kinetochore catalyzes the generation of SAC signal [*De Antoni et al.*, 2005]. The involvement of Mps1 phosphorylation in each step of this cascade is notable [*London et al.*, 2012; *London and Biggins*, 2014; *Hewitt et al.*, 2010]. It probably localizes the signaling cascade to unattached kinetochores, and ensures that it occurs only when the kinetochore is unattached. (b) Left: Schematic to generate a single-pair of unattached kinetochores. Right: Micrographs show localization of Bub1-GFP and Mad1-GFP to the unattached kinetochores labeled with Spc24-mCherry, localizing away from the bioriented kinetochore clusters. Quantification on the right shows a $\approx$ 2:15 distribution of kinetochores amongst the unattached cluster that recruited SAC proteins and each kinetochore cluster on spindle, respectively. Scatter plot in the bottom presents the number of Bub1-GFP and Mad1-GFP dimers localizing to each unattached kinetochore. The experiments were repeated at least twice and the scatter plots (mean $\pm$ 95% confidence interval) present pooled data. (c) Representative micrographs show the localization of SAC proteins to unattached kinetochore cluster consisting of $\approx$ 10 kinetochores in nocodazole-treated cells (top) and to all 32 bioriented kinetochores, when Mps1 was anchored at Ndc80 (bottom). (d) Number of Bub1 or Mad1-dimers (mean $\pm$ s.d.) bound to kinetochores with increasing number of SAC active kinetochores. 2, $\approx$ 10 and 32 signaling kinetochores were generated using techniques described in (b) and (c). Gray line marks half-maximal binding for Mad1-dimers. The curves present fit to a bimolecular saturation binding model. (e) Mad1-GFP dimers recruited to the kinetochores (data presented in (d) above) increases linearly with the number of Bub1-GFP at the kinetochores at a 2:1 proportionality. Error bars represent mean $\pm$ s.d.

Protein	Moleculescell [*Ghaemmaghami et al.*, 2003]	Estimated nuclear concentration (nM)	Measured concentration (nM)
Bub1	414	230	< 81 nM (western blot)
Bub3	1430	794	-
Mad1	656	364	-
Mad2	1110	616	-
Bub1-Bub3	-	> 52 (kd < 3.6 uM) [*Larsen et al.*, 2007]	28 nM
MELTp (at 10 unattached kinetochores)	200 (Ref. [*Joglekar et al.*, 2006])(> 4 MELTp/Spc105)	111	-

Table 4.1: **SAC protein numbers and concentration that affect SAC biochemistry** Concentration estimated assuming a nuclear volume of $2.9\mu m^3$ ref. [*Jorgensen et al.*, 2007]

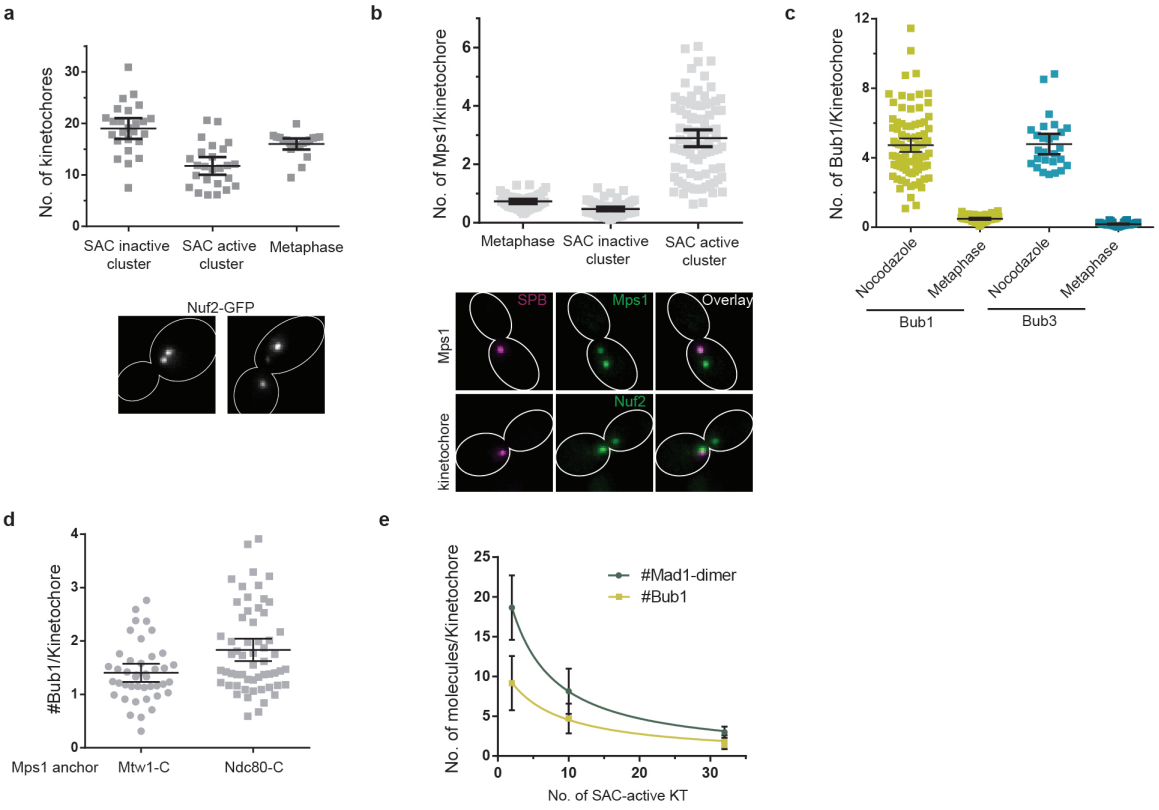

Figure 4.3: **Establishing techniques to generate defined numbers of signaling kinetochores in the cell** (a) Number of kinetochores present in clusters in cells treated with nocodazole compared to that aligned in metaphase spindle. Spindle depolymerization with nocodazole creates 2-3 clusters of kinetochores in the cell as previously described. The clusters with lesser number of kinetochores (≈10) recruit the SAC proteins and therefore defined as 'SAC active', whereas the larger 'SAC inactive' cluster (with ≈ 20 kinetochores) recruits little Bub1 and no Mad1 [*Aravamudhan et al.*, 2015]. (b) Localization of Mps1 to kinetochore clusters (defined in (a)) in nocodazole-treated cells relative to bioriented kinetochores in cells artificially arrested in metaphase through Cdc20 depletion [*Aravamudhan et al.*, 2015]. Horizantal bars represent mean ± 95% confidence intervals. Preferential recruitment of SAC proteins to the smaller kinetochore clusters is consistent with this biased localization

of Mps1 at these clusters. (c) Bub1 and Bub3 localize exclusively to unattached kinetochores in nocodazole-treated cells and are removed in the presence of attachment in metaphase. The 1:1 stoichiometry between Bub1 and Bub3 at the kinetochore is consistent with the specific binding of Bub1-Bub3 complex to the phosphorylated MELT motifs in Spc105. Horizontal bars represent mean ± 95% confidence intervals. (d) Similar quantities of Bub1 are recruited to kinetochore when Mps1 is anchored at the indicated kinetochore locations, which are separated by ≈ 24 nm along the MT axis. (e) Number of molecules of Bub1-GFP and Mad1-GFP dimers (mean ± s.d.) recruited by each kinetochore decreases with increasing numbers of unattached kinetochores in the cell.

We next investigated factors that limit the steady-state occupancy of Spc105 by the Bub3-Bub1 complex. These factors may be kinetochore-intrinsic, e.g. phosphoregulation of Spc105 by Mps1 and Glc7 [*Zhang et al.*, 2014], cooperativity in SAC protein recruitment by Spc105, etc [*Krenn et al.*, 2014; *Kern et al.*, 2014].; or kinetochore-extrinsic, e.g. the cellular concentration of SAC proteins [*Heinrich et al.*, 2013]. We first tested whether multiple copies of Spc105 within each kinetochore acted cooperatively (positive or negative) to recruit Bub3-Bub1. We systematically reduced the average number of Spc105 molecules per kinetochore in order to indirectly interfere with cooperative recruitment (Figure 4.4a). Even though Spc105 is an integral kinetochore protein, neither kinetochore bi-orientation nor the recruitment of the Ndc80 complex was affected even when the kinetochore contained only ≈ 1 Spc105 molecule on average (Figure 4.4b and Figure 4.5a). Therefore, any changes in SAC protein recruitment can be attributed solely to the reduced number of Spc105 molecules.

We reduced the average number of Spc105 molecules per kinetochore and measured the number of Bub1 molecules per kinetochore in cells treated with nocodazole (Figure 4.4b). As the cumulative number of signaling Spc105 molecules decreased, the total number of Bub1 molecules also decreased (Figure 4.4c). However, the number of Bub1 molecules per Spc105 increased modestly (Figure 4.5d). It is informative to contrast the result of this experiment, wherein the number of Spc105 molecules was reduced but the number of signaling kinetochores remained the same, with the result of a previous experiment wherein the number of signaling kinetochores was reduced, but the number of Spc105 molecules per kinetochore remained the same (Figure 4.2d vs. Figure 4.5b).

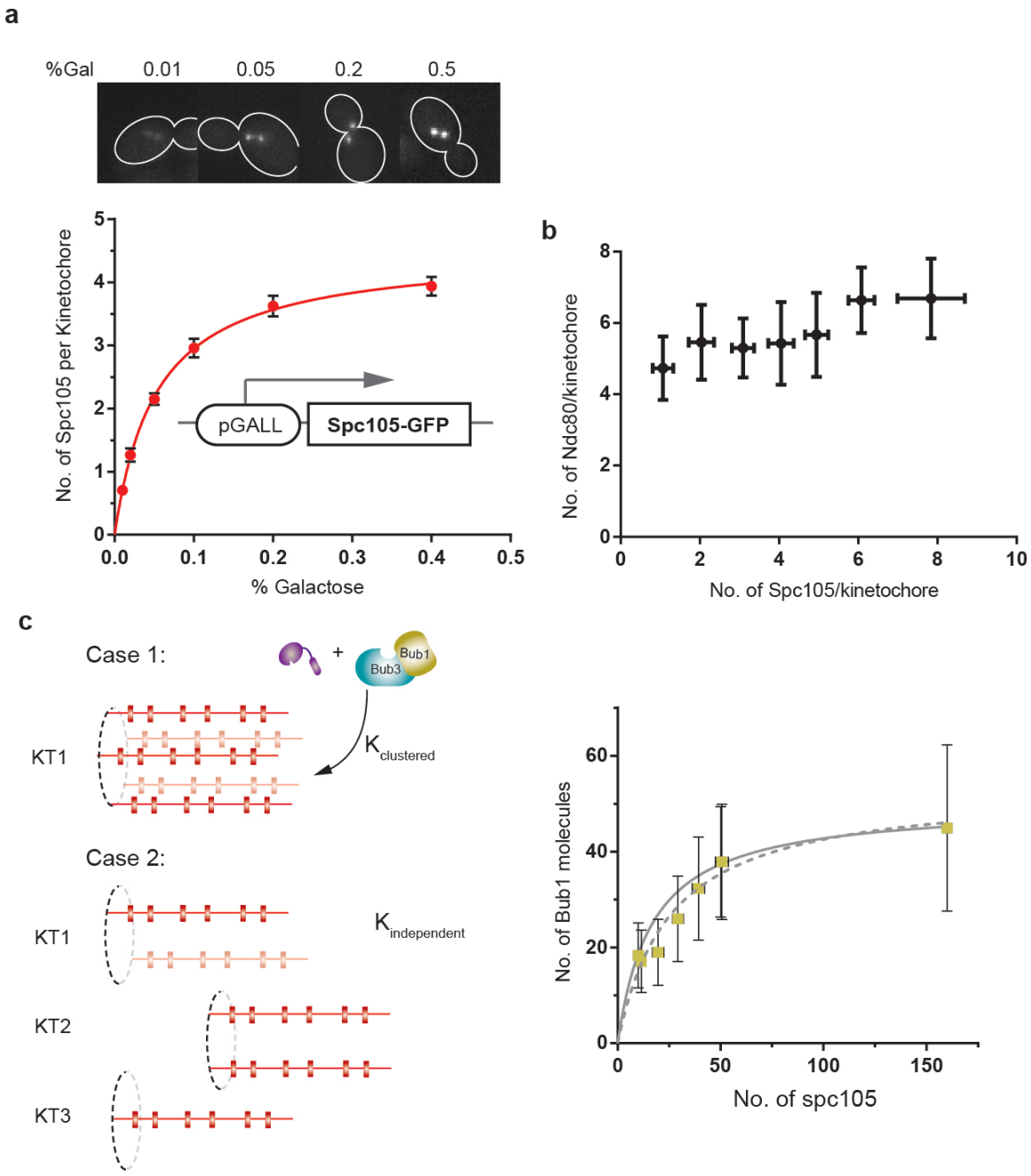

Figure 4.4: **Multiple copies of Spc105 at the kinetochore act independently in recruiting SAC proteins** (a) Representative micrographs at the top display differential recruitment of Spc105-GFP at the kinetochore upon controlled expression from a pGALL promoter at different concentrations of galactose in the cell culture medium. The corresponding quantification (mean ± s.e.m.) of Spc105-GFP at the

kinetochore is presented in the bottom. Curve represents saturation binding fit of the data. (b) Recruitment of Ndc80-mcherry to kinetochores containing different copy numbers of Spc105-GFP, like the experiment in (a). Individual data points represent mean ± s.d. from binned data. (c) Left: Cartoon represents the experimental strategy. Case 1 presents the wild-type scenario where each kinetochore contains ≈ 5 Spc105 molecules. Case 2 presents reduced expression from galactose-inducible promoter where each kinetochore contains less Spc105 such that 5 Spc105 molecules are distributed amongst three kinetochores. Bub3-Bub1 binding to phosphorylated MELT motifs in both scenarios is the parameter of interest. Right: Recruitment of Bub1 (mean ± s.d.) to ≈ 10 kinetochores containing different numbers of Spc105 (due to controlled expression from pGALL promoter), overlaid on data from Figure 4.2d. Dashed and solid curves represents saturation binding fit for data from Figure 4.2d or the entire data set presented, respectively.

Bub1 recruitment per Spc105 is the same in both cases, revealing that the number of Bub1 recruited depends only on the total number of Spc105 molecules, and not on how the molecules are distributed among the signaling kinetochores (Figure 4.4c). Thus, Bub1 recruitment by Spc105 molecules is additive, and not cooperative. The number of Mad1 molecules did not change significantly in this experiment, most likely because of the relatively modest reduction in Bub1 and 2:1 Bub1:Mad1 stoichiometry.

Based on the above results, we concluded that either the dynamic phosphoregulation of Spc105 [*Zhang et al.*, 2014] or the cellular concentration of Bub3-Bub1 limits the recruitment of Bub1. Testing the role of Spc105 phosphoregulation using Mps1 over-expression and Glc7 inhibition was complicated by the global changes resulting from the perturbation of Mps1 or Glc7 activities (data not shown). Therefore, we focused on the concentration of Bub3 and Bub1. Bub1 has the lowest cellular abundance amongst SAC proteins: there are $\approx$ 150 molecules per cell as compared to $\approx$ 400 molecules of Bub3 and 600 molecules of Mad1 (Table 4.1, ref. [*Ghaemmaghami et al.*, 2003]). Therefore, we tested whether Bub1 overexpression can increase its own steady-state binding to unattached kinetochores, and that of downstream SAC proteins [*Larsen et al.*, 2007] (Figure 4.6, cartoon). When over-expressed using a galactose-inducible promoter, Bub1 bound to unattached kinetochores in significantly higher numbers than what was measured under wild-type expression (Figure 4.6a). At maximal expression (at least 25-fold higher wild-type levels, Figure 4.5d), 28$\pm$0.8 Bub1 molecules bound to each kinetochore (5.6$\pm$0.16 per Spc105 on average, Figure 4.6a). The binding of additional molecules was mediated by phosphorylated MELT motifs, because the number of kinetochore-bound Bub3 molecules increased proportionally with Bub1 (Figure 4.6b).

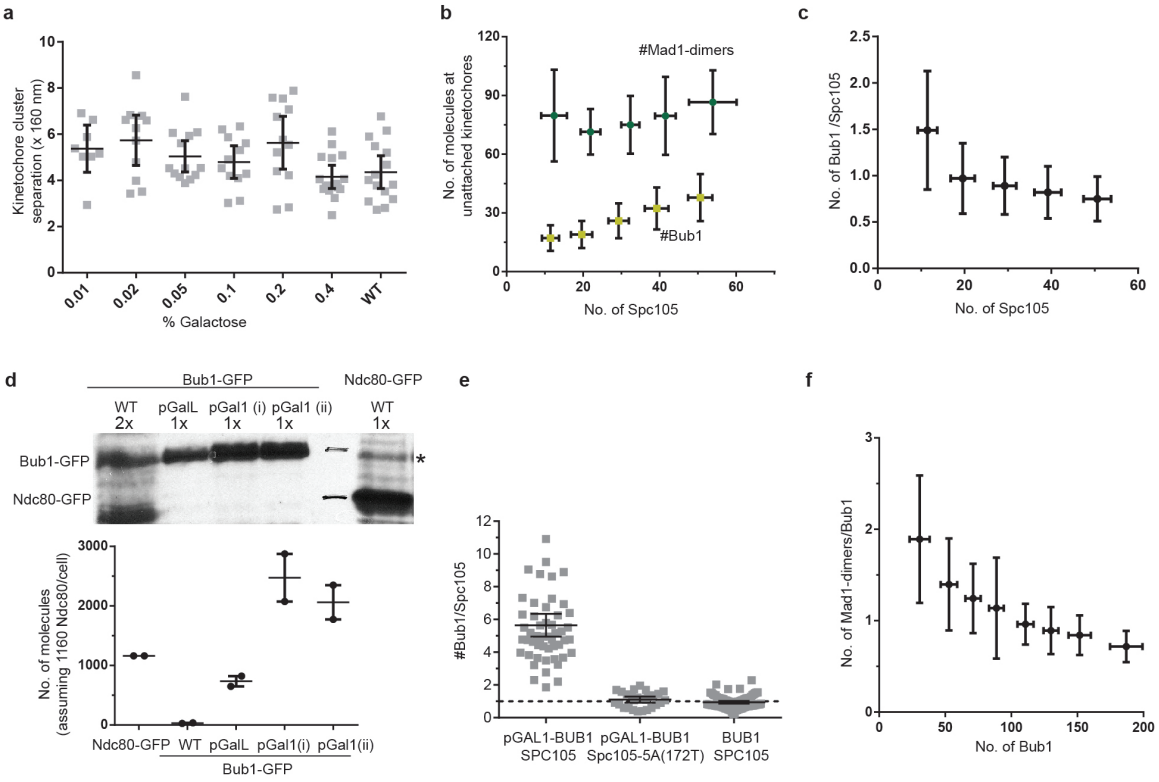

Figure 4.5: **Establishing techniques to generate defined numbers of signaling kinetochores in the cell**(a) Separation between kinetochore clusters in metaphase (mean ± 95% confidence intervals) does not vary significantly with reduced Spc105 copy numbers at the kinetochore upon under-expression from pGALL. (b) Changes in the recruitment of Bub1 and Mad1-dimers to kinetochore cluster in nocodazole-treated cells with varying number of Spc105 at the kinetochore (achieved through controlled expression from pGALL. Data points on the graph represent binned mean ± s.d with a bin size of numbers of Spc105 =10. Mad1 numbers do not vary significantly, whereas Bub1 numbers decrease with decrease in Spc105 at the kinetochore. (c) Changes in the number of Bub1 bound per Spc105 (mean ± s.d.) from the same experiment as in (b) above. (d) Immunoblotting of Bub1-GFP expressed from indicated promoters or Ndc80-GFP expressed from its endogenous locus (WT) probed with -GFP antibody. Bub1-GFP overexpression from pGAL1 promoter was measured

in strains expressing Spc105 (i) and Spc105-5A(172T) (ii). Twice as much lysate was loaded for Bub1-GFP expressed from its endogenous locus (WT), which was still undetectable in the blots. * indicates a non-specific band. 1.5% Galactose was used for inducing Bub1 expression from GAL promoters. Graph represents quantification of copy numbers of proteins in the cell from western blots (mean ± s.e.m.) from two experimental repeats. Bub1 numbers were calculated from band intensities (after subtracting background and signal from the non-specific band) assuming 1160 Ndc80 molecules per cell. (e) Number of Bub1 bound to unattached kinetochores in nocodazole upon overexpression from pGAL1 (quantified in (c)) in cells expressing wildtype Spc105 or an allele with a single phosphorylatable MELT motif. Bub1 recruitment in the latter case is comparable to its recruitment at endogenous expression to wildtype Spc105. (f) Number of Mad1-mCherry dimers recruited per Bub1-GFP (mean ± s.d.) decreases with recruitment of Bub1-GFP at unattached kinetochores in nocodazole upon over expression from from pGAL1.

To further confirm this, we overexpressed Bub1 in a strain expressing spc105-5A(172T), an Spc105 allele wherein 5 out of the 6 MELT motifs are non-phosphorylatable. Despite significant Bub1 over-expression, only 5.5+2.3 Bub1 molecules were recruited per kinetochore ($\approx$ 1 per Spc105, Figure 4.5d-e). Thus, Bub1 over-expression is sufficient to increase the steady-state binding of the Bub3-Bub1 complex.

We tested whether increased Bub1 recruitment leads to increased Mad1 binding to unattached kinetochores. Increased Mad1 binding will be significant, because it will provide additional templates for SAC signal generation [*Collin et al.*, 2013]. The number of Mad1 molecules increased robustly with the number of Bub1 molecules, with $\approx$ 3-fold increase at the highest Bub1 expression over wild-type conditions (Figure 4.6d). Interestingly, the stoichiometry between Mad1 and Bub1 gradually reduced from 2:1 at lower Bub1 concentrations to 1:1 at the highest concentration (Figure 4.5f). This is likely because either Mps1 phosphorylation of Bub1, which is essential for Mad1 binding, or Mad1 concentration in the cell limits recruitment. Our data suggests that the MELT motifs of Spc105 are efficiently phosphorylated by Mps1 in unattached kinetochores.

The recruitment of Bub3-Bub1 to the unattached kinetochore emerges as a key factor that modulates steady-state behavior of the kinetochore-based cascade. Therefore, we examined the binding affinity of MELT motifs for the Bub3-Bub1 complex by modeling Bub3-Bub1 recruitment to the kinetochore as a simple bimolecular reaction with ligand depletion. Assuming this mechanism, our in vivo data estimates the apparent dissociation constant for the MELT-Bub3-Bub1 complex as $\approx$ 37 nM (see Methods for details).

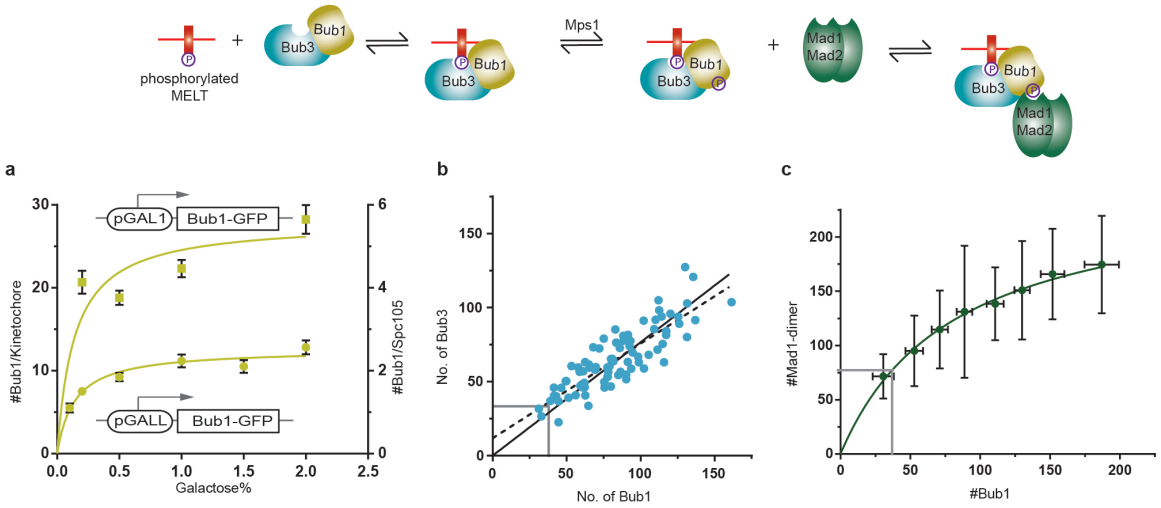

Figure 4.6: **Bub1 concentration in the cell limits the SAC signaling capacity of unattached kinetochores** Schematic at the top present the steady-state reaction products measured in the data below (a) Recruitment of Bub1-GFP to unattached kinetochores (mean ± s.e.m.) in nocodazole-treated cells upon overexpression of Bub1 from two different galactose-inducible promoters. The curves represent fit of the data to one-site specific binding model. The dissociation constant obtained from the fit for pGALL was used to constrain the fit pGAL1. (b-c) Increase in Bub3-mCherry or Mad1-mCherry dimers (mean ± s.d.) binding to unattached kinetochores in nocodazole upon overexpression of Bub1-GFP from pGALL as in (a). The dashed and solid lines in (b) are linear fits of the data unconstrained and constrained through origin, respectively. The curve in (c) represents fit of the data to one-site saturation binding. The gray lines represent the number of respective molecules that bind to kinetochores upon expression of Bub1-GFP at wild-type levels.

Although the comparison of in vivo and in vitro data is not always reliable, this value is an order of magnitude lower than the dissociation constant measured for a single MELT motif in vitro [*Primorac et al.*, 2013]. The significantly stronger binding observed in vivo could be the due to an unexpected intra-molecular cooperation amongst the six MELT motifs in each Spc105. To test this possibility, we created two Spc105 alleles: spc105-5A(172T) and spc105-5A(313T). These alleles containing 5 non-phosphorylatable MELT motifs, and a single phosphorylatable motif, either at the second or the last position from the N-terminus (Figure 4.7a).

We counted the number of Bub1 molecules recruited to unattached kinetochores in nocodazole-treated cells expressing the two Spc105 alleles. Based on the apparent dissociation constant for the wild-type Spc105, we expected that only $\approx$ 25% of the spc105-5A molecules should bind Bub3-Bub1. Surprisingly, we found that nearly 100% of the molecules of both spc105-5A(172T) and spc105-5A(313T) bound Bub3-Bub1 complex (Figure 4.7b). Mad1 recruitment by all these alleles maintained similar stoichiometry with Bub1 as in case of wild-type Spc105 (Figure 4.7c). The steady-state binding of Bub1 translates into a dissociation constant of 1.4 nM, which is significantly lower than that for the wild-type Spc105 molecule containing 6 MELT motifs (Table 2). In fact, the apparent binding affinity of a single Spc105 molecule containing two MELT motifs is significantly lower than that calculated for each independent motif (Figure 4.7b). This behavior is strongly suggestive of negative cooperativity: binding of the first Bub3-Bub1 complex to one of the MELT motifs in Spc105 lowers the affinity for subsequent binding.

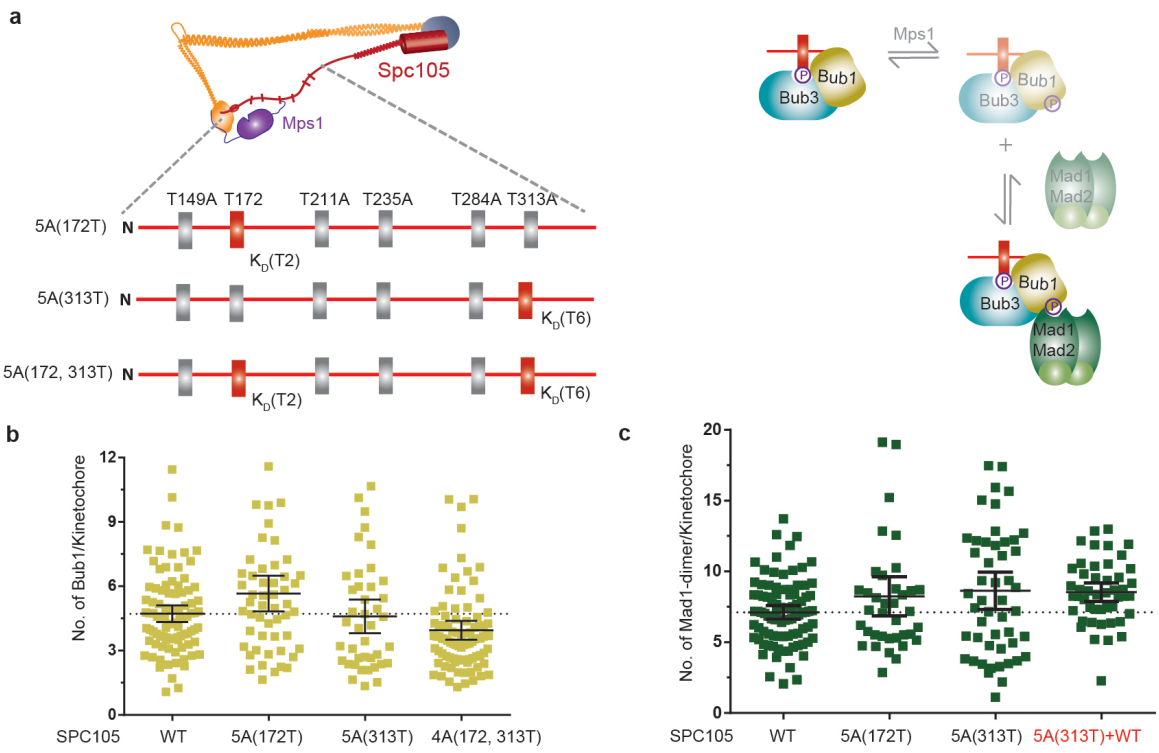

Figure 4.7: **Multiple MELT motifs within Spc105 exhibit negative cooperativity in binding Bub1-Bub3 complex** (a) Left: Cartoon depicts the likely relative localization of Mps1 bound to Ndc80 and the MELT motifs in Spc105 N-terminus. The motifs mutated to non-phosphorylatable forms are shown as grey bars. KD dissociation constant for Bub1-Bub3 binding to individual MELT motifs. Left: Cartoon shows the steady state reaction intermediates that are measured in (b) and (c). (b-c) Scatter plots (mean ± 95% confidence intervals) present the number of Bub1-GFP or Mad1-GFP dimers localizing per kinetochore in nocodazole-treated cells expressing the indicated variant of Spc105.

4.3 Discussion

Our work demonstrates that each step in the kinetochore-based reaction cascade of SAC signaling can be modeled effectively as a simple, bimolecular reaction. This analysis reveals novel features of the kinetochore-based signaling cascade of the SAC, as well as kinetochore-intrinsic and extrinsic mechanisms that modulate individual reactions in the cascade. We find that despite the very small copy numbers of Mps1 and Spc105 in the cell, Spc105 is maximally phosphorylated in unattached kinetochores and poised to recruit the maximal number of SAC proteins. Thus, the steady-state behavior of the first step in SAC signaling works like a switch. However, cellular concentrations of Bub1 and Mad1 modulate the activity of phosphorylated Spc105, and determine the upper limit on steady-state signaling from unattached kinetochores.

The limiting Bub1 and Mad1 concentrations in the cell also modulate the cumulative signal output from many unattached kinetochores. We find that the steady-state signaling from individual kinetochores scales inversely with the total number of unattached kinetochores in the cell. This inverse scaling is significant for two reasons. A small number of unattached kinetochores in a dividing cell must signal strongly in order to arrest the cell cycle. In contrast, when the cell contains a large number of unattached kinetochores, the steady-state signaling is automatically distributed among all the kinetochores. Consequently, the cumulative inhibitory signal generated saturates, potentially ensuring that the inhibition can be overcome in a reasonable time period after the last kinetochore establishes MT attachment.

Our analysis also uncovers key kinetochore-intrinsic mechanisms that modulate SAC signaling. We find that the yeast kinetochore can recruit 2 Mad1 dimers for every Bub1 molecule. This 2:1 stoichiometry between the two suggests that either Bub1 can bind two Mad1-dimers, or alternatively, a Bub1-dependent binding site

in the kinetochore also recruits Mad1 [*Scott et al.*, 2005]. In any case, additional Mad1-dimer may amplify the SAC signal generating capacity of the kinetochore. We also find that the 5-6 copies of Spc105 molecules within each kinetochore recruit SAC proteins independently despite their tight spatial clustering in the kinetochore [*Krenn et al.*, 2014; *Kern et al.*, 2014]. Instead, there is negative cooperativity in the binding of more than one Bub3-Bub1 complex to the same Spc105 molecule. We speculate that this negative cooperativity reflects the physical constraints imposed by the binding of the Bub3-Bub1 complex to Spc105, and subsequently, two Mad1-Mad2 hetero-tetramers. These events may induce a conformational change in the phospho-domain of Spc105, and make the binding of additional molecules less likely.

The proteins studied here are highly conserved from yeast to humans. Therefore, many of the mechanisms discussed here are likely to be conserved. At the same time, the complex signaling cascade of the SAC is also inherently adaptable. This adaptability will enable each organism or cell-type to optimize SAC signaling for unique cellular constraints such as the volume of the cell, chromosome number, the complexity of the spindle apparatus, the duration of the cell-cycle, etc. Our study identifies the kinetochore-based mechanisms that will play key roles in optimizing SAC signaling. It also provides the road-map for studying similar mechanisms in other eukaryotes.

CHAPTER V

Summary and Future directions

Accurate segregation of chromosomes during mitosis is essential for cell viability. This accuracy relies heavily on the SAC, which prevents anaphase onset until sister chromatids are attached to the spindle and are bioriented to track MTs into the daughter cells. SAC failure is implicated in cancer, embryonic lethality and other disease conditions [*Dobles et al.*, 2000; *Kitagawa and Rose*, 1999]. Enforcing checkpoint robustness or sometimes even inducing complete SAC failure are important strategies in treating these conditions [*Kops et al.*, 2005; *Huang et al.*, 2009]. Efficient design of such strategies requires a clear understanding how the SAC operates and knowledge of all the molecular players. My thesis work provides novel insights into the operation of the biochemical cascade of SAC at the kinetochore. The mechanisms presented here enhance our understanding of this fundamental process and also pave way for further studies.

5.1 Reconstructed kinetochore architecture sets the stage to understand its evolutionary design

The biggest challenge in understanding attachment-sensitive SAC signaling arises from the complexity of kinetochore architecture. Functions of a majority of kineto-

chore proteins rely on the spatial and molecular context in which they are present [*Santaguida and Musacchio*, 2009; *Cheeseman*, 2014]. A key achievement of the work presented here is the reconstruction of kinetochore architecture that elucidates the relative arrangement of multiple copies of protein complexes. This reconstruction was primarily facilitated by the ease of genetic manipulation in budding yeast, and the fact that each kinetochore binds to a single MT made it easier to interpret FRET measurements compared to other systems. This reconstruction in the presence of attachment shows that multiple copies of kinetochore proteins are well-aligned relative to each other along the length of the MT, and also likely distributed uniformly around the circumference [*Aravamudhan et al.*, 2014; *Joglekar et al.*, 2009]. This has important implications on how multiple copies of MT binding proteins track dynamic MT ends to move chromosomes, and also in the operation of SAC signaling (as discussed below).

The reconstructed kinetochore architecture from budding yeast also provides a foothold to investigate the mechanistic basis for the evolution of its structural features. Ongoing work in the lab will dissect how well-designed modifications in kinetochore architecture affect force generation, processivity of kinetochores and the resulting functionality in segregation. It is also interesting to think about how the length of centromeric foundation offered to build kinetochores evolved with the genome size and cellular/nuclear volume. Although the correlations between genome size and centromere length are very weak, it may be important to have more attachments above a threshold level for better force coupling with increasing genome size, and to work against the drag force experienced during chromosome motion [*Zhang et al.*, 2012; *Cherry et al.*, 1989]. Furthermore, having more attachment sites may also improve the overall processivity of the kinetochore, maintaining attachments over longer distances traversed during division. An experimental strategy of probing this aspect

would be to fuse chromosomes to make larger chromosomes. The processivity of a single kinetochore built on the centromere can be measured as a function of this increasing size of chromosomes.

It should also be possible to test the effect of load bearing capacity with purified kinetohcore particles by studying how these reconstituted particles are able to bear differently sized loads [*Akiyoshi et al.*, 2010]. The reconstituted systems can also be used to test how the processivity of kinetochores varies between tracking single versus bundled MTs to understand how the distance-to-traverse plays into the requirement for single vs. multiple attachment sites at each kinetochore [*Scott et al.*, 1992].

5.2 Mechanistic insights into SAC signaling enable investigation of its molecular components

The second part of my work provides insight into the mechanism of execution of SAC signaling by attachment-dependent kinetochore architecture. Elucidating this mechanism was enabled primarily by the first part of my thesis work that established the *in vivo* architecture of kinetochore. A key feature of this attached architecture is the alignment of multiple copies of protein complexes along the MT axis [*Aravamudhan et al.*, 2014]. Such alignment is important to allow the switch-like, attachment-sensitive operation of the SAC through spatial separation of Mps1 from multiple copies of Spc105 molecules with in the kinetochore, following attachment [*Aravamudhan et al.*, 2015]. If the molecules are staggered, then Mps1 can potentially phosphorylate staggered neighboring copies of Spc105 even in the presence of attachment. Perhaps this necessitates additional mechanisms such as attachment dependent removal of Mps1and stripping of SAC proteins following MT attachment

in higher organisms [*Howell et al.*, 2001; *Nijenhuis et al.*, 2013]. In scenarios where multiple MT attachment sites are present at each kinetochore, staggering and cross communication between adjacent sites may lead to aberrant SAC activation in the presence of Mps1 at attached kinetochores.

It will be interesting to examine the above hypothesis by mimicking higher order kinetochore in budding yeast. For instance incorporation of an additional centromeric sequence ($\approx$ 125 bp adjacent to the endogenous centromere on one of the chromosomes may initiate the formation of two kinetochores at proximal loci on the same chromosome [*Henikoff and Henikoff*, 2012]. If such a system works, it can be used to address a number of questions regarding force generation and SAC signaling at kinetochores containing multiple attachment sites. First of all, if the incorporated sequence makes multiple MT attachments, is budding yeast equipped to resolve merotelic attachments? If successful bipolar attachments are made in this system, how does the crosstalk between adjacent sites affect SAC silencing through the toggle-switch mechanism demonstrated in this work? Even further, how does this influence kinetochore-MT attachments and segregation during meiosis I, where the sisters have to make attachment to the same pole [*Watanabe*, 2012]?

Further work is also required to fully understand the biochemical roles for kinetochore components in operating the toggle-switch mechanism. Our data strongly suggest a primary role for Ndc80 CH-domains in recruiting Mps1 kinase to trigger SAC signaling. This requirement for Ndc80 has to be biochemically established. It will also be important to verify that the sole function of Ndc80 in SAC signaling is presenting Mps1. It should be possible to completely deplete Ndc80 (using degron tags) or cleave off its CH domain (using TEV protease cleavage sites) in synchronized cultures, and then test whether this leads to an SAC defect that can be completely

compensated by anchoring Mps1 at the kinetochore [*Kemmler et al.*, 2009; *Uhlmann et al.*, 2000]. This will also be important to support or rule out a role for Ndc80 in recruiting Mad1 to the kinetochore for SAC signaling [*Kemmler et al.*, 2009].

Next, the geometry and the minimal structural requirements for Ndc80 and Spc105 in SAC signaling is also an area that invites further investigation. For instance, how does the length of both Ndc80 and Spc105 affect their physical proximity, and thereby SAC signaling through positioning of Mps1 relative to Spc105. Are there favored conformations for Ndc80/Mps1 and Spc105 that promote maximal efficiency of the SAC cascade or is it simply a random, proximal positioning of the two in the absence of attachment that drives SAC signaling? It is important to note that this proximity is not only important in triggering Spc105 phosphorylation but also in driving downstream reactions, where Mps1 plays a significant role. This can be tested in parts with a bonsai version of Ndc80 that is shorter in length, and also by changing the length and flexibility of Spc105 N-terminus that contains the MELT motifs [*Ciferri et al.*, 2008; *Zhang et al.*, 2014; *Petrovic et al.*, 2010]. For instance, I have shown that even a single MELT motif (chapter 4, Fig 4.4) can sustain SAC signaling upon MT disruption with nocodazole. One can test how the signaling ability of this motif is affected, when the unstructured region of N-Spc105 is replaced with rigid, structured (predictable) motifs. Lastly, the role of Dam1 complex in acting as a barrier that prevents Spc105 phosphorylation upon MT attachment remains to be tested. This requires a clever strategy that can separate the role of Dam1 in making attachment, from that in silencing.

The role of phosphorylation of Mad1 and Mad2 in generating the SAC signal from kinetochores also remains an enigma [*Kim et al.*, 2010; *Hewitt et al.*, 2010]. The requirement for Mps1 in driving SAC from Mad1 artificially localized to the kineto-

chores implies the necessity for Mps1 in this reaction [*Maldonado and Kapoor*, 2011; *Ballister et al.*, 2014]. It has been known for a long time that Mps1 hyperphosphorylates Mad1 during SAC [*Palframan et al.*, 2006]. Identifying the phosphorylation sites in Mad1 and also those proposed in Mad2 will form the first step in systematically testing their roles in SAC. Ongoing work in the lab, initiated from the work presented here (by Alan Goldfarb), is aimed at identifying phosphorylation sites on Mad1. I further propose testing the sites on Mad2 concomitantly to dissect how phosphorylation at these sites influence conformational transition of Mad2 [*Kim et al.*, 2010]. It will also be interesting to induce reversible dimerization of Mad2 with Mps1 to understand if this is sufficient to induce the conformational transition in Mad2 and promote its incorporation in MCC.

5.3 Kinetochore-based SAC biochemistry provides the first step in understanding the operation of SAC

The primary goal of SAC signaling, when activated, is to stall cell cycle progression to ensure fidelity in genome segregation. In this context, it is important not just for the kinetochores to be responsive to attachment status, but also for the signal generated downstream to be strong to buy enough time to make correct attachments [*Meraldi et al.*, 2004; *Dick and Gerlich*, 2013a]. The kinetochore-based biochemical cascade of SAC provides the precursor to generate this signal. The work presented in Chapter 4 of this thesis provides insights into the regulatory mechanisms that operate at each step of this kinetochore-based biochemical cascade. This knowledge would allow further investigation of whether and how these parameters are utilized by cells to generate an optimal SAC signal that strikes a balance between robustness and optima. A starting point for this investigation would be to measure missegregation and

cell cycle delay as a function of biochemical perturbations used in this work in yeast, following an insult with nocodazole. This will provide an idea of how perturbations observed in the number of SAC proteins assembled at the kinetochores translate to the capacity to generate an effector signal that mediates cell cycle delay.

For a comprehensive understanding of the operation of SAC, future work should systematically answer the following: (1) What is the flux of SAC signal (i.e., Closed Mad2) indeed from an unattached kinetochore to achieve a complete inhibition of APC activity? In other words what fraction of Cdc20 should be sequestered in cells in order to effectively block APC [*Ciliberto and Shah*, 2009]? (2) How should the cells tune molecular biochemistry at the kinetochore to satisfy the above requirement, and finally, (3) how should these parameters scale with cellular volume, and the number and size of signaling kinetochores in the cell for an optimal performance? Purified and reconstituted *in vitro* system will provide a good way to systematically establish some of these parameters [*Kulukian et al.*, 2009]. Even better, Xenopus egg extracts will provide a beautiful mimic of the molecular complexity of the cells to study these parameters. Partial depletion or enrichment of selected SAC proteins in the extracts will allow measurement of MCC generation as a function of concentration of the respective elements [*Cross and Powers*, 2009; *Chen and Murray*, 1997]. To measure the rate of MCC generation as a function of different parameters, a real time reporter for MCC is needed. A FRET pair designed within purified MCC components can be used to measure the rate of MCC generation in extracts, from bulk FRET measurements [*Chao et al.*, 2012].

The ultimate aim of such comprehensive analysis will be to quantitatively define the minimal requirements of SAC components, at the level of kinetochore architecture, molecular affinities and also the relative concentrations of SAC protein machinery

that can drive optimal SAC signaling to ensure fidelity in chromosome segregation. Comprehensive mechanistic and quantitative understanding of the SAC cascade will enable us to model this process mathematically to predict whether SAC will succeed or fail under commonly observed perturbations that are linked to genetic instability and cancer, and also to identify the apt targets for therapy [*Kops et al.*, 2005; *Huang et al.*, 2009].

BIBLIOGRAPHY

BIBLIOGRAPHY

Akiyoshi, B., et al. (2010), Tension directly stabilizes reconstituted kinetochore-microtubule attachments., *Nature*, *468*(7323), 576–579, doi:10.1038/nature09594.

Alushin, G. M., V. H. Ramey, S. Pasqualato, D. A. Ball, N. Grigorieff, A. Musacchio, and E. Nogales (2010), The Ndc80 kinetochore complex forms oligomeric arrays along microtubules, *Nature*, *467*(7317), 805–810.

Alushin, G. M., V. Musinipally, D. Matson, J. Tooley, P. T. Stukenberg, and E. Nogales (2012), Multimodal microtubule binding by the Ndc80 kinetochore complex., *Nature structural & molecular biology*, *19*(11), 1161–7, doi:10.1038/nsmb.2411.

Amor, D. J., K. Bentley, J. Ryan, J. Perry, L. Wong, H. Slater, and K. H. A. Choo (2004), Human centromere repositioning "in progress"., *Proceedings of the National Academy of Sciences of the United States of America*, *101*(17), 6542–7, doi:10.1073/pnas.0308637101.

Aravamudhan, P., I. Felzer-Kim, and A. P. Joglekar (2013), The budding yeast point centromere associates with two Cse4 molecules during mitosis, *Curr Biol*, *23*(9), 770–774, doi:10.1016/j.cub.2013.03.042.

Aravamudhan, P., I. Felzer-Kim, K. Gurunathan, and A. P. Joglekar (2014), Assembling the protein architecture of the budding yeast kinetochore-microtubule attachment using FRET, *Curr Biol*, *24*(13), 1437–1446, doi:10.1016/j.cub.2014.05.014.

Aravamudhan, P., A. A. Goldfarb, and A. P. Joglekar (2015), The kinetochore encodes a mechanical switch to disrupt spindle assembly checkpoint signaling, *Nat Cell Biol*, *17*(7).

Ballister, E. R., M. Riegman, and M. A. Lampson (2014), Recruitment of Mad1 to metaphase kinetochores is sufficient to reactivate the mitotic checkpoint, *J Cell Biol*, *204*(6), 901–908, doi:10.1083/jcb.201311113.

Bevington, P. R., and D. K. Robinson (1969), Data reduction and error analysis, *McGraw–Hill, New York*.

Biggins, S. (2013), The composition, functions, and regulation of the budding yeast kinetochore., *Genetics*, *194*(4), 817–46, doi:10.1534/genetics.112.145276.

Biggins, S., and A. W. Murray (2001), The budding yeast protein kinase Ipl1/Aurora allows the absence of tension to activate the spindle checkpoint, *Genes & development*, *15*(23), 3118–29, doi:10.1101/gad.934801.

Biggins, S., F. F. Severin, N. Bhalla, I. Sassoon, A. A. Hyman, and A. W. Murray (1999), The conserved protein kinase Ipl1 regulates microtubule binding to kinetochores in budding yeast, *Genes Dev*, *13*(5), 532–544.

Bollen, M. (2014), Kinetochore signalling: the KIss that MELTs Knl1., *Current biology : CB*, *24*(2), R68–70, doi:10.1016/j.cub.2013.11.053.

Bouck, D. C., and K. S. Bloom (2005), The kinetochore protein Ndc10p is required for spindle stability and cytokinesis in yeast, *Proc Natl Acad Sci U S A*, *102*(15), 5408–5413.

Boveri, T. (1929), *The origin of malignant tumors,*, The Williams & Wilkins Company, Baltimore.

Brinkley, B. R., and E. Stubblefield (1966), The fine structure of the kinetochore of a mammalian cell in vitro., *Chromosoma*, *19*(1), 28–43.

Burke, D. J., and P. T. Stukenberg (2008), Linking kinetochore-microtubule binding to the spindle checkpoint., *Developmental cell*, *14*(4), 474–9, doi:10.1016/j.devcel.2008.03.015.

Chao, W. C., K. Kulkarni, Z. Zhang, E. H. Kong, and D. Barford (2012), Structure of the mitotic checkpoint complex, *Nature*, *484*(7393), 208–213.

Cheeseman, I. M. (2014), The Kinetochore, *Cold Spring Harbor Perspectives in Biology*, *6*(7), a015,826–a015,826, doi:10.1101/cshperspect.a015826.

Cheeseman, I. M., M. Enquist-Newman, T. Muller-Reichert, D. G. Drubin, and G. Barnes (2001), Mitotic spindle integrity and kinetochore function linked by the Duo1p/Dam1p complex, *J Cell Biol*, *152*(1), 197–212.

Cheeseman, I. M., J. S. Chappie, E. M. Wilson-Kubalek, and A. Desai (2006), The conserved KMN network constitutes the core microtubule-binding site of the kinetochore., *Cell*, *127*(5), 983–97, doi:10.1016/j.cell.2006.09.039.

Chen, R.-H., and A. Murray (1997), Characterization of spindle assembly checkpoint in xenopus egg extracts., *Methods in enzymology*, *283*, 572.

Cherry, L. M., A. J. Faulkner, L. Grossberg, and R. Balczon (1989), Kinetochore size variation in mammalian chromosomes: an image analysis study with evolutionary implications, *Journal of cell science*, *92*(2), 281–289.

Chevance, F. F. V., and K. T. Hughes (2008), Coordinating assembly of a bacterial macromolecular machine., *Nature reviews. Microbiology*, *6*(6), 455–65, doi:10.1038/nrmicro1887.

Ciferri, C., et al. (2005), Architecture of the human ndc80-hec1 complex, a critical constituent of the outer kinetochore., *The Journal of biological chemistry*, *280*(32), 29,088–95, doi:10.1074/jbc.M504070200.

Ciferri, C., et al. (2008), Implications for kinetochore-microtubule attachment from the structure of an engineered Ndc80 complex, *Cell*, *133*(3), 427–439, doi:10.1016/j.cell.2008.03.020.

Ciliberto, A., and J. V. Shah (2009), A quantitative systems view of the spindle assembly checkpoint., *The EMBO journal*, *28*(15), 2162–73, doi:10.1038/emboj.2009.186.

Coffman, V. C., P. Wu, M. R. Parthun, and J. Q. Wu (2011), CENP-A exceeds microtubule attachment sites in centromere clusters of both budding and fission yeast, *J Cell Biol*, *195*(4), 563–572, doi:jcb.201106078 [pii] 10.1083/jcb.201106078.

Collin, P., O. Nashchekina, R. Walker, and J. Pines (2013), The spindle assembly checkpoint works like a rheostat rather than a toggle switch, *Nat Cell Biol*, *15*(11), 1378–1385, doi:10.1038/ncb2855.

Coudreuse, D., and P. Nurse (2010), Driving the cell cycle with a minimal CDK control network., *Nature*, *468*(7327), 1074–9, doi:10.1038/nature09543.

Cross, M. K., and M. A. Powers (2009), Learning about cancer from frogs: analysis of mitotic spindles in xenopus egg extracts, *Disease models & mechanisms*, *2*(11-12), 541–547.

Daum, J. R., J. D. Wren, J. J. Daniel, S. Sivakumar, J. N. McAvoy, T. A. Potapova, and G. J. Gorbsky (2009), Ska3 Is Required for Spindle Checkpoint Silencing and the Maintenance of Chromosome Cohesion in Mitosis, *Current Biology*, *19*(17), 1467–1472.

De Antoni, A., et al. (2005), The Mad1/Mad2 complex as a template for Mad2 activation in the spindle assembly checkpoint., *Current biology : CB*, *15*(3), 214–25, doi:10.1016/j.cub.2005.01.038.

De Wulf, P., A. D. McAinsh, and P. K. Sorger (2003), Hierarchical assembly of the budding yeast kinetochore from multiple subcomplexes., *Genes & development*, *17*(23), 2902–21, doi:10.1101/gad.1144403.

DeLuca, J. G., B. J. Howell, J. C. Canman, J. M. Hickey, G. Fang, and E. D. Salmon (2003), Nuf2 and Hec1 are required for retention of the checkpoint proteins Mad1 and Mad2 to kinetochores, *Curr Biol*, *13*(23), 2103–2109.

Demirel, P. B., B. E. Keyes, M. Chaterjee, C. E. Remington, and D. J. Burke (2012), A redundant function for the N-terminal tail of Ndc80 in kinetochore-microtubule interaction in Saccharomyces cerevisiae., *Genetics*, *192*(2), 753–6, doi:10.1534/genetics.112.143818.

Dick, A. E., and D. W. Gerlich (2013a), Kinetic framework of spindle assembly checkpoint signalling, *Nature cell biology*, *15*(11), 1370–1377.

Dick, A. E., and D. W. Gerlich (2013b), Kinetic framework of spindle assembly checkpoint signalling, *Nat Cell Biol*, *15*(11), 1370–1377, doi:10.1038/ncb2842.

Dobles, M., V. Liberal, M. L. Scott, R. Benezra, and P. K. Sorger (2000), Chromosome missegregation and apoptosis in mice lacking the mitotic checkpoint protein mad2, *Cell*, *101*(6), 635–645.

Doncic, A., E. Ben-Jacob, and N. Barkai (2005), Evaluating putative mechanisms of the mitotic spindle checkpoint, *Proc Natl Acad Sci U S A*, *102*(18), 6332–6337, doi:10.1073/pnas.0409142102.

Efremov, A., E. L. Grishchuk, J. R. McIntosh, and F. I. Ataullakhanov (2007), In search of an optimal ring to couple microtubule depolymerization to processive chromosome motions, *Proc Natl Acad Sci U S A*, *104*(48), 19,017–19,022.

Espeut, J., D. K. Cheerambathur, L. Krenning, K. Oegema, and A. Desai (2012), Microtubule binding by KNL-1 contributes to spindle checkpoint silencing at the kinetochore, *J Cell Biol*, *196*(4), 469–482, doi:jcb.201111107 [pii] 10.1083/jcb.201111107.

Flemming, W. Zellsubstanz, K. u. Z. (1882), Zellsubstanz, kern und zelltheilung.. : Flemming, Walther, 1843-1905, *FCW Vogel, Leipzig*.

Fraschini, R., A. Beretta, G. Lucchini, and S. Piatti (2001), Role of the kinetochore protein Ndc10 in mitotic checkpoint activation in Saccharomyces cerevisiae, *Mol Genet Genomics*, *266*(1), 115–125.

Funabiki, H., and D. J. Wynne (2013), Making an effective switch at the kinetochore by phosphorylation and dephosphorylation, *Chromosoma*, *122*(3), 135–158, doi:10.1007/s00412-013-0401-5.

Gascoigne, K. E., and I. M. Cheeseman (2011), Kinetochore assembly: if you build it, they will come., *Current opinion in cell biology*, *23*(1), 102–8, doi:10.1016/j.ceb.2010.07.007.

Gascoigne, K. E., and I. M. Cheeseman (2013), CDK-dependent phosphorylation and nuclear exclusion coordinately control kinetochore assembly state., *The Journal of cell biology*, *201*(1), 23–32, doi:10.1083/jcb.201301006.

Ghaemmaghami, S., W. K. Huh, K. Bower, R. W. Howson, A. Belle, N. Dephoure, E. K. O'Shea, and J. S. Weissman (2003), Global analysis of protein expression in yeast, *Nature*, *425*(6959), 737–741, doi:10.1038/nature02046.

Goh, P. Y., and J. V. Kilmartin (1993), NDC10: a gene involved in chromosome segregation in Saccharomyces cerevisiae, *J Cell Biol*, *121*(3), 503–512.

Gonen, S., B. Akiyoshi, M. G. Iadanza, D. Shi, N. Duggan, S. Biggins, and T. Gonen (2012), The structure of purified kinetochores reveals multiple microtubule-attachment sites., *Nature structural & molecular biology*, *19*(9), 925–9, doi: 10.1038/nsmb.2358.

Grishchuk, E. L., M. I. Molodtsov, F. I. Ataullakhanov, and J. R. McIntosh (2005), Force production by disassembling microtubules., *Nature*, *438*(7066), 384–8, doi: 10.1038/nature04132.

Grishchuk, E. L., I. S. Spiridonov, V. A. Volkov, A. Efremov, S. Westermann, D. Drubin, G. Barnes, F. I. Ataullakhanov, and J. R. McIntosh (2008), Different assemblies of the DAM1 complex follow shortening microtubules by distinct mechanisms, *Proc Natl Acad Sci U S A*, *105*(19), 6918–6923.

Guimaraes, G. J., Y. Dong, B. F. McEwen, and J. G. Deluca (2008), Kinetochore-microtubule attachment relies on the disordered N-terminal tail domain of Hec1, *Curr Biol*, *18*(22), 1778–1784.

Hardwick, K. G., E. Weiss, F. C. Luca, M. Winey, and A. W. Murray (1996), Activation of the budding yeast spindle assembly checkpoint without mitotic spindle disruption, *Science*, *273*(5277), 953–956.

Haruki, H., J. Nishikawa, and U. K. Laemmli (2008), The anchor-away technique: rapid, conditional establishment of yeast mutant phenotypes, *Mol Cell*, *31*(6), 925–932, doi:10.1016/j.molcel.2008.07.020.

Heinrich, S., H. Windecker, N. Hustedt, and S. Hauf (2012), Mph1 kinetochore localization is crucial and upstream in the hierarchy of spindle assembly checkpoint protein recruitment to kinetochores, *J Cell Sci*, *125*(Pt 20), 4720–4727, doi: 10.1242/jcs.110387.

Heinrich, S., et al. (2013), Determinants of robustness in spindle assembly checkpoint signalling, *Nat Cell Biol*, *15*(11), 1328–1339, doi:10.1038/ncb2864.

Henikoff, S., and J. G. Henikoff (2012), "Point" centromeres of Saccharomyces harbor single centromere-specific nucleosomes., *Genetics*, *190*(4), 1575–7, doi: 10.1534/genetics.111.137711.

Hewitt, L., A. Tighe, S. Santaguida, A. M. White, C. D. Jones, A. Musacchio, S. Green, and S. S. Taylor (2010), Sustained Mps1 activity is required in mitosis to recruit O-Mad2 to the Mad1-C-Mad2 core complex, *J Cell Biol*, *190*(1), 25–34, doi:10.1083/jcb.201002133.

Holland, A. J., and D. W. Cleveland (2009), Boveri revisited: chromosomal instability, aneuploidy and tumorigenesis., *Nature reviews. Molecular cell biology*, *10*(7), 478–87, doi:10.1038/nrm2718.

Hooke, R. (1665), Micrographia: or, Some physiological descriptions of minute bodies made by magnifying glasses, *London: J. Martyn and J. Allestry*.

Hornung, P., M. Maier, G. M. Alushin, G. C. Lander, E. Nogales, and S. Westermann (2010), Molecular Architecture and Connectivity of the Budding Yeast Mtw1 Kinetochore Complex, *J Mol Biol*, *405*(2), 548–559.

Howell, B. J., B. F. McEwen, J. C. Canman, D. B. Hoffman, E. M. Farrar, C. L. Rieder, and E. D. Salmon (2001), Cytoplasmic dynein/dynactin drives kinetochore protein transport to the spindle poles and has a role in mitotic spindle checkpoint inactivation, *J Cell Biol*, *155*(7), 1159–1172, doi:10.1083/jcb.200105093.

Howell, B. J., B. Moree, E. M. Farrar, S. Stewart, G. Fang, and E. D. Salmon (2004), Spindle checkpoint protein dynamics at kinetochores in living cells, *Curr Biol*, *14*(11), 953–964, doi:10.1016/j.cub.2004.05.053.

Hoyt, M. A., L. Totis, and B. T. Roberts (1991), S. cerevisiae genes required for cell cycle arrest in response to loss of microtubule function., *Cell*, *66*(3), 507–17.

Hsu, K.-S., and T. Toda (2011), Ndc80 Internal Loop Interacts with Dis1/TOG to Ensure Proper Kinetochore-Spindle Attachment in Fission Yeast, *Current Biology*, *21*(3), 214–220.

Huang, H.-C., J. Shi, J. D. Orth, and T. J. Mitchison (2009), Evidence that mitotic exit is a better cancer therapeutic target than spindle assembly., *Cancer cell*, *16*(4), 347–58, doi:10.1016/j.ccr.2009.08.020.

Ito, D., Y. Saito, and T. Matsumoto (2012), Centromere-tethered Mps1 pombe homolog (Mph1) kinase is a sufficient marker for recruitment of the spindle checkpoint protein Bub1, but not Mad1, *Proc Natl Acad Sci U S A*, *109*(1), 209–214, doi:10.1073/pnas.1114647109.

Jelluma, N., T. B. Dansen, T. Sliedrecht, N. P. Kwiatkowski, and G. J. Kops (2010), Release of Mps1 from kinetochores is crucial for timely anaphase onset, *J Cell Biol*, *191*(2), 281–290, doi:10.1083/jcb.201003038 jcb.201003038 [pii].

Joglekar, A. P., D. C. Bouck, J. N. Molk, K. S. Bloom, and E. D. Salmon (2006), Molecular architecture of a kinetochore-microtubule attachment site, *Nat Cell Biol*, *8*(6), 581–585.

Joglekar, A. P., D. Bouck, K. Finley, X. Liu, Y. Wan, J. Berman, X. He, E. D. Salmon, and K. S. Bloom (2008), Molecular architecture of the kinetochore-microtubule attachment site is conserved between point and regional centromeres, *J Cell Biol*, *181*(4), 587–594.

Joglekar, A. P., K. Bloom, and E. D. Salmon (2009), In vivo protein architecture of the eukaryotic kinetochore with nanometer scale accuracy., *Current biology : CB*, *19*(8), 694–9, doi:10.1016/j.cub.2009.02.056.

Joglekar, A. P., K. S. Bloom, and E. D. Salmon (2010), Mechanisms of force generation by end-on kinetochore-microtubule attachments, *Curr Opin Cell Biol.*, *22*(1), 57–67.

Joglekar, A. P., R. Chen, and J. G. Lawrimore (2013), A sensitized emission based calibration of FRET efficiency for probing the architecture of macromolecular machines, *Cell and Molecular Bioengineering*, *6*, 369–382, doi:10.1007/s12195-013-0290-y.

Johnston, K., A. Joglekar, T. Hori, A. Suzuki, T. Fukagawa, and E. D. Salmon (2010), Vertebrate kinetochore protein architecture: protein copy number., *The Journal of cell biology*, *189*(6), 937–43, doi:10.1083/jcb.200912022.

Jorgensen, P., N. P. Edgington, B. L. Schneider, I. Rupes, M. Tyers, and B. Futcher (2007), The size of the nucleus increases as yeast cells grow, *Mol Biol Cell*, *18*(9), 3523–3532, doi:10.1091/mbc.E06-10-0973.

Kaksonen, M., C. P. Toret, and D. G. Drubin (2005), A modular design for the clathrin- and actin-mediated endocytosis machinery., *Cell*, *123*(2), 305–20, doi:10.1016/j.cell.2005.09.024.

Kamenz, J., and S. Hauf (2014), Slow checkpoint activation kinetics as a safety device in anaphase., *Current biology : CB*, *24*(6), 646–51, doi:10.1016/j.cub.2014.02.005.

Kemmler, S., M. Stach, M. Knapp, J. Ortiz, J. Pfannstiel, T. Ruppert, and J. Lechner (2009), Mimicking Ndc80 phosphorylation triggers spindle assembly checkpoint signalling, *Embo J*, *28*(8), 1099–1110.

Kern, D. M., T. Kim, M. Rigney, N. Hattersley, A. Desai, and I. M. Cheeseman (2014), The outer kinetochore protein KNL-1 contains a defined oligomerization domain in nematodes, *Mol Biol Cell*, doi:10.1091/mbc.E14-06-1125.

Khodjakov, A., and J. Pines (2010), Centromere tension: a divisive issue., *Nature cell biology*, *12*(10), 919–23, doi:10.1038/ncb1010-919.

Kim, S., H. Sun, H. L. Ball, K. Wassmann, X. Luo, and H. Yu (2010), Phosphorylation of the spindle checkpoint protein Mad2 regulates its conformational transition, *Proc Natl Acad Sci U S A*, *107*(46), 19,772–19,777, doi:10.1073/pnas.1009000107.

King, J. M., and R. B. Nicklas (2000), Tension on chromosomes increases the number of kinetochore microtubules but only within limits., *Journal of cell science*, *113 Pt 21*, 3815–23.

Kitagawa, R., and A. M. Rose (1999), Components of the spindle-assembly checkpoint are essential in caenorhabditis elegans, *Nature cell biology*, *1*(8), 514–521.

Kiyomitsu, T., C. Obuse, and M. Yanagida (2007), Human Blinkin/AF15q14 is required for chromosome alignment and the mitotic checkpoint through direct interaction with Bub1 and BubR1., *Developmental cell*, *13*(5), 663–76, doi:10.1016/j.devcel.2007.09.005.

Kops, G. J. P. L., B. A. A. Weaver, and D. W. Cleveland (2005), On the road to cancer: aneuploidy and the mitotic checkpoint., *Nature reviews. Cancer*, *5*(10), 773–85, doi:10.1038/nrc1714.

Krenn, V., K. Overlack, I. Primorac, S. van Gerwen, and A. Musacchio (2014), KI motifs of human Knl1 enhance assembly of comprehensive spindle checkpoint complexes around MELT repeats, *Curr Biol*, *24*(1), 29–39, doi:10.1016/j.cub.2013.11.046.

Kuijt, T. E., M. Omerzu, A. T. Saurin, and G. J. Kops (2014), Conditional targeting of MAD1 to kinetochores is sufficient to reactivate the spindle assembly checkpoint in metaphase, *Chromosoma*, doi:10.1007/s00412-014-0458-9.

Kulukian, A., J. S. Han, and D. W. Cleveland (2009), Unattached kinetochores catalyze production of an anaphase inhibitor that requires a mad2 template to prime cdc20 for bubr1 binding, *Developmental cell*, *16*(1), 105–117.

Lampert, F., P. Hornung, and S. Westermann (2010), The Dam1 complex confers microtubule plus end-tracking activity to the Ndc80 kinetochore complex, *J Cell Biol*, *189*(4), 641–649, doi:jcb.200912021 [pii] 10.1083/jcb.200912021.

Larsen, N. A., J. Al-Bassam, R. R. Wei, and S. C. Harrison (2007), Structural analysis of Bub3 interactions in the mitotic spindle checkpoint, *Proc Natl Acad Sci U S A*, *104*(4), 1201–1206, doi:10.1073/pnas.0610358104.

Lawrimore, J., K. S. Bloom, and E. D. Salmon (2011), Point centromeres contain more than a single centromere-specific Cse4 (CENP-A) nucleosome, *J Cell Biol*, *195*(4), 573–582, doi:jcb.201106036 [pii] 10.1083/jcb.201106036.

Li, R., and A. W. Murray (1991), Feedback control of mitosis in budding yeast, *Cell*, *66*(3), 519–531, doi:10.1016/0092-8674(81)90015-5.

Li, X., and R. B. Nicklas (1995), Mitotic forces control a cell-cycle checkpoint., *Nature*, *373*(6515), 630–2, doi:10.1038/373630a0.

Li, Y., J. Bachant, A. A. Alcasabas, Y. Wang, J. Qin, and S. J. Elledge (2002), The mitotic spindle is required for loading of the DASH complex onto the kinetochore, *Genes Dev*, *16*(2), 183–197, doi:10.1101/gad.959402.

Liu, X., and M. Winey (2012), The MPS1 family of protein kinases, *Annu Rev Biochem*, *81*(1), 561–585, doi:10.1146/annurev-biochem-061611-090435.

London, N., and S. Biggins (2014), Mad1 kinetochore recruitment by Mps1-mediated phosphorylation of Bub1 signals the spindle checkpoint, *Genes Dev*, doi:10.1101/gad.233700.113.

London, N., S. Ceto, J. A. Ranish, and S. Biggins (2012), Phosphoregulation of Spc105 by Mps1 and PP1 regulates Bub1 localization to kinetochores, *Curr Biol*, *22*(10), 900–906, doi:10.1016/j.cub.2012.03.052.

Maddox, P. S., K. Oegema, A. Desai, and I. M. Cheeseman (2004), "Holo"er than thou: chromosome segregation and kinetochore function in C. elegans., *Chromosome research : an international journal on the molecular, supramolecular and evolutionary aspects of chromosome biology*, *12*(6), 641–53, doi: 10.1023/B:CHRO.0000036588.42225.2f.

Maldonado, M., and T. M. Kapoor (2011), Constitutive Mad1 targeting to kinetochores uncouples checkpoint signalling from chromosome biorientation, *Nat Cell Biol*, *13*(4), 475–482, doi: http://www.nature.com/ncb/journal/v13/n4/abs/ncb2223.html#supplementary-information.

Maresca, T. J., and E. D. Salmon (2009), Intrakinetochore stretch is associated with changes in kinetochore phosphorylation and spindle assembly checkpoint activity, *J Cell Biol*, *184*(3), 373–381, doi:10.1083/jcb.200808130.

Marston, A. L. (2014), Chromosome segregation in budding yeast: sister chromatid cohesion and related mechanisms., *Genetics*, *196*(1), 31–63, doi: 10.1534/genetics.112.145144.

Martin-Lluesma, S., V. M. Stucke, and E. A. Nigg (2002), Role of Hec1 in spindle checkpoint signaling and kinetochore recruitment of Mad1/Mad2., *Science (New York, N.Y.)*, *297*(5590), 2267–70, doi:10.1126/science.1075596.

Maskell, D. P., X.-W. Hu, and M. R. Singleton (2010), Molecular architecture and assembly of the yeast kinetochore MIND complex, *J Cell Biol*, *190*(5), 823–834, doi:10.1083/jcb.201002059.

McAinsh, A. D., J. D. Tytell, and P. K. Sorger (2003), Structure, function, and regulation of budding yeast kinetochores., *Annual review of cell and developmental biology*, *19*, 519–39, doi:10.1146/annurev.cellbio.19.111301.155607.

McCleland, M. L., R. D. Gardner, M. J. Kallio, J. R. Daum, G. J. Gorbsky, D. J. Burke, and P. T. Stukenberg (2003), The highly conserved Ndc80 complex is required for kinetochore assembly, chromosome congression, and spindle checkpoint activity, *Genes Dev*, *17*(1), 101–114, doi:10.1101/gad.1040903.

McEwen, B. F., A. B. Heagle, G. O. Cassels, K. F. Buttle, and C. L. Rieder (1997), Kinetochore fiber maturation in PtK1 cells and its implications for the mechanisms of chromosome congression and anaphase onset, *J Cell Biol*, *137*(7), 1567–1580.

McEwen, B. F., G. K. Chan, B. Zubrowski, M. S. Savoian, M. T. Sauer, and T. J. Yen (2001), CENP-E Is Essential for Reliable Bioriented Spindle Attachment, but Chromosome Alignment Can Be Achieved via Redundant Mechanisms in Mammalian Cells, *Molecular Biology of the Cell*, *12*(9), 2776–2789, doi:10.1091/mbc.12.9.2776.

McIntosh, J. R. (1991), Structural and mechanical control of mitotic progression, *Cold Spring Harb Symp Quant Biol*, *56*, 613–619.

McIntosh, J. R., V. Volkov, F. I. Ataullakhanov, and E. L. Grishchuk (2010), Tubulin depolymerization may be an ancient biological motor., *Journal of cell science*, *123*(Pt 20), 3425–34, doi:10.1242/jcs.067611.

Meraldi, P., V. M. Draviam, and P. K. Sorger (2004), Timing and checkpoints in the regulation of mitotic progression, *Developmental cell*, *7*(1), 45–60.

Moyle, M. W., T. Kim, N. Hattersley, J. Espeut, D. K. Cheerambathur, K. Oegema, and A. Desai (2014), A Bub1-Mad1 interaction targets the Mad1-Mad2 complex to unattached kinetochores to initiate the spindle checkpoint., *The Journal of cell biology*, *204*(5), 647–57, doi:10.1083/jcb.201311015.

Muller, E. G., et al. (2005), The organization of the core proteins of the yeast spindle pole body, *Mol Biol Cell*, *16*(7), 3341–3352.

Murray, A. W. (2011), A brief history of error., *Nature cell biology*, *13*(10), 1178–82, doi:10.1038/ncb2348.

Musacchio, A. (2011), Spindle assembly checkpoint: the third decade., *Philosophical transactions of the Royal Society of London. Series B, Biological sciences*, *366*(1584), 3595–604, doi:10.1098/rstb.2011.0072.

Nasmyth, K. (2005), How do so few control so many?, *Cell*, *120*(6), 739–746, doi:10.1016/j.cell.2005.03.006.

Nasmyth, K., and C. H. Haering (2009), Cohesin: Its Roles and Mechanisms, *Annual Review of Genetics*.

Nezi, L., and A. Musacchio (2009), Sister chromatid tension and the spindle assembly checkpoint, *Current Opinion in Cell Biology*, *21*(6), 785–795, doi:10.1016/j.ceb.2009.09.007.

Nicklas, R. B., and C. A. Koch (1969), Chromosome micromanipulation. 3. Spindle fiber tension and the reorientation of mal-oriented chromosomes., *The Journal of cell biology*, *43*(1), 40–50.

Nijenhuis, W., et al. (2013), A TPR domain-containing N-terminal module of MPS1 is required for its kinetochore localization by Aurora B, *J Cell Biol*, *201*(2), 217–231, doi:10.1083/jcb.201210033.

Padilla-Parra, S., N. Audugé, H. Lalucque, J.-C. Mevel, M. Coppey-Moisan, and M. Tramier (2009), Quantitative Comparison of Different Fluorescent Protein Couples for Fast FRET-FLIM Acquisition, *Biophysical Journal*, *97*(8), 2368–2376, doi:10.1016/j.bpj.2009.07.044.

Pagliuca, C., V. M. Draviam, E. Marco, P. K. Sorger, and P. De Wulf (2009), Roles for the Conserved Spc105p/Kre28p Complex in Kinetochore-Microtubule Binding and the Spindle Assembly Checkpoint, *PLoS ONE*, *4*(10), e7640.

Palframan, W. J., J. B. Meehl, S. L. Jaspersen, M. Winey, and A. W. Murray (2006), Anaphase inactivation of the spindle checkpoint, *Science*, *313*(5787), 680–684, doi: 10.1126/science.1127205.

Petrovic, A., et al. (2010), The MIS12 complex is a protein interaction hub for outer kinetochore assembly., *The Journal of cell biology*, *190*(5), 835–52, doi: 10.1083/jcb.201002070.

Petrovic, A., et al. (2014), Modular assembly of RWD domains on the Mis12 complex underlies outer kinetochore organization, *Mol Cell*, *53*(4), 591–605, doi: 10.1016/j.molcel.2014.01.019.

Pinsky, B. A., C. Kung, K. M. Shokat, and S. Biggins (2006), The Ipl1-Aurora protein kinase activates the spindle checkpoint by creating unattached kinetochores, *Nat Cell Biol*, *8*(1), 78–83.

Pinsky, B. A., C. R. Nelson, and S. Biggins (2009), Protein phosphatase 1 regulates exit from the spindle checkpoint in budding yeast, *Curr Biol*, *19*(14), 1182–1187, doi:10.1016/j.cub.2009.06.043.

Piston, D. W., and G.-J. Kremers (2007), Fluorescent protein FRET: the good, the bad and the ugly, *Trends in Biochemical Sciences*, *32*(9), 407–414, doi: 10.1016/j.tibs.2007.08.003.

Powers, A. F., A. D. Franck, D. R. Gestaut, J. Cooper, B. Gracyzk, R. R. Wei, L. Wordeman, T. N. Davis, and C. L. Asbury (2009), The Ndc80 kinetochore complex forms load-bearing attachments to dynamic microtubule tips via biased diffusion, *Cell*, *136*(5), 865–875.

Primorac, I., J. R. Weir, E. Chiroli, F. Gross, I. Hoffmann, S. van Gerwen, A. Ciliberto, and A. Musacchio (2013), Bub3 reads phosphorylated MELT repeats to promote spindle assembly checkpoint signaling, *Elife*, *2*, e01,030, doi: 10.7554/eLife.01030.

Quénet, D., and Y. Dalal (2012), The CENP-A nucleosome: a dynamic structure and role at the centromere., *Chromosome research : an international journal on the molecular, supramolecular and evolutionary aspects of chromosome biology*, *20*(5), 465–79, doi:10.1007/s10577-012-9301-4.

Ramey, V. H., H.-W. Wang, Y. Nakajima, A. Wong, J. Liu, D. Drubin, G. Barnes, and E. Nogales (2011), The Dam1 ring binds to the E-hook of tubulin and diffuses along the microtubule, *Mol. Biol. Cell*, *22*(4), 457–466, doi:10.1091/mbc.E10-10-0841.

Rieder, C. L. (1981), The structure of the cold-stable kinetochore fiber in metaphase PtK1 cells, *Chromosoma*, *84*(1), 145–158, doi:10.1007/BF00293368.

Rieder, C. L., A. Schultz, R. Cole, and G. Sluder (1994), Anaphase onset in vertebrate somatic cells is controlled by a checkpoint that monitors sister kinetochore attachment to the spindle, *J Cell Biol*, *127*(5), 1301–1310.

Rosenberg, J. S., F. R. Cross, and H. Funabiki (2011), KNL1/Spc105 Recruits PP1 to Silence the Spindle Assembly Checkpoint., *Current biology : CB*, *21*(11), 942–7, doi:10.1016/j.cub.2011.04.011.

Roy, B., N. Varshney, V. Yadav, and K. Sanyal (2013), The process of kinetochore assembly in yeasts., *FEMS microbiology letters*, *338*(2), 107–17, doi:10.1111/1574-6968.12019.

Santaguida, S., and A. Musacchio (2009), The life and miracles of kinetochores., *The EMBO journal*, *28*(17), 2511–31, doi:10.1038/emboj.2009.173.

Santaguida, S., C. Vernieri, F. Villa, A. Ciliberto, and A. Musacchio (2011), Evidence that Aurora B is implicated in spindle checkpoint signalling independently of error correction., *The EMBO journal*, *30*(8), 1508–19, doi:10.1038/emboj.2011.70.

Schmidt, J. C., et al. (2012), The kinetochore-bound Ska1 complex tracks depolymerizing microtubules and binds to curved protofilaments., *Developmental cell*, *23*(5), 968–80, doi:10.1016/j.devcel.2012.09.012.

Schmitzberger, F., and S. C. Harrison (2012), Rwd domain: a recurring module in kinetochore architecture shown by a ctf19–mcm21 complex structure, *EMBO reports*, *13*(3), 216–222.

Schwartz, T. U. (2005), Modularity within the architecture of the nuclear pore complex., *Current opinion in structural biology*, *15*(2), 221–6, doi:10.1016/j.sbi.2005.03.003.

Scott, C., A. Klika, M. Lo, T. Norris, and C. Caputo (1992), Tau protein induces bundling of microtubules in vitro: comparison of different tau isoforms and a tau protein fragment, *Journal of neuroscience research*, *33*(1), 19–29.

Scott, R. J., C. P. Lusk, D. J. Dilworth, J. D. Aitchison, and R. W. Wozniak (2005), Interactions between Mad1p and the nuclear transport machinery in the yeast Saccharomyces cerevisiae, *Mol Biol Cell*, *16*(9), 4362–4374, doi:10.1091/mbc.E05-01-0011.

Screpanti, E., A. De Antoni, G. M. Alushin, A. Petrovic, T. Melis, E. Nogales, and A. Musacchio (2011), Direct binding of Cenp-C to the Mis12 complex joins the inner and outer kinetochore, *Curr Biol*, *21*(5), 391–398, doi:10.1016/j.cub.2010.12.039.

Sear, R. P., and M. Howard (2006), Modeling dual pathways for the metazoan spindle assembly checkpoint, *Proceedings of the National Academy of Sciences*, *103*(45), 16,758–16,763, doi:10.1073/pnas.0603174103.

Shen, Z. (2011), Genomic instability and cancer: an introduction., *Journal of molecular cell biology*, *3*(1), 1–3, doi:10.1093/jmcb/mjq057.

Shepperd, L. A., J. C. Meadows, A. M. Sochaj, T. C. Lancaster, J. Zou, G. J. Buttrick, J. Rappsilber, K. G. Hardwick, and J. B. A. Millar (2012), Phosphodependent recruitment of Bub1 and Bub3 to Spc7/KNL1 by Mph1 kinase maintains the spindle checkpoint., *Current biology : CB*, *22*(10), 891–9, doi:10.1016/j.cub.2012.03.051.

Shimogawa, M. M., et al. (2006), Mps1 phosphorylation of Dam1 couples kinetochores to microtubule plus ends at metaphase., *Current biology : CB*, *16*(15), 1489–501, doi:10.1016/j.cub.2006.06.063.

Sironi, L., M. Mapelli, S. Knapp, A. De Antoni, K.-T. Jeang, and A. Musacchio (2002), Crystal structure of the tetrameric Mad1-Mad2 core complex: implications of a 'safety belt' binding mechanism for the spindle checkpoint., *The EMBO journal*, *21*(10), 2496–506, doi:10.1093/emboj/21.10.2496.

Spencer, F., and P. Hieter (1992), Centromere DNA mutations induce a mitotic delay in Saccharomyces cerevisiae, *Proc Natl Acad Sci U S A*, *89*(19), 8908–8912, doi:10.1073/pnas.89.19.8908.

Tanaka, K., N. Mukae, H. Dewar, M. van Breugel, E. K. James, A. R. Prescott, C. Antony, and T. U. Tanaka (2005), Molecular mechanisms of kinetochore capture by spindle microtubules, *Nature*, *434*(7036), 987–994, doi:10.1038/nature03483.

Tien, J. F., N. T. Umbreit, D. R. Gestaut, A. D. Franck, J. Cooper, L. Wordeman, T. Gonen, C. L. Asbury, and T. N. Davis (2010), Cooperation of the Dam1 and Ndc80 kinetochore complexes enhances microtubule coupling and is regulated by aurora B., *The Journal of cell biology*, *189*(4), 713–723, doi:jcb.200910142 [pii] 10.1083/jcb.200910142.

Tien, J. F., et al. (2014), Kinetochore Biorientation in Saccharomyces cerevisiae Requires a Tightly Folded Conformation of the Ndc80 Complex, *Genetics*, doi:10.1534/genetics.114.167775.

Tipton, A. R., W. Ji, B. Sturt-Gillespie, M. E. Bekier, K. Wang, W. R. Taylor, and S.-T. Liu (2013), Monopolar Spindle 1 (MPS1) Kinase Promotes Production of Closed MAD2 (C-MAD2) Conformer and Assembly of the Mitotic Checkpoint Complex, *Journal of Biological Chemistry*, *288*(49), 35,149–35,158, doi:10.1074/jbc.M113.522375.

Uchida, K. S., K. Takagaki, K. Kumada, Y. Hirayama, T. Noda, and T. Hirota (2009), Kinetochore stretching inactivates the spindle assembly checkpoint, *J Cell Biol*, *184*(3), 383–390, doi:jcb.200811028 [pii] 10.1083/jcb.200811028.

Uhlmann, F., D. Wernic, M.-A. Poupart, E. V. Koonin, and K. Nasmyth (2000), Cleavage of cohesin by the cd clan protease separin triggers anaphase in yeast, *Cell*, *103*(3), 375–386.

Varma, D., et al. (2012), Recruitment of the human Cdt1 replication licensing protein by the loop domain of Hec1 is required for stable kinetochore-microtubule attachment, *Nat Cell Biol*, *14*(6), 593–603, doi:10.1038/ncb2489.

Vig, B. K., N. Paweletz, and D. Broccoli (1989), Centromere separation and aneuploidy: a lesson from multicentric chromosomes., *Progress in clinical and biological research*, *318*, 137–48.

Vink, M., et al. (2006), In vitro FRAP identifies the minimal requirements for Mad2 kinetochore dynamics., *Current biology : CB*, *16*(8), 755–66, doi: 10.1016/j.cub.2006.03.057.

Wan, X., et al. (2009), Protein architecture of the human kinetochore microtubule attachment site, *Cell*, *137*(4), 672–684.

Wang, H. W., V. H. Ramey, S. Westermann, A. E. Leschziner, J. P. Welburn, Y. Nakajima, D. G. Drubin, G. Barnes, and E. Nogales (2007), Architecture of the Dam1 kinetochore ring complex and implications for microtubule-driven assembly and force-coupling mechanisms, *Nat Struct Mol Biol*, *14*(8), 721–726, doi: 10.1038/nsmb1274.

Wang, H. W., S. Long, C. Ciferri, S. Westermann, D. Drubin, G. Barnes, and E. Nogales (2008), Architecture and flexibility of the yeast Ndc80 kinetochore complex, *J Mol Biol*, *383*(4), 894–903.

Watanabe, Y. (2012), Geometry and force behind kinetochore orientation: lessons from meiosis., *Nature reviews. Molecular cell biology*, *13*(6), 370–82, doi: 10.1038/nrm3349.

Wei, R. R., P. K. Sorger, and S. C. Harrison (2005), Molecular organization of the Ndc80 complex, an essential kinetochore component, *Proc Natl Acad Sci U S A*, *102*(15), 5363–7, doi:10.1073/pnas.0501168102.

Wei, R. R., J. R. Schnell, N. A. Larsen, P. K. Sorger, J. J. Chou, and S. C. Harrison (2006), Structure of a central component of the yeast kinetochore: the Spc24p/Spc25p globular domain, *Structure*, *14*(6), 1003–1009, doi: 10.1016/j.str.2006.04.007.

Welburn, J. P. I., E. L. Grishchuk, C. B. Backer, E. M. Wilson-Kubalek, J. R. Yates, and I. M. Cheeseman (2009), The human kinetochore Ska1 complex facilitates microtubule depolymerization-coupled motility., *Developmental cell*, *16*(3), 374–85, doi:10.1016/j.devcel.2009.01.011.

Westermann, S., I. M. Cheeseman, S. Anderson, J. R. Yates 3rd, D. G. Drubin, and G. Barnes (2003), Architecture of the budding yeast kinetochore reveals a conserved molecular core, *J Cell Biol*, *163*(2), 215–222, doi:10.1083/jcb.200305100.

Yeong, F. M., H. H. Lim, C. G. Padmashree, and U. Surana (2000), Exit from mitosis in budding yeast: biphasic inactivation of the Cdc28-Clb2 mitotic kinase and the role of Cdc20, *Mol Cell*, *5*(3), 501–511.

Yuen, K. W., C. D. Warren, O. Chen, T. Kwok, P. Hieter, and F. A. Spencer (2007), Systematic genome instability screens in yeast and their potential relevance to cancer, *Proc Natl Acad Sci U S A*, *104*(10), 3925–3930, doi:10.1073/pnas.0610642104.

Zhang, G., C. D. Kelstrup, X. W. Hu, M. J. Kaas Hansen, M. R. Singleton, J. V. Olsen, and J. Nilsson (2012), The Ndc80 internal loop is required for recruitment of the Ska complex to establish end-on microtubule attachment to kinetochores, *J Cell Sci*, *125*(Pt 13), 3243–3253, doi:10.1242/jcs.104208.

Zhang, G., T. Lischetti, and J. Nilsson (2014), A minimal number of MELT repeats supports all the functions of KNL1 in chromosome segregation, *J Cell Sci*, *127*(Pt 4), 871–884, doi:10.1242/jcs.139725.

Zhou, H. X. (2004), Polymer models of protein stability, folding, and interactions, *Biochemistry*, *43*(8), 2141–2154, doi:10.1021/bi036269n.